MINISTRY OF PUBLIC WORKS

****

MINISTÈRE DES TRAVAUX PUBLICS

****

MINISTRY OF HIGHER EDUCATION

****

MINISTÈRE DE L'ENSEIGNEMENT SUPÉRIEUR

****

DEPARTMENT OF CIVIL ENGINEERING

DEPARTEMENT DE GENIE CIVIL

DEPARTMENT OF CIVIL, ARCHITECTURAL

AND ENVIRONMENTAL ENGINEERING

FORENSIC ENGINEERING IN REINFORCED CONCRETE STRUCTURES AND ANALYSIS OF CRACK PROPAGATION: CASE STUDY OF THE NEW ADMINISTRATIVE BUILDING OF THE NATIONAL ADVANCED SCHOOL OF PUBLIC WORKS YAOUNDE

A thesis submitted in partial fulfilment of the requirements for the degree of Master of Engineering (MEng) in Civil Engineering

Curriculum: Structural engineering

Presented by:

TIWA Stanislas

Student number: 15TP20996

Supervised by:

Prof. Carmelo MAJORANA

Co-Supervised by:

Dr. Eng. Guillaume Hervé POH'SIE

Eng. Giuseppe CARDILLO

ACADEMIC YEAR: 2019/2020

MINISTRY OF PUBLIC WORKS

****

MINISTÈRE DES TRAVAUX PUBLICS

****

MINISTRY OF HIGHER EDUCATION

****

MINISTÈRE DE L'ENSEIGNEMENT SUPÉRIEUR

****

Ecole Nationale Supérieure des Travaux Publics

UNIVERSITÀ DEGLI STUDI DI PADOVA

DEPARTMENT OF CIVIL ENGINEERING

DEPARTEMENT DE GENIE CIVIL

DEPARTMENT OF CIVIL, ARCHITECTURAL AND ENVIRONMENTAL ENGINEERING

FORENSIC ENGINEERING IN REINFORCED CONCRETE STRUCTURES AND ANALYSIS OF CRACK PROPAGATION: CASE STUDY OF THE NEW ADMINISTRATIVE BUILDING OF THE NATIONAL ADVANCED SCHOOL OF PUBLIC WORKS YAOUNDE

A thesis submitted in partial fulfilment of the requirements for the degree of Master of Engineering (MEng) in Civil Engineering

Curriculum: Structural engineering

Presented by:

TIWA Stanislas

Student number: 15TP20996

Supervised by:

Prof. Carmelo MAJORANA

Co-Supervised by:

Dr. Eng. Guillaume Hervé POH'SIE

Eng. Giuseppe CARDILLO

ACADEMIC YEAR: 2019/2020

DEDICATION

To my beloved mother, ***TATIO LONTSI Fabienne.***

ACKNOWLEDGEMENTS

First of all, I thank the Almighty God for giving me the courage, strength and patience to complete this modest work. This thesis is the fruit of the combined efforts of several individuals who contributed either directly or indirectly to its elaboration. It is therefore with gratitude that I address my sincere thanks to:

- The **President of the jury** for the honor of accepting to preside this jury;
- The **Examiner** of this jury for accepting to bring his criticisms and observations to ameliorate this work;
- My supervisors Prof. Eng. **Carmelo MAJORANA,** Dr Eng. **Guillaume Hervé POH'SIE** and Eng. **Giuseppe CARDILLO** for all the guidance, the advices and the patience provided to me during this work;
- The Director of the National Advanced School of Public Works (NASPW) of Yaounde Prof. **NKENG George ELAMBO**, and Prof. **Carmelo MAJORANA** of University of Padua in Italy for all their academic and administrative support during these five years spent at NASPW;
- Prof. **MBESSA Michel**, the head of department of Civil Engineering for his tutoring and valuable advices;
- **All the teaching staff** of NASPW and University of Padua for their good quality teaching and the motivation they developed in us to continue our studies;
- My mother Mrs **TATIO LONTSI Fabienne** for the trust, love, unconditional support, valuable advices and efforts invested in me for the obtaining of this degree;
- My grandparents, uncles and aunts especially the families **TATIO** and **MEGOZE** for the education and financial support during all these years;
- **All my classmates** and my friends of the 6th batch of MEng in the National Advanced School of Public Works especially the group **MATRICE** who were a source of motivation and tenacity;
- Eng. **MASSING Samuel Jonathan** and Eng. **BILE BILE ABESSOLO Davy Marcel** for their support and guidance to achieve the set objectives of this thesis.
- To all people who, from near or far, have given me their heartfelt help in carrying out this work.

GLOSSARY

NOTATIONS AND SYMBOLS

ACI	*American Concrete Institute*
ASCE	*American Society of Civil Engineers*
CAE	*Complete Abaqus Environment*
DCH	*Ductility Class High*
DCL	*Ductility Class Low*
DMRF	*Ductile Moment Resisting Frame*
EC	*Eurocode*
FE	*Finite Element*
FEA	*Finite Element Analysis*
FEM	*Finite Element Method*
FEMA	*Federal Emergency Agency*
NASPW	*National Advanced School of Public Works*
RC	*Reinforced Concrete*
SMRF	*Special Moment Resisting Frame*
SAP	*Structural Analysis Program*
SLS	*Serviceabilty Limit State*
ULS	*Ultimate Limit State*
A	*Area of the cross section*
A_c	*Area of the concrete cross section*
A_{min}	*Minimum section area*
A_{net}	*Net area of the cross section*
A_s	*Area of the steel reinforcement section*
A_{sw}	*Cross sectional area of the shear reinforcement*
A_{jv}	*Area of vertical shear reinforcement*
A_g	*Gross area of concrete*
A_{st}	*Total are of stirrups*
A_{jh}	*Area of horizontal shear reinforcements*
A_{sh}	*Area of horizontal steel reinforcement*
A_{s1}	*Area of steel at the top of beam section*

A_{s2}	*Area of steel section at the bottom of beam section*
b	*Width of bottom flange of beam*
b_c	*Width of column*
b_w	*Width of the beam*
$C_{min,\mathrm{b}}$	*Minimum cover due to bond requirement*
$C_{min,dur}$	*Minimum cover due to environmental conditions*
C_{min}	*Minimum concrete cover*
d	*Effective depth section*
d_t	*Concrete tensile damage parameter*
d_c	*Concrete compressive damage parameter*
f_{ywd}	*Design yield strength of stirrups*
f_{yv}	*Yield strength of vertical shear reinforcements*
f_v	*Unconfined compressive strength of concrete*
f_h	*Horizontal confinement effect due to steel hoops*
f_{yh}	*Yield stress of horizontal shear reinforcements*
f_h	*Horizontal confinement effect due to steel hoops*
V_{jh}^{Rd}	*Horizontal joint shear capacity*
V_{juh}	*Maximum induced horizontal shear force in the joint*
N_{Ed}	*Design axial compression force*
N_{Ed}	*Tensile axial force inside the element*
$N_{Pl,Rd}$	*Design tension resistance of a steel section*
N_{Rd}	*Minimum area section of the column*
N_{Sd}	*Axial load compute using the recovery area of the column*
$N_{u,Rd}$	*Designed ultimate resistance*
$S_{cl,max}$	*Minimum spacing of the transverse reinforcement*
V_{Ed}	*Acting shear*
V_{Rdc}	*Design shear resistance of the member without shear reinforcement*
c	*Concrete cover*
$s_{l,max}$	*Maximum longitudinal spacing*
$s_{t,max}$	*Maximum transversal spacing*
x	*Neutral Axis Position*

α	*Angle between shear reinforcement and the beam axis perpendicular to the shear force*
α_{cw}	*Coefficient taking account the state of stress in the compression cord*
$\Delta C_{dur,d}$	*Add reduction of minimum cover for use of additional protection*
$\Delta C_{dur,st}$	*Reduction of minimum cover for use of stainless steel*
$\Delta C_{dur,\gamma}$	*Additive safety element*
$\emptyset_{l,min}$	*Minimum diameter of the longitudinal bars*
φ_{ef}	*Effective creep ratio*
γ	*Specific weight*
γ_c	*Partial factor for concrete*
γ_s	*Partial safety factor for steel*
Ψ_E	*Combination coefficient for variable action*
λ	*Slenderness*
λ_{lim}	*Limit value of slenderness*
v	*Poisson's ratio*
ν_1	*Reduction factor for concrete cracked on shear*
ϕ	*Strength reduction factor*
V_j	*Joint horizontal shear force*
v_n	*Nominal joint shear stress*
τ_c	*Shear stress in concrete*

ABSTRACT

The aim of this work was to extend the field of application of FEM to the understanding of cracks pattern in a beam subjected to vertical transverse displacements and why is such a knowledge important for a forensic engineer. A six-storey building was modelled under static load conditions. Horizontal structural, vertical structural and foundation elements were designed according to Eurocode. Next, the reinforced concrete beam was analyzed to failure using ABAQUS/CAE. To conveniently simulate the nonlinear behaviour of concrete material, the Concrete Damage Plasticity model (CDP) was applied to the numerical model. A displacement based control method was used, with an imposed displacement of 30mm to be applied incrementally in 1 second on the beam to trace out the crack pattern from its initiation to complete beam failure. Comparison between experimental results and numerical results indicated that the FE model is able to simulate the performance of the RC beam. The results revealed that under vertical displacements of a beam, flexural and diagonal tension cracks appears caused by tensile stresses and compressive cracks also appears caused by compressive stresses. As mid spans displacements increases, flexural cracks extends upward towards the supports while compressive cracks moves downward through the beam section inclined at almost 45^{o}, with the evolution of flexural cracks in terms of speed and magnitude faster than that of compressive cracks. Further displacements leads to the appearance of diagonal tensile cracks also almost inclined at 45^{o}. Cracks due to tension later on appears at the supports and at the beam-column joints. The results obtained can provide the lead information necessary for a structural forensic engineer to discover the actual source of the defect (in this case deflection of the beam) during an investigation. Deflection in the beam causes partition walls and floor finishes to crack, so when cracks on these finishes are noticed, it should serve as a warning that it can be due to beam deflection avoiding any remedial solution which may not be effective.

Keywords: Forensic engineering, Reinforced concrete structures Crack propagation, Finite Element Method.

RESUME

Le but de ce travail était d'étendre le champ d'application de la méthode des éléments finis (MEF) à la compréhension des schémas de fissures dans une poutre soumise à des déplacements transversaux verticaux et pourquoi une telle connaissance est-elle importante pour un ingénieur légiste. Un bâtiment de six étages a été modélisé dans des conditions de charge statique. Les éléments structurels horizontaux, verticaux et de fondations ont été conçus selon l'Eurocode. Ensuite, une poutre en béton armé a été analysée jusqu'à la rupture à l'aide d'ABAQUS/CAE. Pour simuler de manière pratique le comportement non linéaire du béton, la notion << concrete damage plasticity (CDP) >> a été appliqué au modèle numérique. Une méthode de contrôle basée sur le déplacement a été utilisée, avec un déplacement imposé de 30 mm à appliquer progressivement en 1 seconde sur la poutre pour tracer le schéma des fissures depuis son déclenchement jusqu'à la rupture complète de la poutre. La comparaison entre les résultats expérimentaux et les résultats numériques a indiqué que le modèle par éléments finis est capable de simuler les performances de la poutre en béton armé. Les résultats ont révélé que sous les déplacements verticaux d'une poutre, des fissures de flexion et de tension diagonale apparaissent causées par la tension et des fissures de compression apparaissent également causées par la compression. Lorsque les déplacements aux mi- travées augmentent, les fissures de flexion s'étendent vers le haut et vers les supports tandis que les fissures de compression se déplacent vers le bas à travers la section de poutre inclinée à près de 45^{o}, l'évolution des fissures de flexion en termes de vitesse et d'ampleur étant plus rapide que celle des fissures de compression. Plus de déplacements entraînent l'apparition de fissures de tension diagonales également presque inclinées à 45^{o}. Des fissures dues à la tension apparaissent plus tard au niveau des supports et des joints poutre-poteaux. Les résultats obtenus peuvent fournir les informations de plomb nécessaires à un ingénieur légiste pour découvrir la source réelle du défaut (dans ce cas, déflection de la poutre) au cours d'une enquête. La déflection de la poutre provoque la fissuration des cloisons et des finitions de plancher, de sorte que lorsque des fissures sur ces finitions sont remarquées, elles devraient servir d'avertissement que cela peut être dû à la déflection de la poutre, évitant toute solution corrective qui pourrait ne pas être efficace.

Mots clés: Ingénierie légiste, Structures en béton armé, Propagation de fissures, Méthode des éléments finis

LIST OF FIGURES

LIST OF TABLES

TABLE OF CONTENTS

GENERAL INTRODUCTION

Reinforced concrete constructions involves a number of uncertainties and risks, many of them associated with the inherent variability and unknown properties and behaviour of the materials involved. These and other factors may lead to deficiencies in structural performance, to the collapse of parts or the entire structure, and on occasion, to the loss of life. It is therefore inevitable that when a failure occurs, an investigation is carried out which brings about the field of forensic engineering. In the context of structural engineering, forensic engineering is taken to be the application of engineering principles to investigate and determine the causes of deficiencies in structural performance, the collapse of a structure or its inability to perform the services for which it was constructed which generally is accompanied by the appearance of cracks. Notions on crack patterns can provide the lead information necessary for a structural forensic engineer to discover the actual source of the defects (deflection of the beam in the case of this work) during an investigation. Numerical methods are being developed to analyse crack growth in a concrete member and to detect fracture failure at an early stage. More recently, computer-generated simulations have assumed a similar role. FEM softwares such as ANSYS, ABAQUS and DIANA can all be used to simulate flexural behaviour of RC beams

The main objective of this work is to study extend the field of application of FEM to the understanding of crack patterns in a beam subjected to vertical deflection and why is such a knowledge important for a forensic engineer.

In order to achieve this objective, the study is divided in three parts. The first part (Chapter 1) consists of a literature review on reinforced concrete structures, forensic engineering as well as crack propagation. The second part (Chapter 2) presents the methodology of the study, it elaborates on the collection of data, analysis and design procedures used. The third part (Chapter 3) is the application of the detailed methodology outlined in chapter 2 to obtain the results of the analysis. The model presented in this work and the results are conducted by means of the FEA software ABAQUS and calibrated by modelling and analysing a RC frame in which the governing failure mode during simulations under vertical displacements was the flexural failure mode.

CHAPTER 1: LITERATURE REVIEW

Introduction

Failure need not involve a complete or even partial collapse; failure may involve a less catastrophic deficiency or performance problem, such as unacceptable deformation, cracking, water or weather resistance, or other such phenomena. Cracks in reinforced concrete buildings are signs of distress and can be due to different reasons. A structural forensic engineer needs notions about the nature of cracks in order to efficiently carry out investigations to determine their causes. All through this chapter, the aim is to elaborate the concept of reinforced concrete structures in which the components, properties of the components, fields of use and the defects of reinforced concrete are discussed followed by a general nature on forensic engineering and its application in structural engineering. Also, a literature review on the concept of cracks, their classification, their causes in concrete buildings, the danger they may represent will been presented. Finally, a historical background concerning crack patterns experimental and FEM analysis will be presented

1.1. Reinforced concrete

Reinforced concrete is a strong durable building material that can be formed into many varied shapes and sizes. Its utility and versatility are achieved by combining the best features of concrete and steel. When they are combined, steel is able to provide the tensile strength and probably some of the shear strength while the concrete, strong in compression, protects the steel to give durability and fire resistance. The different forms of steel reinforcements can be reinforcing bars, welded wire fabric and various reinforcing fibers (Reinforced concrete design to Eurocode 2 by Bill Mosley, John Bungey and Ray Hulse).

1.1.1. Components of reinforced concrete

The main components of reinforced concrete are concrete and steel.

1.1.1.1. Concrete

Concrete is defined as a mixture of several very different components, some of which are active and the other inert [Georges Dreux and Jean Festa, 1998]. Ordinary concrete is a generic term for a composite building material made up of a mixture of aggregates (sand, gravel) clumped by a binder. The binder can be "hydraulic" because it is taken by hydration. It is called cement and

in this case you get a concrete of cement, or concrete at all. The binder can also be a hydrocarbon also called bitumen, which leads to the manufacture of oil concrete.

(a) Components of concrete

The components of concrete are aggregates, cement, water and admixtures.

(i) Aggregates

Aggregates are a broad category of fine to coarse grained particle materials used in construction, including sand, gravel, crushed stone, slag, recycled concrete and geosynthetic aggregates. This mixture of grains ranges from 0 to 125mm. Aggregates occupy more than 70% of concrete volume and intervene directly on its properties of dried concrete as well as wet (Mbessa, 2000). Their availability in nature and consequently its relatively low cost gives it an advantage both economically and mechanically (Dreux & Festa, 1998). The range of particle sizes in aggregate is illustrated in figure 1.1.

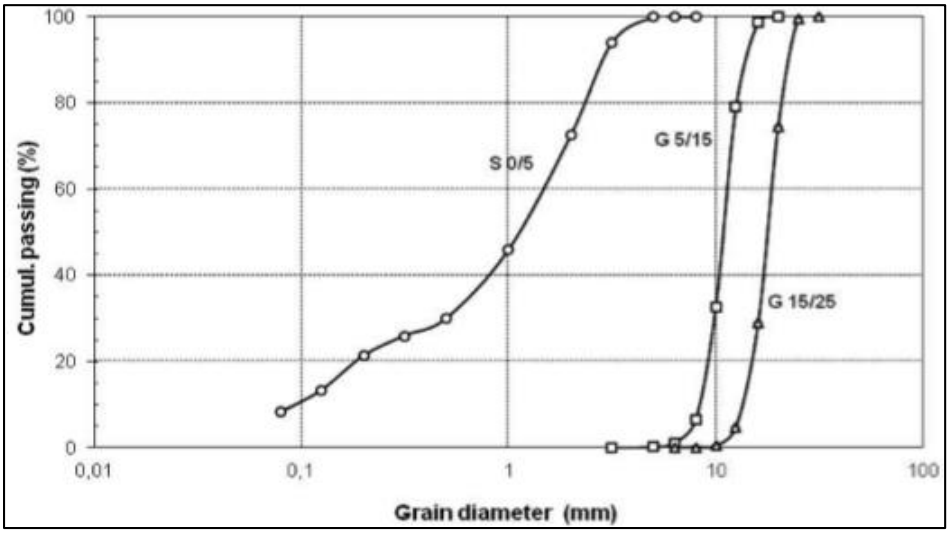

Figure 1.1. Particle size distribution curves of sand and gravel (Makhloufi et al., 2014)

(ii) Cement

Cement is a binder, a substance used for construction that sets, hardens, and adheres to other materials to bind them together. Cement mixed with fine aggregate produces mortar for masonry, or with sand and gravel, produces concrete. The 27 products in the family of common cements, covered by EN 197-1, they are grouped into five main cement types as follows:

- CEM I Portland cement
- CEM II Portland-composite cement

- CEM III Blast-furnace cement
- CEM IV Pozzolanic cement
- CEM V Composite cement

The standard strength of a cement is the compressive strength determined in accordance with EN 196-1 at 28 days of maturation and is shown in table 1.1.

Table 1.1. Classification of common cement types by strength (EN 197-1:2000).

Strength class	Characteristic compressive strength (N/mm2)	Absolute minima (N/mm2)		Characteristic 28-day compressive strength (N/mm2)		Absolute minima (N/mm2)
	2 days	7 days	2/7 days	Minimum	Maximum	28 days
32.5N	-	≥16	≥14	32.5	52.5	≥30.0
32.5R	≥10	-	≥8			
42.5N	≥10	-	≥8	42.5	62.5	≥40.0
42.5R	≥20	-	≥8			
52.5N	≥20	-	≥18	52.5	-	≥50.0
52.5R	≥30	-	≥28		-	

Where N: Normal (subclass; indicates the rate of early strength development)

R: Rapid

(iii) Water

Water is essential for concrete manufacturing. It is added when mixing to moisturize the cement and allows the concrete constituents to be bonded together. The water also makes the mixture much more workable, making it easier to apply the concrete. The characteristics of water are standardized by the 2003 NF EN 1008 standard, which specifies the criteria used to define water quality and the limited values to be met depending on the type of concrete to be made. To be suitable for making concrete, water must not contain compounds that are likely to chemically attack cement, aggregates or frames, or suspended particles whose quantity could alter its original

qualities. Water plays a triple role in making concrete, which is to wet the surface of the aggregates so that the cement paste can adhere to them, to enable the hydration of the cement powder and to favour the placement of concrete (Mbessa Michel, 2000).

(iv) Admixtures

Admixtures are those ingredients in concrete other than cement, water, and aggregates that are added to the mixture immediately before or during mixing (Kosmatka et al., 2003). The amount of admixture recommended by the manufacturer or the optimum amount determined by laboratory tests should be used. Admixtures can be classified into air-entraining and water-reducing admixtures, plasticizers, accelerating and retarding admixtures and many others.

(b) Properties of the concrete

The different properties of concrete are strength, durability and stress-strain relation.

(i) Strength

Among all the characteristics of the material, the most common factor used to measure concrete quality is its compressive strength. It is the fundamental parameter, which allows identifying the concrete class of resistance.

It is defined, in accordance with EN 206-1, by the characteristic value f_{ck} (5% fractile of distribution) obtained through the elaboration of compression tests executed at 28 days on cylindrical specimens of diameter 150mm and height 300mm as show in figure 1.2. It can also be defined by another characteristic value $f_{ck,cube}$ obtained from a cubic specimen.

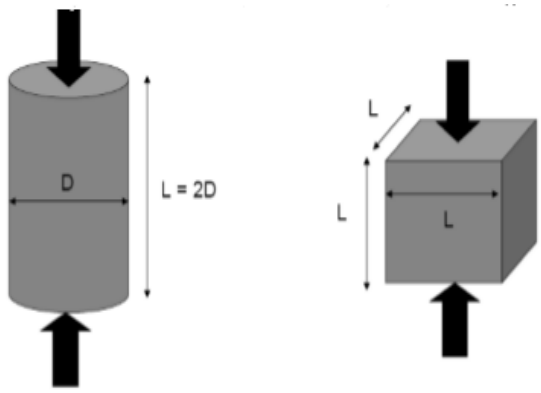

Figure 1.2. Cylinder and cubic specimens in compressive strength evaluation (EN 1992-1-1:2004)

(ii) Durability

(J. Gonzalez, 2018) defined durability as the conservation of the physical and mechanical characteristics of the structure and the materials with which the structures are constructed. One of the main properties of concrete is its ability to be durable. By (Mosley et al., 2007). The durability of concrete is affected by factors such as:

- The exposure conditions;
- The cement type;
- The concrete cover reinforcement

(iii) Stress- strain relation for nonlinear structural analysis

As the load is applied on concrete, the ratio between stresses and strains is approximately linear at first and the concrete behaves almost as an elastic material with virtually full recovery of displacement if the load is removed. Eventually, the curve is no more linear and the concrete behaves more and more as a plastic material. If the load were removed during the plastic range, the recovery will no longer be complete and a permanent deformation will remain. Stress-strain curve of concrete is a graphical representation of concrete behaviour under load is shown in figure 1.3. It is produced by plotting concrete compress strain at various interval of concrete compressive loading (stress).

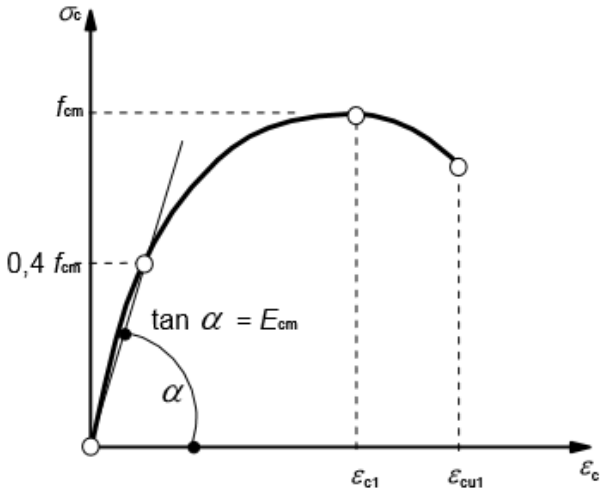

Figure 1.3. Stress Strain Curve for concrete under compression (EN 1992-1-1:2004)

1.1.1.2. Reinforcing steel

Steel reinforcement bar, also known as rebar (reinforcing bar, and reinforcing steel) is a steel bar or mesh of steel wires used as tension device in reinforced concrete and reinforced masonry structures to strengthen and aid the concrete under tension. Concrete (Rafi et al., 2013) is a weak material in tension and cracks when local tensile stresses exceed its tensile strength.

(a) Types of reinforcing steel bars

The two main types are hot-rolled and cold-rolled steel bars.

(i) Hot-rolled steel bars

Here we have mainly two types:

- Smooth raw rolling rounds;
- High adhesion bars with lateral surface equipped with regularly spaced oblique ribs (HA bars).

These two types can be made of:

- Natural steel (no mechanical treatment at the exit of the rolling mill);
- Heat-treated natural steel;
- Hardened steel (with mechanical cold treatment).

(ii) Cold-rolled steels bars

Steel with a lateral surface provided with impressions or ribs (HA threads). Welded mesh obtained by assembling bars or wires, smooth or HA, in square or rectangular meshes, with factory electric welding of each crossing point. The properties of these products are defined by EN 100802.

(a)Properties of the reinforcing steel

Reinforcing steel bars have different properties.

(i) Strength

Reinforcing steel must be strong in tension and, at the same time, be ductile enough to be shaped or bent cold. The application rules for design and detailing in Eurocode are valid for a specified yield strength range, f_{yk} = 400 to 600 N/mm^2. The grade of reinforcement steel denotes the specified characteristic yield stress (f_{yk}). The stress-strain diagram for both hot rolled steel and cold worked steel is shown in figure 1.4. The curves exhibit an initial linear elastic portion.

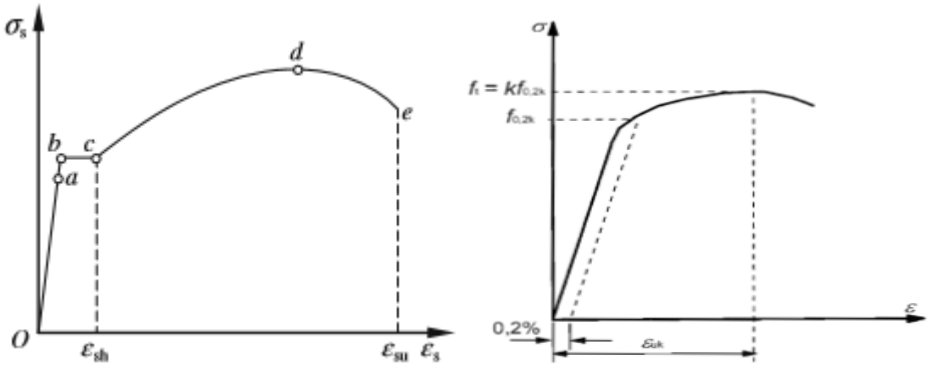

a) Hot rolled steel b) Cold worked steel

Figure 1.4. Stress-strain diagrams for reinforcing steel (EN 1992-1-1:2004)

(ii) Ductility

Designing structures to remain elastic in large earthquakes is likely to be uneconomic as the force demands will be very large. A more economical design can be achieved by accepting some level of damage short of complete collapse and making use of the ductility of the structure to reduce the force demands to acceptable levels. Ductility is defined as the ability of a structure or member to withstand large deformations beyond its yield point without fracture and can be expressed in terms of the maximum imposed deformation. Ductility characterizes the deformation capacity of members after yielding, or their ability to dissipate energy. Yielding of a structure also has the effect of limiting the peak force that it must sustain. Figure 1.5 shows the ductility and behaviour factor of a system.

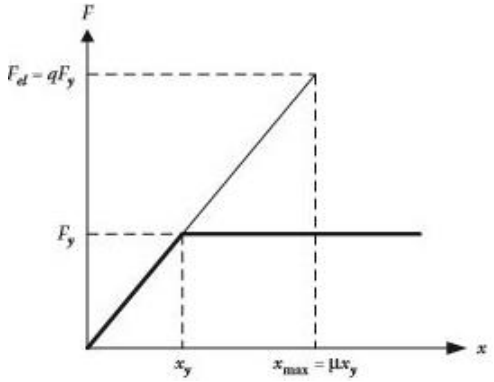

Figure 1.5. Equivalence of ductility and behaviour factor with equal elastic and inelastic displacements (Ahmed Y., 2016)

The reinforcement shall have adequate ductility as defined by the ratio of tensile strength to yield stress (f_t/f_{yk}) and elongation (ε_{uk}) at maximum force. With reference to the ultimate strain of the material, three ductility classes are distinguished:

- Class A (Low ductility) with $\varepsilon_{uk} \geq 2.5\%$ $f_t/f_{yk} \geq 1.05$
- Class B (Normal ductility) with $\varepsilon_{uk} \geq 5.0\%$ $f_t/f_{yk} \geq 1.08$
- Class C (High ductility) with $\varepsilon_{uk} \geq 7.5\%$ $f_t/f_{yk} \geq 1.15$ =7,5

1.1.2. Field of use of reinforced concrete

CIM BÉTON experts in one of their technical sheets entitled " Les bétons: formulation, fabrication et mise en œuvre " divided the use of concrete into two major areas of construction which are buildings and public works.

1.1.2.1. Buildings

Concrete plays an essential role in modern urban planning. This seems normal when considering its use in the construction of dwellings (for the construction of walls, structural elements and for floors, concrete is practically the ideal material). Concrete has also been heavily established in the construction of other buildings such as offices, hospitals, premises, as well as large public buildings and industrial buildings.

1.1.2.2. Public works

In the domain of public works, concrete is widely used.

(a) Bridges

Technological advances and, in particular, the evolution of concrete characteristics, allow ranges of up to several hundred meters to be achieved.

(b) Tunnels

For large tunnels whose examples are multiplying in the world, concrete is either poured on site or used as prefabricated. These are laid to the advancement of the tunneling machine.

(c) Dams

Large dams are most often made of concrete, allowing settlements in the most difficult sites.

(d) Roads

Concrete pavement is becoming increasingly important in major road and motorway roads, thanks to the development of modern techniques such as continuous reinforced concrete, thick slabs, surface treatment, low-traffic roads and urban developments show a renewed interest in concrete solutions, which ensure them durability and low maintenance costs.

(e) Other works

It is also important to mention unusual structures: offshore structures or nuclear power plants, whose requirements require concretes with high mechanical characteristics and durability.

1.1.3. Defects of reinforced concrete

Like any other material, concrete is subjected to chemical attack by an aggressive environment or suffers some physical damage. Alkali aggregate reaction, cracking, spalling and honeycombing due to poor-quality materials or workmanship, and/or corrosion of the reinforcement are some signs of distress that indicate a concrete of low durability (figure 1.6). (L. H. Son et al., Building Maintenance Technology, 1993)

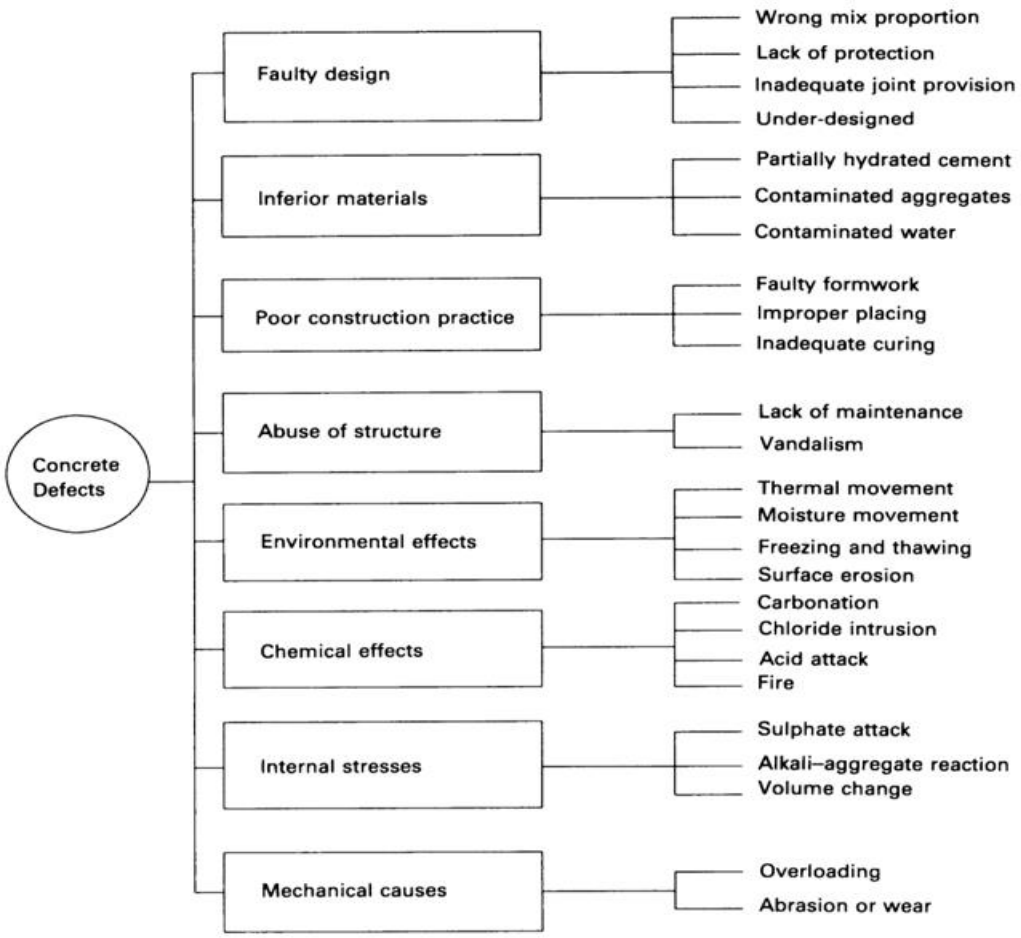

Figure 1.6. Factors affecting concrete durability (L. H. Son et al., 1993)

1.2. Forensic engineering

The role of the forensic engineer may be that of an investigator of the causes of the failure, or it may extend into litigation support and testimony in legal proceeding. Forensic engineers are also involved in devising repairs or mitigating consequences of failures.

Specter (1987) defines forensic engineering as "the art and science of professional practice of those qualified to serve as engineering experts in matters before courts of law or in arbitration proceedings".

Similarly, Noon (2001) defines forensic engineering as "the application of engineering principles, knowledge, skills, and methodologies to answer questions of fact that may have legal ramifications".

In line with Noon (2001) and Carper (2000) as stated by Brown (2006), in the context of structural engineering, forensic engineering is the application of engineering principles to investigate and determine the causes of deficiencies in structural performance, the collapse of a structure or its inability to perform the services for which it was constructed.

1.2.1. General goals of forensic structural engineering investigation

In 2014, according to Azlan Ab. Rahman, the main goals of forensic engineering investigation are:

- To determine the causes of failures (most commonly desired information);
- To compare statements by witnesses or injured parties with physical evidence;
- To ascertain whether an illegal or an improper activity was causative;
- To assess damage to materials, products or structures and evaluate repair estimate.

1.2.2. General nature of forensic engineering

Initially, only the end result of an investigation is known. From this starting point, the forensic engineer gathers evidence to "reverse engineer" how the failure occurred. Like a good journalist, a forensic engineer endeavors to determine who, what, where, when, why, and how.

When a particular failure has been explained, it is said that the failure has been "reconstructed." Because of this, forensic engineers are also sometimes called reconstruction experts. Forensic engineering is similar to failure analysis and root cause analysis with respect to the science and engineering methodologies employed. Often the terms are used interchangeably. A typical forensic engineering investigation is shown in figure 1.7.

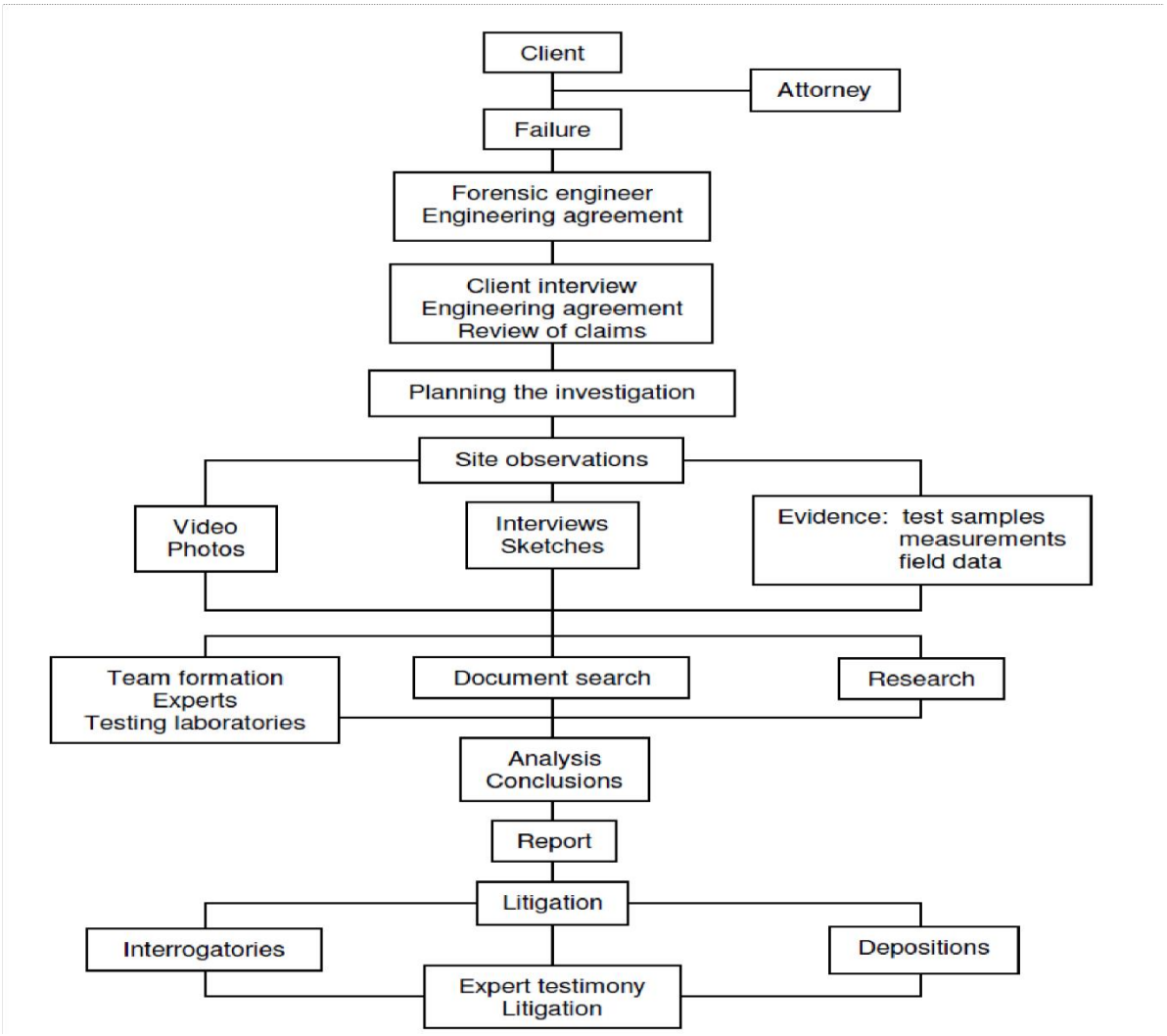

Figure 1.7. Flow chart of a typical forensic engineering investigation (Greenspan et al., 1989).

1.2.3. Competencies and qualifications of forensic structural engineers

Investigation, evaluation, and litigation involving highly complicated topics have led to the need for experts with specialized technical knowledge who can skillfully explain that knowledge and effectively offer relevant opinions. It is therefore important to understand what competencies a forensic engineer and an engineer expert witness could have, and what abilities may be worthwhile for a forensic engineer and an engineer expert witness to possess. These competencies according to Azlan Ab. Rahman (2014) are:

- Familiarity with building codes, specifications and industry standards;

- Understanding of structural and soil behavior to know how structures behave and why they fail;
- Ability to collect and analyze data (detective skills), develop failure hypothesis and reach to correct conclusions regarding the causes of the failure;
- Having some knowledge of legal procedures;
- Good oral and written communication skills;
- Have high ethical standards.

1.3. Cracks propagation

A crack is a linear fracture in concrete which extends partly or completely through the member. Cracks in concrete occur as a result of tensile stresses introduced in the concrete. Tensile stresses are initially carried by the concrete and reinforcement until the level of the tensile stresses exceeds the tensile capacity (modulus of rupture) of the concrete. After this point the concrete cracks and the tensile force is transferred completely to the steel reinforcement. (K.Ohno, in Acoustic Emission and Related Non-Destructive Evaluation Techniques in the Fracture Mechanics of Concrete, 2015).

1.3.1. Causes of cracks in reinforced concrete structures

Building cracks are the most common type of problem in any type of buildings. So, it is important to understand the causes. The main causes of cracking according to (Thaguna, 2015) :

1.3.1.1. Permeability of concrete

As deterioration process begins with penetration of various aggressive agent, low permeability is the key to its durability. Concrete durability is controlled by factors like water-cement ratio, degree of hydration/curing, air voids due to deficient compaction, micro-cracks due to loading and cyclic exposure to thermal variations. The permeability of concrete is a direct function of the porosity and the interconnection of pores of the cement paste.

1.3.1.2. Thermal movement

Thermal movement is one of the most potent causes of cracking in concrete. All materials more or less expand on heating and contract on cooling. The thermal movement in a component depends on a number of factors such as temperature variations, dimensions, coefficient of thermal expansion of brickwork in the vertical direction is fifty percent greater than that in horizontal

direction because there is no restraint to movement in the vertical direction. Thermal variation in the internal walls and intermediate floors are not much and thus do not cause cracking. It is mainly the external walls especially thin walls exposed to direct solar radiation and the roof which are subjected to substantial thermal variation that are liable to cracking.

1.3.1.3. Corrosion of reinforcement

A properly designed and constructed concrete is initially water-tight and the reinforcement steel within it is well protected by a physical barrier of concrete cover which has low permeability and high density. Concrete also gives steel within it a chemical protection. Steel will not corrode as long as the concrete around it is impervious and does not allow moisture or chlorides to penetrate within the cover area. Steel corrosion will also not occur as long as concrete surrounding it is alkaline in nature having a high pH value. Notwithstanding it there are large number of cases in which corrosion of reinforcement has caused damage to concrete structures within a few years from the time of construction resulting in loss of mass, stiffness and bond in concrete and therefore repair becomes inevitable as considerable of strength takes place.

1.3.1.4. Moisture movement

The common cause of cracking in concrete is shrinkage due to drying. This type of shrinkage is caused by the loss of moisture from the cement paste constituent, which can shrink by as much as 1 percent per unit length. These moisture-induced volume changes are a characteristic of concrete. If the shrinkage of the concrete could take place without any restraint, concrete will not crack. It is the combination of shrinkage and restraint, which is provided by another part of the structure or by the subgrade that causes tensile stresses to develop. When the tensile stresses of the concrete are exceeded, the concrete will crack. Cracks may propagate at much lower stresses than are required to cause crack initiation. Most of the building materials with pores in their structure in the form of intermolecular space expand on absorbing moisture and shrink on drying. These movement are cyclic in nature and are caused by increase or decrease in inter pore pressure with moisture changes. Initial shrinkage occurs in all building materials that are cement/lime based such as concrete, mortar, masonry and plasters. Generally heavy aggregate concrete shows less shrinkage than light weight aggregate.

1.3.1.5. Creep

Concrete when subjected to sustained loading exhibits a gradual and slow time dependent deformation known as creep. Creep increases with increase in cement and water content, water cement ratio and temperature. It decreases with increase in humidity of surrounding atmosphere and age of material at the time loading. Use of admixtures in concrete increases creep.

1.3.1.6. Poor construction practices

The construction industry has fallen prey to non-technical persons most of whom have little or no knowledge of correct construction practices. Some of the main causes for poor construction practices and inadequate quality of building are: improper selection of materials; selection of poor-quality cheap materials; Inadequate and improper proportioning of mix constituents of concrete, mortar, etc.; Inadequate control on various step of concrete production such as batching, mixing, transporting, placing, finishing and curing; Inadequate quality control and supervision causing large voids and cracks resulting in leakages and ultimately causing faster deterioration of concrete; Improper construction joints between subsequent concrete pours or between concrete framework and masonry; Addition of excess water in concrete and water mixes

1.3.1.7. Poor maintenance

A structure needs to be maintained after a lapse of certain period from its construction completion. Some structures may need a very early look into their deterioration problem, while others can sustain themselves very well for many years depending on the quality of design and construction. But early identification of probable problems and correcting them within time is wise idea rather.

1.3.1.8. Movement due to chemical reactions

The concrete may crack as a result of expansive reactions between aggregate containing active silica and alkali derived from cement hydration. The alkali silica reaction results in the formation of swelling gel, which tends to draw water from other portions of concrete. This cause local expansion results in cracks structure.

1.3.1.9. Foundation settlement

The place where concrete generally subsides is near a house. Whether the home is built on a crawlspace or a basement, the over-dig is subsequently backfilled. Unless the backfill material is

compacted in lifts as the over-dig is filled, it will settle over the time. This settling will cause any concrete poured atop at it to settle along with it. The other reasons for foundation settle are change in moisture content of soil below or around the foundation, or overload of superstructure and decay of organic matters present in subsoil. Uniform settlement up to some tolerance does not cause the problem but differential settlement is something that result in severe crack problem.

1.3.2. Dangers represented by cracks

Cracks resulting from material shrinkage due to changes in the weather, especially when the construction materials are still green, are in the group of simple cracks. These cracks are commonly referred to as “hair” or “aesthetic” cracks. They do not cause serious damage to the structure or component where they appear. However, cracks resulting from excessive movement of the supporting soil, vibrations within or around the structure, deflections of supporting members, and change in use require careful site inspection.

The diagonal cracks appearing close to the end support of beams are an indication of shear failure; cracks at the bottom face of slabs or beams suggests deflection problem at mid span; the longitudinal cracks appearing on columns indicates buckling of column under excessive load or under reinforcement (Grew 1996, Kaklauskas et al. 1999, Johnson 2002, and Pryke 2007)

In elements subjected to high bending moments (beams for example), overloading generally results in an excessive deflection of the element causing different types of cracks to appear. Excessive beam deflection can also have some adverse effects on the building.

- Residents would be alarmed to see a deflected beam in their home. Even if it is structurally still able of carrying load.
- If a beam is deflected, the slab which it supports also gets deflected. As a result, the floor may not be perfectly horizontal. Due to that brittle finishes like ceramic tiles and pipe ducts would crack, water may stagnate in that low lying area, wheelers move automatically if placed, etc. So problems may arise for users.
- If the wall or floor is supported by a deflected beam, cracks could develop and frames for windows and doors wouldn’t fit correctly in their openings.

1.3.3. Classification of cracks on RC beams

There are: flexural cracks, shear cracks, torsion cracks, corrosion cracks, shrinkage cracks and sliding cracks.

1.3.3.1. Flexural cracks in reinforced concrete beams

Cracking in reinforced concrete beams subjected to bending usually starts in the tensile zone i.e. lower part of the beam. Originates in maximum moment region and varies as per support conditions of beam. It may be single or in groups with its maximum width at bottom/top of beam. It is caused by inadequate flexural capacity of the beam, insufficient cross section of the beam or main reinforcement (it is loaded more than defined loads). Figure 1.8 shows flexural cracks inside RC beams.

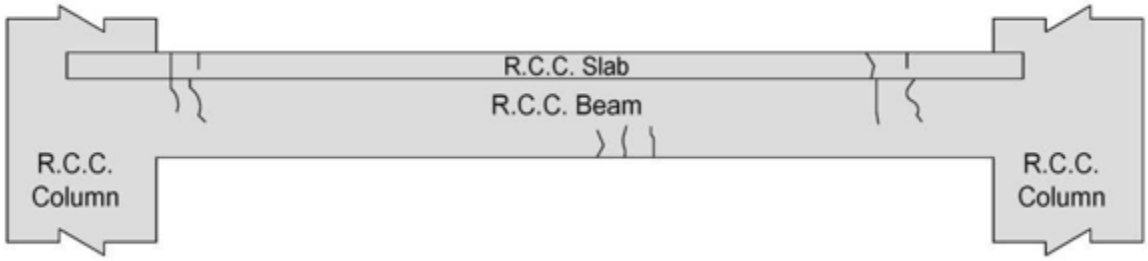

Figure 1.8. Flexural cracks in RC beams (Jaydutt Tailor, 2017).

1.3.3.2. Shear cracks in reinforced concrete beams

Shear cracks in RC beams occur in hardened stage and it is usually caused by structural (self-weight) loading or movement. These types of cracks are better illustrated as diagonal tension cracks due to combined effects of flexural (bending) and shearing action. It originates nearer to supports and maybe single or in groups. Its maximum width is at neutral axis region or at bottom of beam. It is caused by inadequate shear capacity of the beam and insufficient cross section or torsional reinforcement insufficient. Figure 1.9 shows shear cracks inside RC beams.

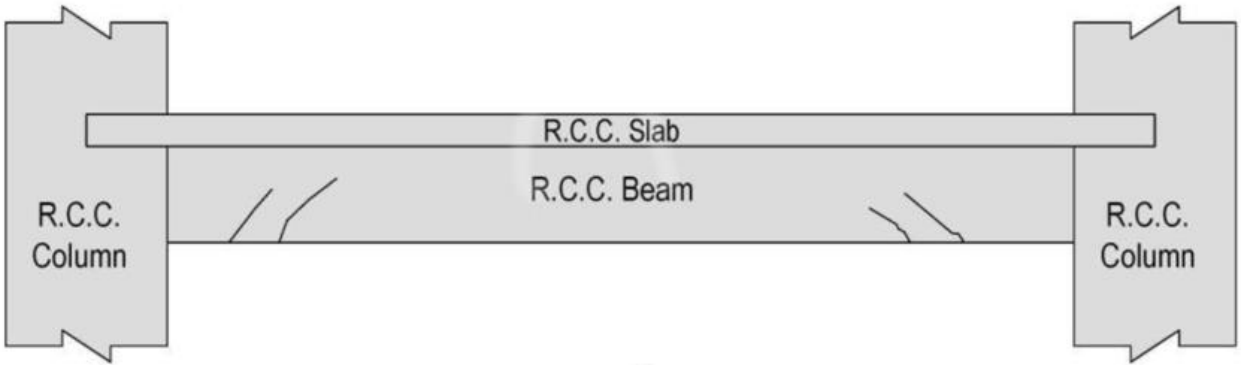

Figure 1.9. Shear cracks in RC beams (Jaydutt Tailor, 2017).

1.3.3.3. Torsional cracks

Usually, beams are subjected to torsion along with bending moment and shear force. Bending moment and shear forces occur as loads act normal to the plane of bending. However, loads away from the bending plane will cause torsional movement. It is caused by inadequate torsional strength of the beam and insufficient cross-section or torsional reinforcement. It originates nearer to maximum torsion region and generally occurs single with uniform width, appearing over the whole periphery in helical form as illustrated in figure 1.10.

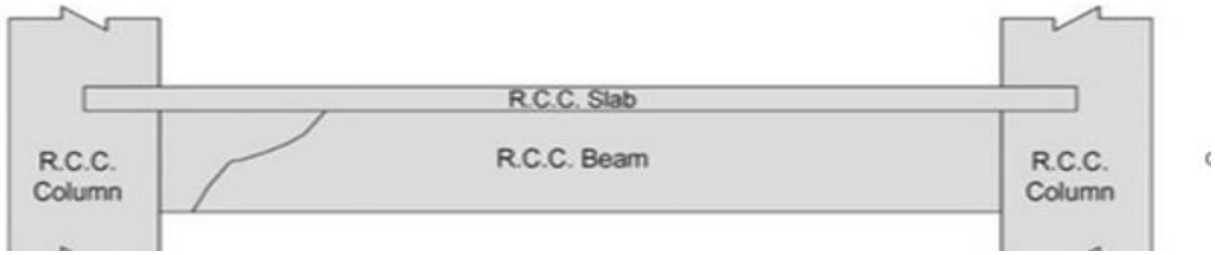

Figure 1.10. Torsional cracks in RC beams (Jaydutt Tailor, 2017).

1.3.3.4. Corrosion cracks

Corrosion cracks in RC beams run along the line of reinforcement. It usually separates the concrete from reinforcing bars. It is mostly manifested by discoloration of paint or stains of rust. It can be caused by unsatisfactory bond between reinforcing bars and concrete or due to corrosion of bars or fire damage. Figure 1.11 shows a RC beam subjected to corrosion cracks.

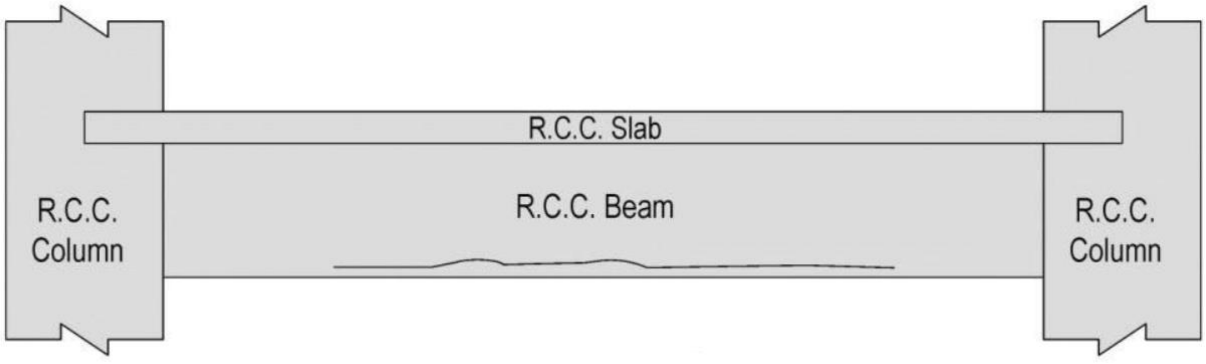

Figure 1.11. Corrosion cracks in RC beams (Jaydutt Tailor, 2017).

1.3.3.5. Shrinkage cracks in RC beams

They occur during two stages, which are pre-hardening stage and hardened stage. In pre-hardening stage, these types of cracks are called as plastic shrinkage cracks and in the hardened

stage they are known as drying shrinkage cracks. Shrinkage cracks occur when fresh concrete is subjected to a very rapid loss of moisture. Figure 1.12 shows clearly how shrinkage cracks develop on RC beam.

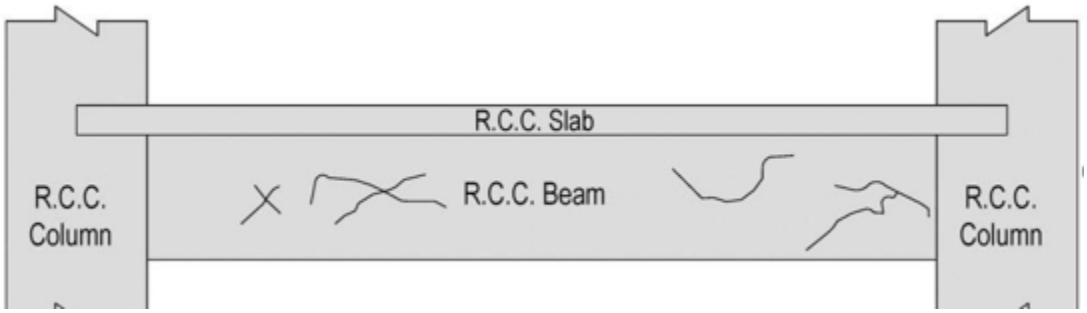

Figure 1.12. . Shrinkage cracks in RC beams (Jaydutt Tailor, 2017).

1.3.3.6. Sliding cracks

The diagonal mode of failure by sliding along the critical cracks is known as a failure by sliding and usually appears vertically at the edge of the supports of the beam. This occurs when concrete in a beam is disturbed at an early age when adequate strength not realized or maybe due to disturbance of formwork at green stage. Figure 1.13 shows sliding cracks in RC beam.

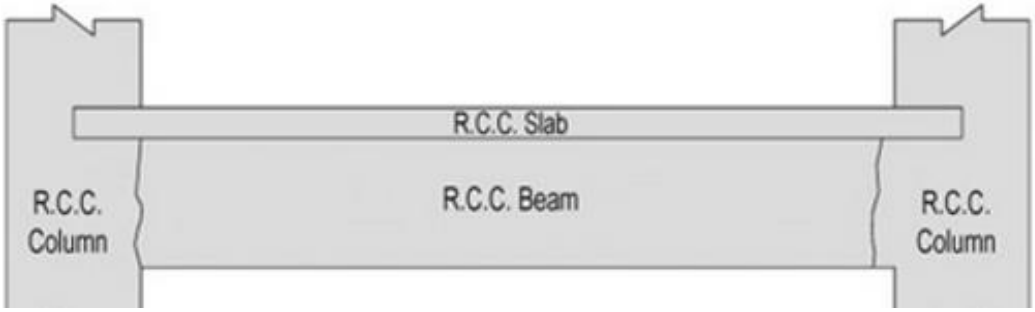

Figure 1.13. Sliding cracks in RC beams (Jaydutt Tailor, 2017).

1.3.4. Historical background on crack analysis of concrete structures

Experimental based testing has been widely used as a means to analyse individual elements and the effects of concrete strength under loading. While this is a method that produces real life response, it is extremely time consuming, and the use of materials can be quite costly. The use of finite element analysis to study these components has increased due to progressing knowledge and capabilities of computer software and hardware. It has now become the choice method to analyse

concrete structural components. The use of computer software to model these elements is much faster, and extremely cost-effective

1.3.4.1. Crack analysis using experiment-based testing of concrete

Here, 02 experiment-based testing of concrete have been studied.

(a) Buckhouse (1997)

Buckhouse (1997) studied external flexural reinforcement of existing concrete beams. The study included experimental testing of control beams that can be used for calibration of finite element models. Three concrete control beams were cast with flexural and shear reinforcing steel. Shear reinforcement was placed in each beam to force a flexural failure mechanism. All three beams were loaded with transverse point loads at third points along the beams. Data acquisition equipment was used to record applied loading, beam deflection at the mid span, and strain in the internal flexural reinforcement. The beam was loaded to flexural failure (figure 1.14)

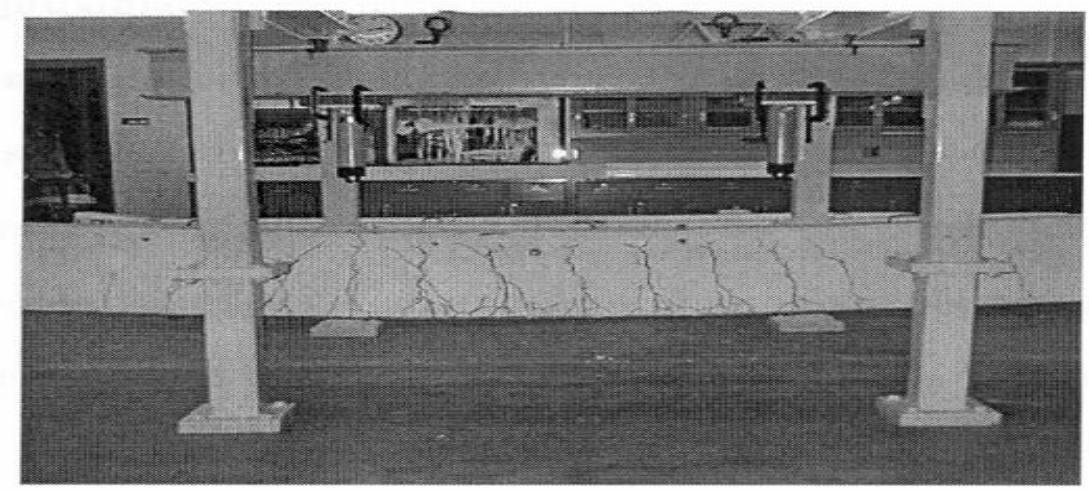

Figure 1.14. Beam failure in flexure (Buckhouse, 1997)

Vertical cracks first formed in the constant moment region, extended upward, and then out towards the constant shear region with eventual crushing of the concrete in the constant moment region. The mode of failure characterized by the beams was compression failure of the concrete in the constant moment region (flexural failure). All failures were ductile, with significant flexural cracking of the concrete in the constant moment region and Load-deflection curves were plotted for each and compared to predicted ultimate loads (figure 1.15).

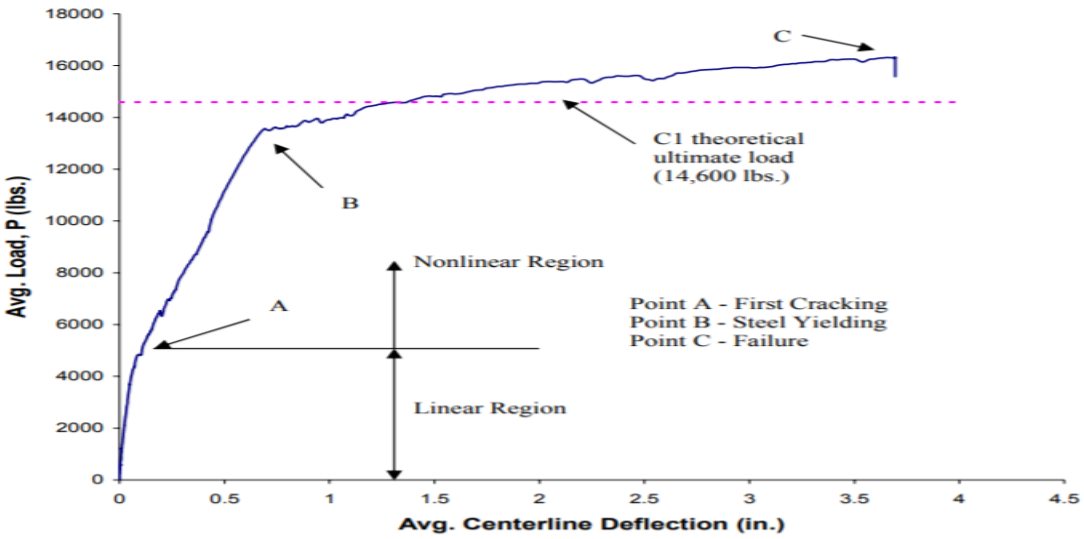

Figure 1.15. Load vs. Deflection Curve for Beam C1 (Buckhouse, 1997)

(b) Leonhardt and Walter (1962)

Leonhardt and Walter (1962) tested several beams to determine the maximum shear stress and the minimum web reinforcement to ensure adequate safety against shear failure. Figure 1.16 shows the crack patterns observed on two of several tested beams.

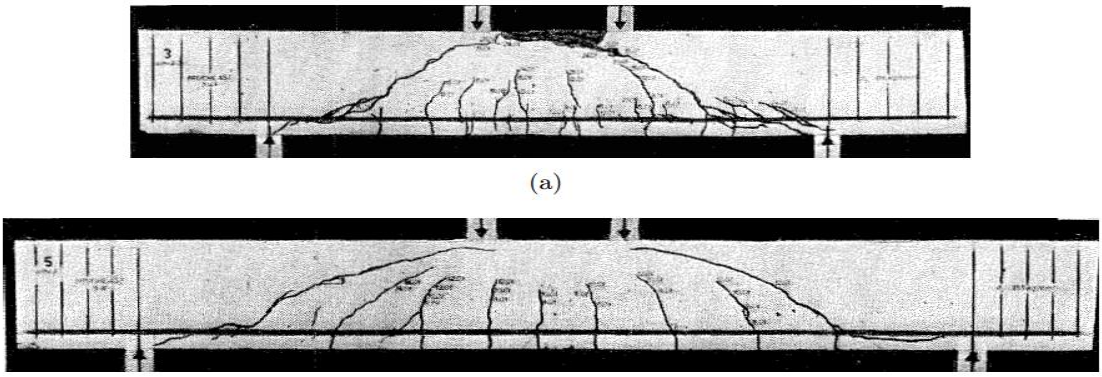

Figure 1.16. Crack patterns observed on beams (Leonhardt and Walter, 1962)

1.3.4.2. Crack analysis using finite element method

Here, 02 finite element method of crack analysis on concrete have been studied.

(a) Kachlakev, (2001)

Kachlakev, et al. (2001) used ANSYS (SAS 2003) to study concrete beam members with externally bonded CFRP fabric. Symmetry allowed one quarter of the beam to be modeled as shown in figure 1.17.

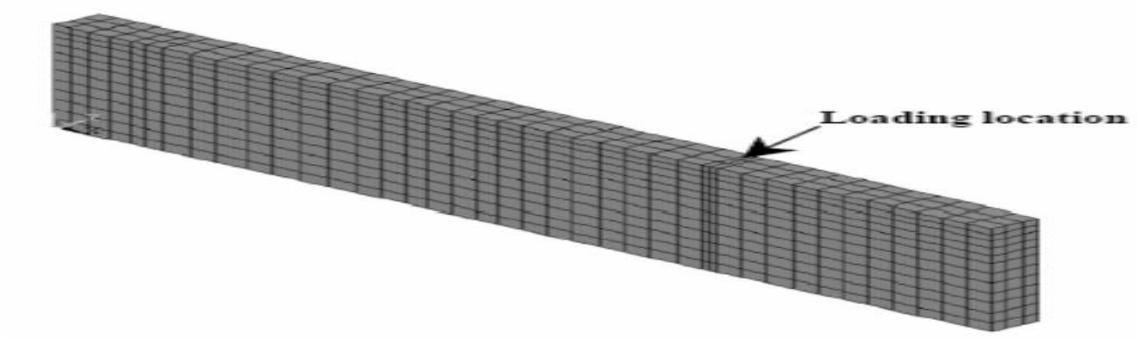

Figure 1.17. FEM Discretization for a Quarter of the Beam (Kachlakev, et al., 2001)

At plane of symmetry, the displacement in the direction perpendicular to the plane was set to zero. A single line support was utilized to allow rotation at the supports. Loads were placed at third points along the full beam on top of steel plates. The mesh was refined immediately beneath the load and no stirrup-type was used. The nonlinear Newton-Raphson approach was utilized to trace the equilibrium path during the load-deformation response. It was found that convergence of solutions for the model was difficult to achieve due to the nonlinear behaviour of reinforced concrete material. At certain stages in the analysis, load step sizes were varied from large (at points of linearity in the response) to small (when instances of cracking and steel yielding occurred). The Load-deflection curve for the non-CFRP reinforced beam that was plotted shows reasonable correlation with experimental data (McCurry and Kachlakev, 2001) as shown in figure 1.18.

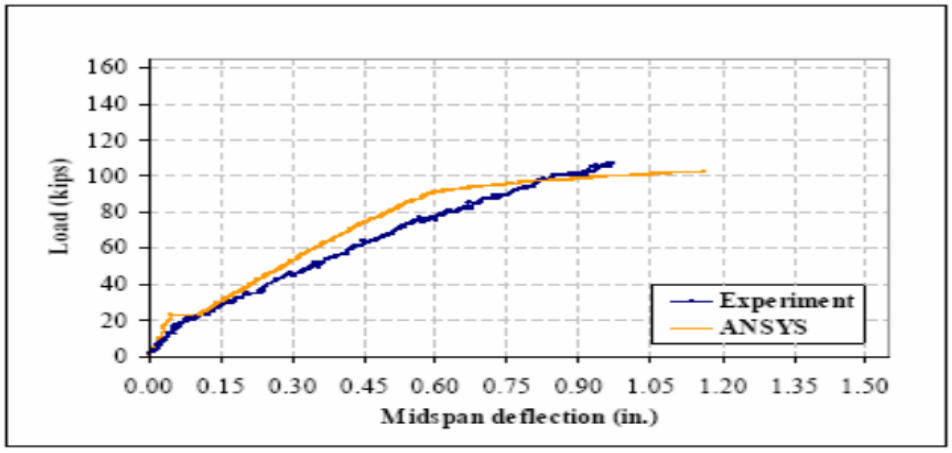

Figure 1.18. Load vs Deflection Plot (Kachlakev, et al., 2001)

The different types of concrete failure that can occur are flexural cracks in figure 1.19a, compression failures in figure 1.19b and diagonal tension cracks in figure 1.19c. Flexural cracks

form vertically up the beam, compression failures are shown as circles and diagonal tension cracks form diagonally up the beam towards the loading that is applied.

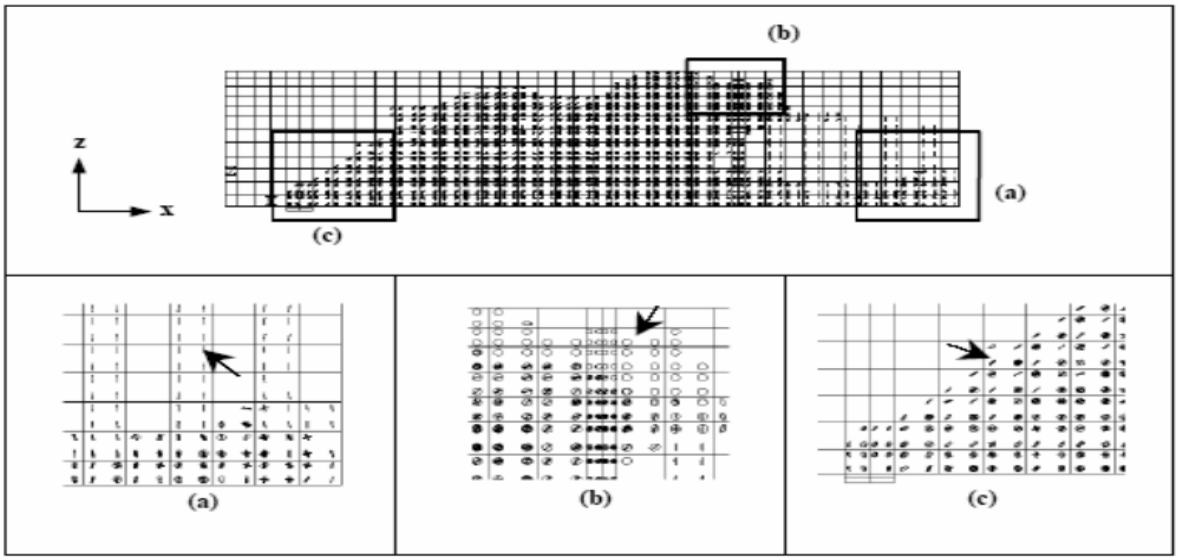

Figure 1.19. Typical Cracking Signs in Finite Element Models: a) Flexural cracks, b) Compressive cracks c) Diagonal Tensile cracks (Kachlakev, et al.2001)

This study indicates that the use of a finite element program to model experimental data is viable and the results that are obtained can indeed model reinforced concrete beam behaviour reasonably well.

(b) Darmansyah Tjitradi, Eliatun Eliatun and Syahril Taufik

Their research was aimed in studying the behaviour of structural elements of single layer reinforced concrete beam under tension, balanced, and compressive collapse mechanisms to be modeled and analyzed using ANSYS software, and compared to manual analysis by code SNI 03-2847-2013. Results obtained from the study was to determine collapse behaviour of the RC beam by the bending capacity, load-deformation relationships, stress-strain relationship of concrete and cracking patterns that occur in every model of the beam. A simple span reinforced concrete beam was modeled with applying ultimate point load until crushing representing the reinforced concrete collapsed mechanism with conditions of under reinforced, balanced reinforced and over-reinforced with dimensions: 200 mm x 400 mm, L = 3000 mm. The load is applied to the middle span beams with concentrated loads, and the observed value of the load, deflection, and the concrete stress that occurred from the first crack load up to fully collapse. The results show that the reinforced concrete

beams can be analyzed using ANSYS software with modified model. The behaviour of reinforced concrete beams can be determined by the analysis of calculation and FEM that beams with tensile collapsed condition has a lower flexural capacity and collapse behaviour is more ductile than that of the beam with the compressive collapse and balanced condition. The observed crack patterns were as shown in figures 1.20 to 1.22.

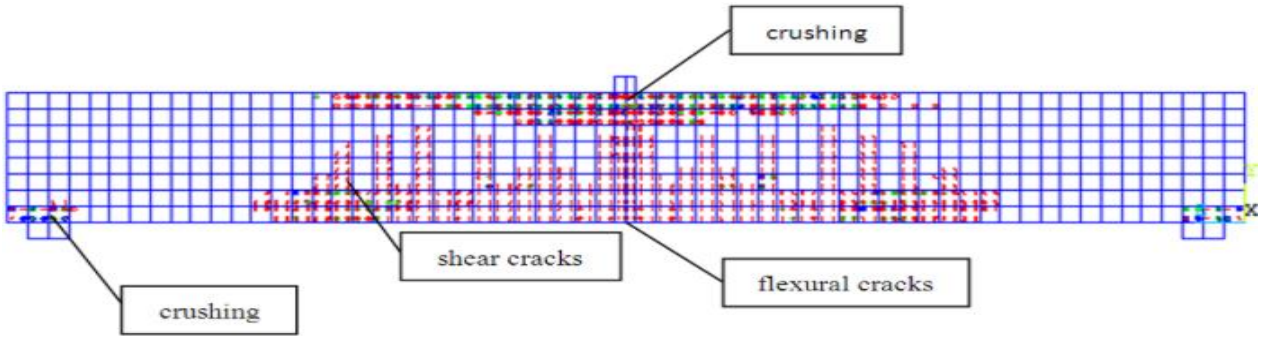

Figure 1.20. Tensile collapse mechanism

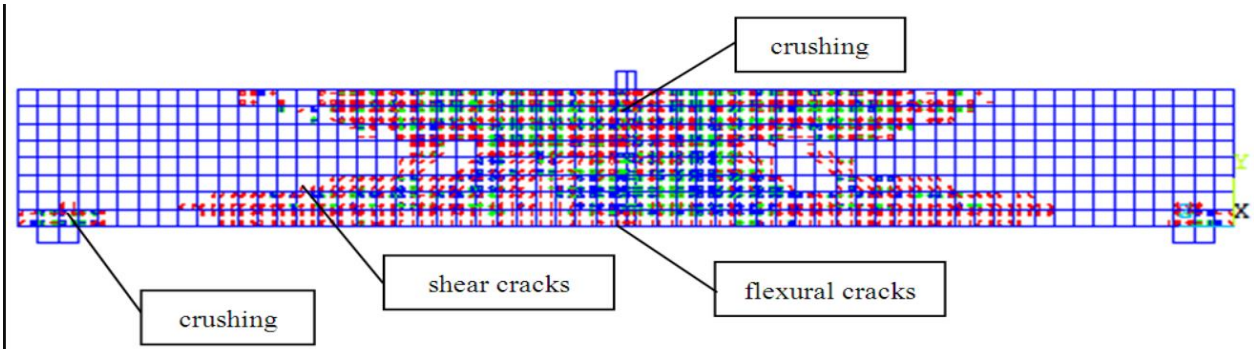

Figure 1.21. Balanced collapse mechanism

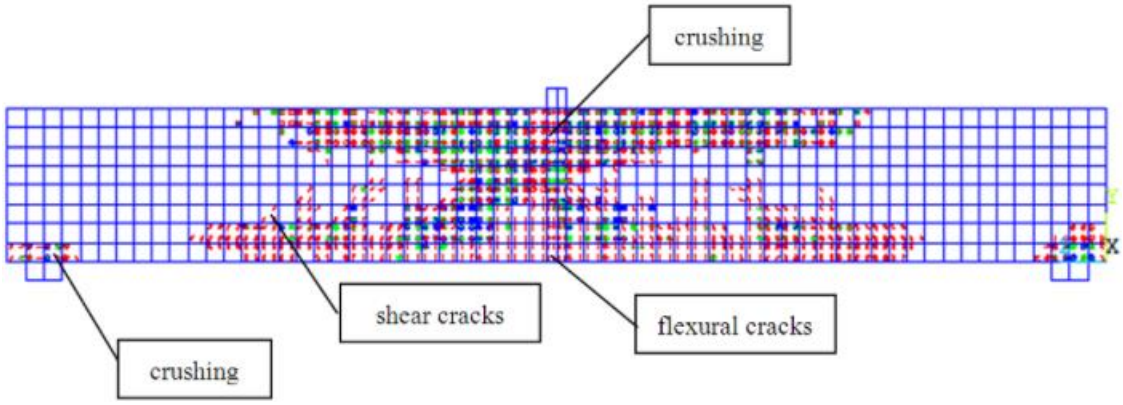

Figure 1.22. Compressive collapse mechanism

The load and the deflection at mid span were illustrated graphically as in figure 1.23.

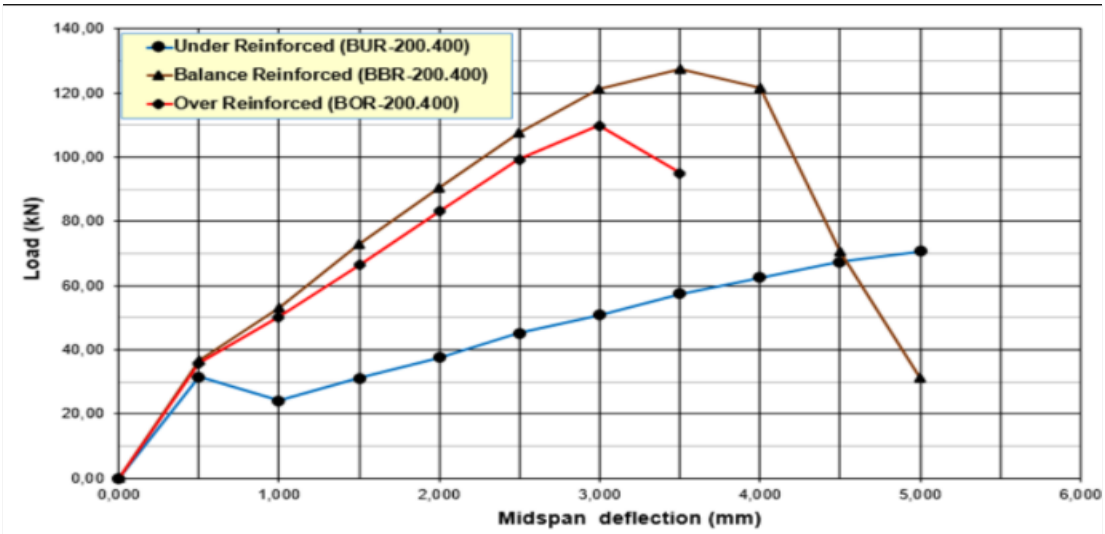

Figure 1.23. FEA Load-Displacement with Various Reinforcement Ratio (Darmansyah Tjitradi, Eliatun Eliatun and Syahril Taufik)

Conclusion

All through this chapter, the aim was to present the concept of reinforced concrete structures in which the components, properties of components, fields of use and the defects of reinforced concrete. It also elaborated the general nature of forensic engineering and its application in structural engineering. A literature review on the concept of cracks, their classification, their causes in concrete buildings, the danger they may represent have been presented. Finally, a historical background concerning crack patterns experimental and FEM analysis were presented. What follows is the methodology in which are found the step by step procedures for the achievement of the set objectives of this work.

CHAPTER 2: METHODOLOGY

Introduction

This chapter is aimed at describing the different constitutive elements of our research. In this work, the first step consists in a site recognition through a documentary research followed by a site visit and the data collection. Then, the linear static design procedure for elements such as beam, column and footings will be presented. Also, for the non-linear finite element analysis of the cracks patterns in a reinforced concrete beam, a brief description of the software used and the concrete damaged plasticity concept are discussed alongside procedures for the modelling of a 3D finite element capable of appropriately representing the concrete stress-strain behaviour, tensile cracking and compressive damage of concrete and indirect modelling of steel-concrete bond.

2.1. General recognition of the site

The site recognition will be carried out from a documentary research whose essential goal is to know the physical parameters and socio-economic parameters of the site.

2.2. Site visit

The purpose of this activity is the building description results from the observation and the presentation of the use category, the floor plans and elevation configuration.

2.3. Data collection

The data collected are the geometrical data and the data concerning the different properties of the materials used on the site.

2.3.1. Geometrical data

These data will be taken from different architectural plans available where we can identify the geometrical dimensions and positions of structural elements (beams and columns). They are collected using AutoCAD software.

2.3.2. Characteristics of materials

This is the data that characterises the materials that were used for the implementation of the structure. Knowing the material properties will help to obtain the resisting forces and moments. The material properties will be divided in two parts, one for the steel members, and the other for the concrete used.

2.4. Linear static design methodology

Static analysis studies the behaviour of the structure under static loads application. The analysis starts with the modelling of the structural members. In that line, the concrete cover, the design and verification of one horizontal (beam), one vertical (column) and foundation structural elements, both considered as representative of the other elements of their respective types. The design code used in this work is the European code (Eurocodes), recommended by the European Committee for standardization. The various parts made use of in this study are: Eurocode 0 (Basis of structural design), Eurocode 1 (Actions on structures), Eurocode 2 (Design of concrete structures), Eurocode 7 (Geotechnical design).

2.4.1. Actions on buildings

A structure can be subjected to a variety of actions and at the same time. The type of actions applied to the chosen structure will be permanent actions and variable actions (imposed loads).

2.4.1.1. Permanent actions

These are actions acting during the whole nominal life of the structure with negligible time variation of their intensity (that can be considered as constant in time):

- Self-weight of structural elements (G1); self-weight of the soil, if present; forces due to the soil (excluding the effects of the service loads applied to the soil); forces due to water pressure (when they are constant in time);
- Self-weight of non-structural elements (G2); imposed displacements and deformations determined by the designer and realized in-situ;
- Prestressing
- shrinkage and creep
- differential displacements

Permanent action or load consist essentially of the weight of the element, whether structural or not. Provisions for the evaluation of the self-weight of these elements are given in Eurocode 1.

2.4.1.2. Variable actions

Variable actions are those which, as the name goes, vary with respect to time. They consist of actions on the structure (or on the structural element) with instantaneous values which can be significantly different in time: That is, their magnitude is time dependent.

- with long duration: acting with a significant intensity, also if non-continuously, for a not negligible time compared to the nominal life of the structure;
- with brief duration: acting with brief duration compared to the nominal life of the structure;

This variation is non-negligible and monotonic. Variable loads fall under two main kinds; imposed loads and seismic-induced loads.

2.4.2. Combination of actions

A combination of actions, as the name indicates, consist of a set of load values applied to the structure simultaneously to verify its structural reliability for a given limit state (design limit states). They are defined as follows, when designing a building.

2.4.2.1. Fundamental combination

Equation 2.1 is the fundamental load combination at Ultimate Limit State (ULS) design situation, where the coefficients $\gamma_{G,j}$ and $\gamma_{Q,i}$ are partials factors or again safety coefficients, which minimize the action which tends to reduce the solicitations and maximize the one which tends to increase it.

$$\sum_{i\geq 1} \gamma_{G,j} G_{k,j} + \gamma_{Q,1} Q_{k,1} + \sum_{i>1} \gamma_{Q,i} \Psi_{0,i} Q_{k,i} \qquad \text{(Eq. 2.1)}$$

The values of these partial factors recommended by the Eurocode 0 for the verifications are:

- $\gamma_{G,} = 1.35$
- $\gamma_{G,} = 1$
- $\gamma_{Q,1} = 1.50$ Where unfavorable (0 where favorable)
- $\gamma_{Q,} = 1.50$ Where unfavorable (0 where favorable)

2.4.2.2. The rare combination

This is the load combination for non-reversible serviceability limit state (SLS) for the verifications with allowable stress method. Equation 2.2 is the fundamental load combination at this serviceability limit state (SLS)

$$\sum_{j\geq 1} G_{k,j} + Q_{k,1} + \sum_{i\geq 1} \Psi_{0,i} Q_{k,i} \qquad \text{(Eq. 2.2)}$$

2.4.3. Concrete cover

Concrete cover is most importantly a measure to protect structural reinforcements against environmental actions (table A1 of the annex). The durability of a structure depends on how long the later can be protected from external factors like environmental actions and others but also the capacity of the structure to perform its function throughout its working life without severe damage. Concrete cover is defined in Eurocode 2 as the distance between the surface of the reinforcement closest to the nearest concrete surface and the nearest concrete surface (figure 2.1). The nominal cover is defined as, according to EN 1992-1-1_E_2004, a minimum cover, C_{min}, plus an allowance in design for deviation, ΔC_{dev} (equation 2.3).

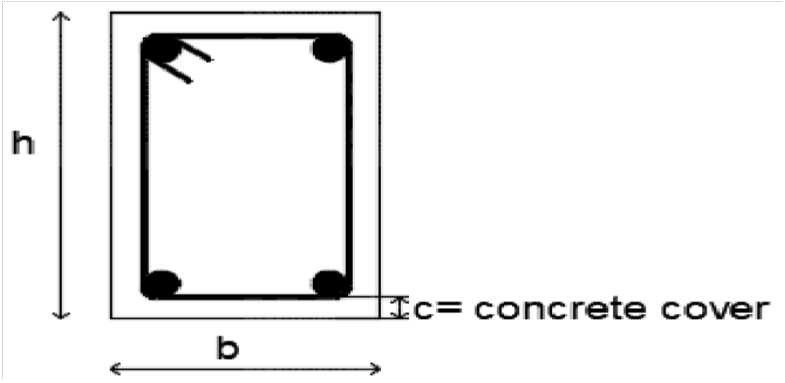

Figure 2.1. Concrete cover representation

$$C_{nom} = C_{min} + \Delta C_{dev} \qquad \text{(Eq. 2.3)}$$

With:

- ΔC is the allowance in design for deviation with a recommended value of 10 mm
- C_{min} is the minimum concrete cover

The minimum concrete cover is computed as shown in equation 2.4.

$$C_{min} = max(C_{min,b}; C_{min,dur} + \Delta C_{dur,\gamma} - \Delta C_{dur,st} - \Delta C_{dur,add}; 10mm) \qquad \text{(Eq. 2.4)}$$

Where:

- $C_{min,}$ is the minimum cover due to bond requirement, equal to the diameter of the bars or the equivalent diameter in the case of bundled bars
- ΔC_{dur} is the additive safety element with a recommended value of 0 mm
- $\Delta C_{dur,}$ is the reduction of minimum cover for use of stainless steel
- $\Delta C_{dur\ add}$ is the add reduction of minimum cover for use of additional protection

- $C_{min,}$ is the minimum cover due to environmental conditions obtain from table A8 of the annex

2.4.4. Modelling of the project

Modelling will consist of creating the appropriate material, section properties, loads and loads combinations. The reinforced concrete elements shall be drawn according to the plans and the supports conditions assigned to be fixed. The structure shall be loaded with respect to specific load patterns discussed in section 2.4. A static linear analysis will be done to obtain the solicitations and verify the different elements in compliance with Eurocode norms.

The software used is SAP2000. This is a software of calculation and design of engineering structures particularly adapted to the buildings and civil engineering works. It offers many possibilities of analysis of the static and dynamic effects with complements of design and verification of the structures in reinforced concrete, metallic frame and others types of structures. The software allows to carry out the modelling steps (definition of geometry, boundary conditions, loading of the structure and more) in a totally graphical, numerical or combined way, using the countless tools available. The software considerably facilitates the analysis of the results by offering the possibility to visualize the distortion of system, the diagrams of the solicitations and envelopes curves, the fields of constraints, the Eigen modes of vibration and more.

2.4.5. Horizontal structural element design

The horizontal structural element to be designed, in this section is a beam. The latter is designed under Ultimate Limit State (ULS) and Serviceability Limit State (SLS). The dimensions of the element are obtained from the data collection. Materials, section properties, loads, loads combinations, restraints and constraints and other design parameters are defined and assigned to the beam to obtain the solicitation parameters and curves. The envelop curve is then obtained for each solicitation parameter.

2.4.5.1. Ultimate Limit State design

Under ULS, the beam will be verified for bending moment and shear force solicitations as there are no axial forces on the beam.

(a) Bending moment design

The design bending moment is obtained from the worst combination of actions shown by the envelope curve of the bending moment solicitation parameter.

(i) Moment reduction

Provisions given by Eurocode 2 recommend moment reduction at the support as shown in figure 2.2. For continuous beams, the value depends on the connection between the beam and the support.

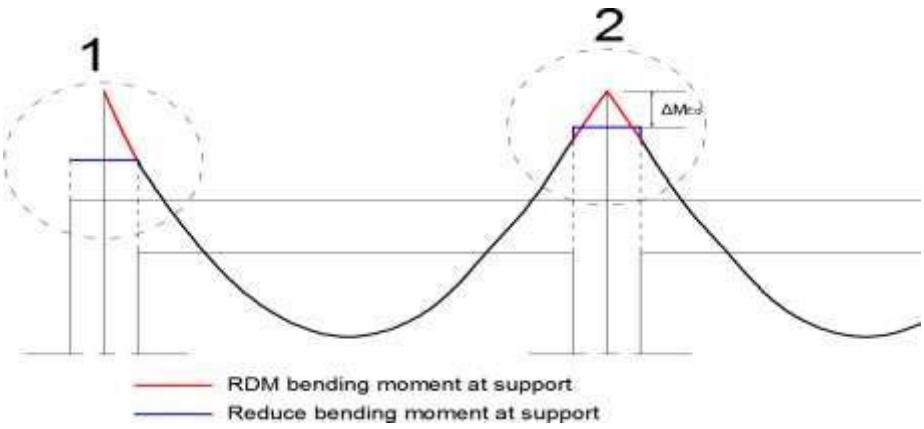

Figure 2.2. Reduction of the bending moment at support (Djeukoua,2018)

Where a beam is monolithic with its supports, the critical design moment at the support should be taken as that at the face of the support. As presented in the figure 2.2 (1). If instead, the beam is continuous over a support (Figure 2.2(2)) the analysis is done considering that the support does not provide no rotational restraint. The amount of this reduction is given by equation 2.5.

$$\Delta M_{Ed} = F_{Ed,}.t/8 \qquad \text{(Eq. 2.5)}$$

Where:

- t, is the breadth of the support
- $F_{Ed,}$ is the design of the support

The curve used for design is obtained by doing a shift of the moment curve a distance of a_i in the worst direction as it is illustrated in figure 2.3 below, accounting for the additional tensile force.

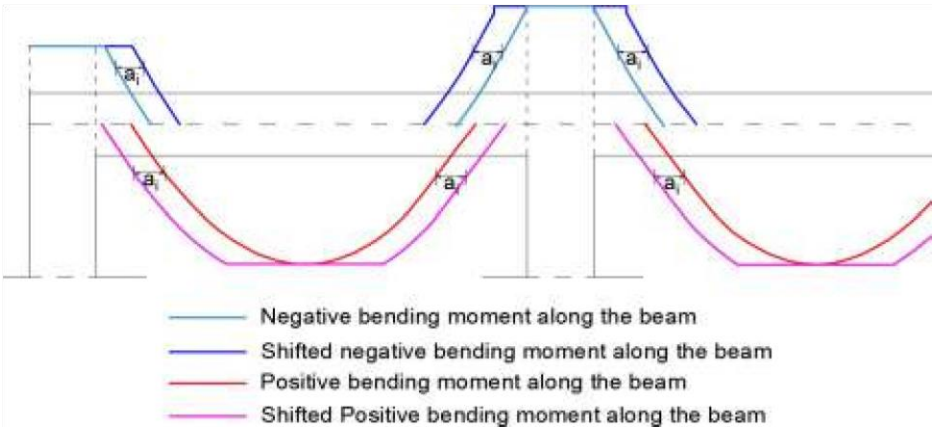

Figure 2.3. Shifting of the moment curve (Djeukoua, 2018)

a_i is computed using equation 2.6.

$$a_i = z(cot\vartheta - cot\alpha)/2 \qquad \text{(Eq. 2.6)}$$

Where:

- Z is the inner lever arm
- ϑ is the angle of concrete compression strut to the beam axis
- α is the angle between shear reinforcement and the beam axis perpendicular to the shear force. The quantity of longitudinal reinforcements is then determined with values of bending moment obtained in the shifted curve.

(ii) Longitudinal steel reinforcement

The section of the beam is a rectangular one. The longitudinal steel reinforcement is computed using equation 2.7.

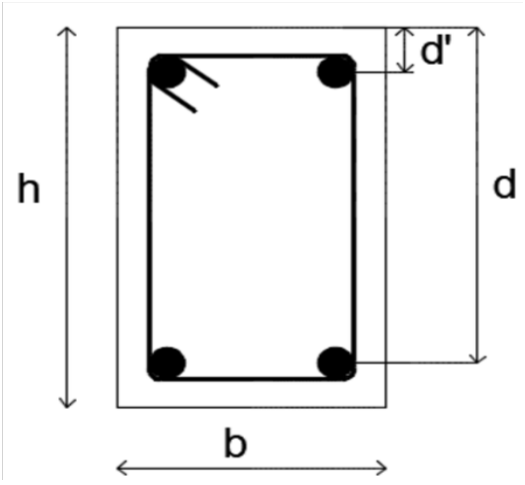

Figure 2.4. Example of transversal beam section with longitudinal reinforcements

The provisions of the Eurocode 2 to be verified by the beam cross section for minimum and maximum reinforcement areas are given in equations 2.8 and 2.9 respectively.

$$A_s = \frac{M_{Ed}}{0.9d.f_{yd}} \quad \text{(Eq. 2.7)}$$

$$A_{s,min} = \max(0.26\frac{f_{ctm}}{f_{yk}}b_t d; 0.0013 b_t d) \quad \text{(Eq. 2.8)}$$

$$A_{s,max} = 0.004 A_c \quad \text{(Eq. 2.9)}$$

Where:

- b_t is the Mean width of the tension zone
- d is the is the effective depth of the section
- f_{ctm} Is the tensile strength of the concrete

(iii) Verification of the steel reinforcement

We compute the number of reinforcement bars needed and the corresponding area of reinforcement. The section is verified, using the position of the neutral axis inside the section (figure 2.5), by calculating the resisting bending moment of the section.

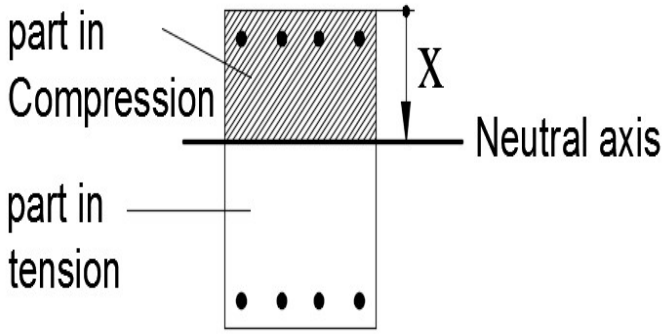

Figure 2.5. Neutral axis position in the beam section

Equation 2.10 shows the computation of the neutral axis position.

$$x = \frac{d}{2\beta_2} - \sqrt{\left(\frac{d}{2\beta_2}\right)^2 - \frac{M_{Ed}}{\beta_1\beta_2.b.f_{cd}}} \quad \text{(Eq. 2.10)}$$

Where:

- d: Effective depth of the section b: Width of the section
- f_{cd}: Design concrete compressive strength
- β_1 and β_2: Correction factors equal to 0.81 and 0.41 respectively

We then calculate the resisting moment using equation 2.11.

$$M_{Rd} = A_{s,}.f_{yd}.(d - \beta_2.x) \qquad \text{(Eq. 2.11)}$$

Where:

- $A_{S.re}$: Effective area of the steel section
- f : Design yielding strength of the steel

(b) Shear verification

The design shear force is obtained from the worst combination of actions shown by the envelope curve of the shear force solicitation parameter. It is usually taken as the shear force at the face of the beam's support. The beam element needs to resist shear forces. This resistance is provided by introducing transversal steel reinforcement inside the beam (figure 2.6). These reinforcements are called stirrups.

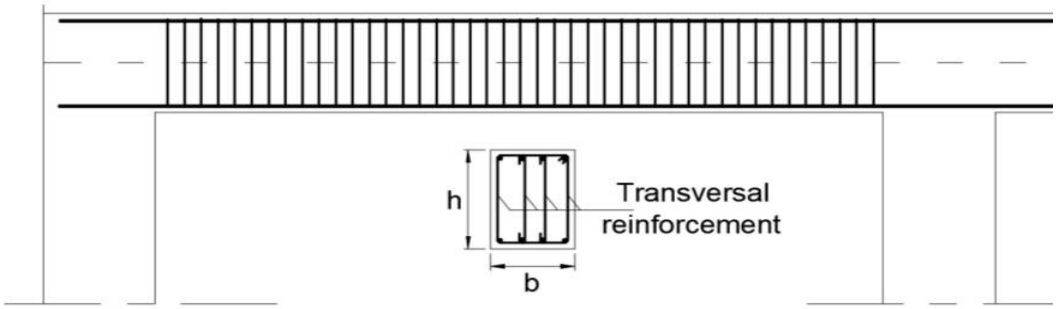

Figure 2.6. Longitudinal and transversal beam section with transversal reinforcement

Whether shear reinforcement is needed or not is agreed on, on comparison of the acting shear, V_{Ed}, with the shear resistance of the members without shear reinforcements, $V_{Rd,C}$.

$$V_{Rd,C} = [C_{Rd,C}k(100\rho_l f_{ck})^3 + k_1\sigma_{cp}]b_w d > V_{Rd,C} = V_{min} + k_1\sigma_{cp})b_w \text{ d} \qquad \text{(Eq. 2.12)}$$

Where:

- $V_{Rd,}$ is the characteristic strength of the reinforcement
- $C_{Rd,}$ = 0.18/γc
- d is the effective depth of the section in mm
- b_w is the smallest width of the cross section in the tensile area in mm
- $\sigma_{cp} = \frac{N_{Ed}}{b_w d} < 0.2 f_{cd}$ $[N/mm^2]$
- N : Axial force of the cross section due to loading or prestressing

- $k = 1 + \sqrt{\frac{200}{d}} \leq 2.0$ With d in mm
- $\rho_l = \frac{A_{sl}}{b_w d} \leq 0.02$

If:

- $V_{Ed} \leq V_{Rd,C}$, specific shear reinforcement is not required and the minimum quantity must be adopted.
- $V_{Ed} > V_{Rd,C}$, then a designed shear reinforcement is required. The shear resistance is the minimum between $V_{Rd,max}$ and $V_{Rd,s}$ defined by the equation 2.13 and equation 2.14 respectively.

$$V_{Rd,max} = \alpha_{cw} b_w z \nu_1 f_{cd} / (cot\theta + tan\theta) \quad \text{(Eq. 2.13)}$$

$$V_{Rd,S} = (A_{sw} / S) z f_{ywd} cot\theta \quad \text{(Eq. 2.14)}$$

Where:

- $z = 0.9d$ for rectangular cross-sections
- s is the stirrup spacing
- f_{ywd} is the design yield stress of the web reinforcement
- θ is the inclination of the cracks or the concrete struts, such that $21.8° \leq \theta \leq 45°$
- α_{cw} is the coefficient of interaction between compressive stresses which can be assumed to be 1 for non-prestressed structures
- ν_1 is the reduction coefficient for shear cracked concrete, ($\nu_1 = 0.6$ for $f_{ck} \leq 60N/mm^2$)
- f_{cd} is the cylindrical concrete compressive strength (design value)
- A_{sw} is the cross sectional area of the shear reinforcement with a maximum value given by the relation: $\frac{A_{sw,max} f_{ywd}}{b_w S} \leq \frac{1}{2} \alpha_{cw} \nu_1 f_{cd}$

In the case of the beam, shear reinforcements are characterized by the maximum longitudinal spacing of the shear assembly, the maximum transversal spacing of the legs in a series of shear link 7and the minimum shear reinforcement ratio (See figure 2.7).

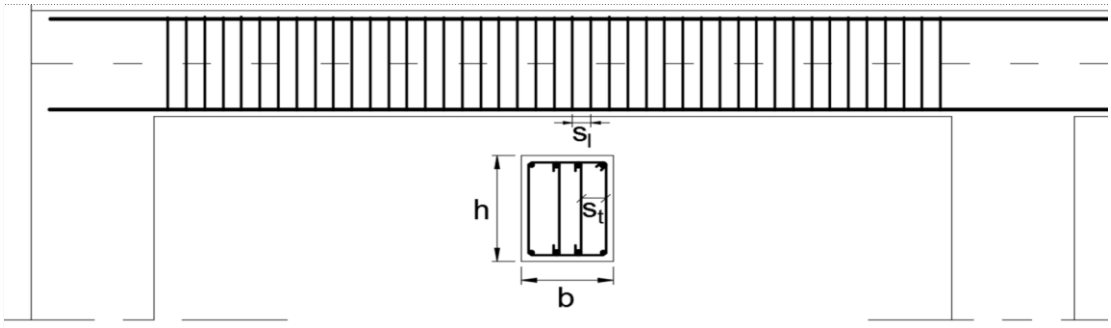

Figure 2.7. Illustration of the maximum longitudinal spacing and maximum transversal spacing of the legs

These limitations is given respectively in the equations 2.15 to 2.18.

$$s_{l,max} = 0.75d(1 + cot\alpha) \quad \text{(Eq. 2.15)}$$

$$s_{t,max} = 0.75d \leq 600mm \quad \text{(Eq. 2.16)}$$

$$\rho_w = A_{sw}/(s.\, b_w.\, sin\alpha) \quad \text{(Eq. 2.17)}$$

$$\rho_{w,min} = (0.08\sqrt{f_{ck}}) \,/\, f_{yk} \quad \text{(Eq. 2.18)}$$

2.4.5.2. Serviceability Limit State

The parameters of interest in this section are the stress limitations and deflection control.

(a)Stress limitation

The rare combination is the combination used for the stress verification because it permits to avoid inelastic deformation of the reinforcement and longitudinal cracks in concrete. Long-term and short-term effects are accounted for by the modular ratio, on which depends the stress value (equations 2.19 and 2.20)

$$n_o = E_s / E_c \quad \text{(Eq. 2.19)}$$

Where $\varphi_L = 0.55$ for shrinkage of concrete and the parameter $\rho_\infty = 2 \div 2.5$. For an uncracked concrete section, the neutral axis is computed thus:

$$x = \frac{-n(A_s^{'}+A_s)+\sqrt{[n(A_s^{'}+A_s)]^2+2bn\,(A_s^{'}d^{'}+A_s)}}{b} \quad \text{(Eq. 2.20)}$$

Where $A_s^{'}$ and A_s are the upper and lower steel reinforcement inside the section respectively.

b, d' and d, are the geometrical characteristics of the section presented in the figure 2.8.

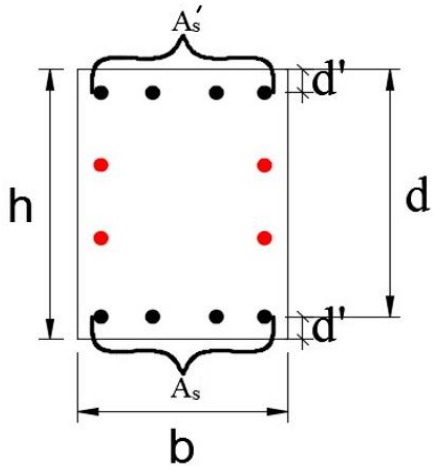

Figure 2.8. Geometric characteristics of a transversal beam section

The moment of inertia of the uncracked section is given by equation 2.21.

$$J_{cr} = \frac{bx^3}{3} + nA_s(d-x)^2 + nA'_s(x-c)^2 \qquad \text{(Eq. 2.21)}$$

The stresses in the concrete and steel can now be computed using equations 2.22 and 2.23 respectively.

$$\sigma_s = \frac{M_{Ed}(d-x)}{J_{cr}} \times n_{\infty} \qquad \text{(Eq. 2.22)}$$

$$\sigma_c = \frac{M_{Ed}.x}{J_{cr}} \qquad \text{(Eq. 2.23)}$$

The verifications of these stresses, as provided by Eurocode 2, are given by equations 2.24 and 2.25.

$$\sigma_c \leq k_1 * f_{ck} \qquad \text{(Eq. 2.24)}$$

$$\sigma_s \leq k_3 * f_{yk} \qquad \text{(Eq. 2.25)}$$

With $k_1 = 0.6$ and $k_3 = 0.8$.

(b) Deflection control

Deflection control is performed on the longest beam span which is the span subjected to the greatest deflection. The quasi-permanent combination is the combination used for the deflection

control. The deflection, f_1 at pre-cracking phase of the concrete, can be obtained with equation 2.26.

$$f_1 = 5*q*l^4 / (384*Ec*I_1) \quad \text{(Eq. 2.26)}$$

I_1 is obtained with Equation 2.27.

$$I_1 = b*h^3/12 + n*A_c\,(h/2 - d')^2 + n*A_t*\,(d - h/2)^2 \quad \text{(Eq. 2.27)}$$

Where A_t is the area of the steel in the tension zone is. It is at a distance d from the edge of the compression zone. The area of the steel in the compression zone is A_c. It is at a distance d' from the edge of the compression zone. The coefficient of homogenization is $n = E_s/E_c$.

The deflection, f_2 at cracking phase of the concrete, when the neutral axis is at a distance y from the edge of the compression zone, can be obtained with equation 2.28.

$$f_2 = 5*q*l^4/(384*E_c*I_2) \quad \text{(Eq. 2.28)}$$

I_2 is obtained with equation 2.29.

$$I_2 = b*y^3/3 + n*A_c(y - d')^2 + n*A_t(d - y)^2 \quad \text{(Eq. 2.29)}$$

y is obtained with equation 2.30.

$$b*y*(y/2) + n*A_c(y - d') - n*A_t*(d - y) = 0 \quad \text{(Eq. 2.30)}$$

The critical moment can be obtained with equation 2.31.

$$M_{cr} = (f_{ctm}*b*h^3/12)/(h/2) \quad \text{(Eq. 2.31)}$$

The final deflection f is obtained with equation 2.32.

$$f = f_1*(M_{cr}/M)^2 + f_2[1 - \beta*(M_{cr}/M)^2] \quad \text{(Eq. 2.32)}$$

Where:

- M is the moment at serviceability limit state
- $\beta = 1$ for short-term loading

For the verification, the deflection f must be lower than the length of the beam over 250 ($f<L/250$).

2.4.6. Vertical structural element design

Before the vertical structural element could be designed, the entire structure has to be modelled on SAP2000 V22. The dimensions of the element are obtained from the data collection. Similar to the beam, different load arrangements and combinations are assigned to the column to obtain the envelope curve that represents the worst case of loading the column could be subjected to, throughout the structure's working life. Only ULS is considered in the case of the column and the verifications done for axial force, bending moment and shear force.

2.4.6.1. Bending moment-axial force verification

Shear forces put aside, each column at each level is subjected to moment and axial force; these solicitations are obtained from the respective envelope curves. Each couple of points, M-N (moment-axial force) should belong to the section M-N interaction diagram. The interaction is a diagram representing all the limit situations deterministic of the section failure and is computed through the determination of points, which will be plotted to obtain the curve. Points lying within the diagram are respectful of the design criteria otherwise failure occurs. When considering a rectangular section, the computation of the points is done as presented in the subsequent sections.

(a) First point

At this point, the section is completely subjected to tension, thus, the concrete is not reacting (concrete resists poorly to tension). We impose $\varepsilon_s = \varepsilon_{su}$, $\varepsilon_s' = \varepsilon_{syd}$. The stress inside the element corresponds to the design yielding strength of the steel reinforcement and the limit axial force and bending moment are obtained from equations 2.33 and 2.34 respectively.

$$N_{Rd} = f_{yd}.A_s + f_{yd}.A'_s \qquad \text{(Eq. 2.33)}$$

$$M_{Rd} = f_{yd}.A_s.\left(\frac{h}{2} - d'\right) - f_{yd}.A_s.\left(\frac{h}{2} - d'\right) \qquad \text{(Eq. 2.34)}$$

(b) Second point

At the second point, the section is completely subjected to tension. We impose that; the strains, $\varepsilon_s = \varepsilon_{su}$, $\varepsilon_c = 0$. The upper steel yielding condition is verified. If the steel has not yielded, then ε_s' is determined. Equations 2.33 and 2.34 are used for the computation of the limit axial force and the bending moment respectively.

(c) Third point

Here failure is due to concrete and the lower reinforcements have yielded. We assume

$\varepsilon_s \geq \varepsilon_{syd}$, $\varepsilon_c = \varepsilon_{cu2}$ and the position of the neutral axis is determined. Yielding condition of the upper steel reinforcement is verified. If the steel is yielded or not is determined by determining ε_s' in order to determine the corresponding stress. The limit axial force and bending moment corresponding to the third point are computed following equations 2.35 and 2.36 respectively.

$$N_{Rd} = -\beta_1 . b . x . f_{cd} + f_{yd} . A_s - f_{yd} . A'_s \quad \text{(Eq. 2.35)}$$

$$M_{Rd} = f_{yd} . A'_s . \left(\frac{h}{2} - d'\right) + f_{yd} . A_s \left(\frac{h}{2} - d'\right) + \beta_1 . b . x . f_{cd} \left(\frac{h}{2} - \beta_2 . x\right) \quad \text{(Eq. 2.36)}$$

(d) Fourth point

We impose that the failure is due to concrete and the lower reinforcement reaches exactly $\varepsilon_s = \varepsilon_{syd}$. Likewise, we determine the neutral axis position and the strain ε_s'. Equations 2.35 and 2.36 are respectively used to compute the limit axial force and bending moment corresponding to fourth point.

(e) Fifth point

We impose that the failure is due to concrete and the lower reinforcement reaches exactly $\varepsilon_s = 0$. Then the neutral axis position is equal to the effective depth of the section. The limit axial force and bending moment are obtained from the equations 2.37 and 2.38 respectively.

$$N_{Rd} = -\beta_1 . b . x . f_{cd} - f_{yd} . A'_s \quad \text{(Eq. 2.37)}$$

$$M_{Rd} = f_{yd} . A'_s . \left(\frac{h}{2} - d'\right) + \beta_1 . b . d . f_{cd} \left(\frac{h}{2} - \beta_2 . x\right) \quad \text{(Eq. 2.38)}$$

(f) Sixth point

We impose that concrete is uniformly compressed and assume the strains $\varepsilon_s = \varepsilon_c \geq \varepsilon_{c2}$. limit values of axial force and bending moment are computed by equations 2.39 and 2.40 respectively.

$$N_{Rd} = -b . h . f_{cd} - f_{ywd} . A'_s - f_{yd} . A_s \quad \text{(Eq. 2.39)}$$

$$M_{Rd} = f_{yd} . A'_s . \left(\frac{h}{2} - d'\right) - f_{yd} . A_s \left(\frac{h}{2} - d'\right) \quad \text{(Eq. 2.40)}$$

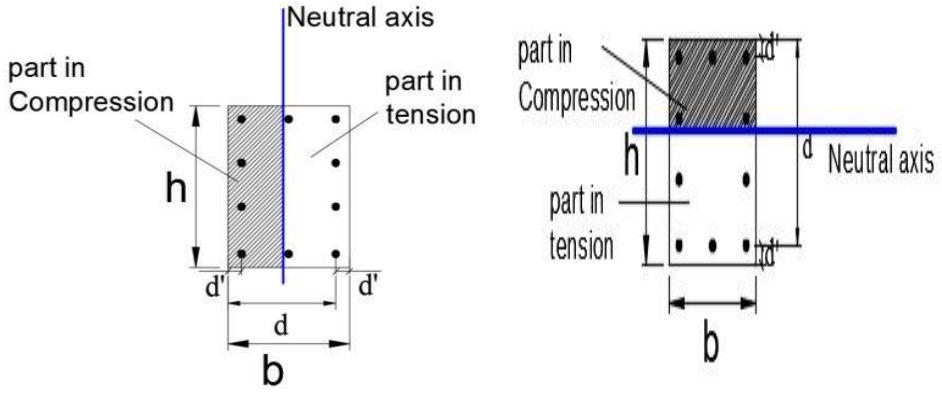

Figure 2.1. Rectangular section to illustrate the computation of the M-N diagram for different direction of the neutral axis (Djeukoua,2018).

Provisions of Eurocode with regards to the steel reinforcement of the column recommend limit values for reinforcing steel section as shown in equations 2.41 and 2.42.

$$A_{s,min} = max\left(\frac{0.10N_{Ed}}{f_{yd}}; 0.002A_c\right) \quad \text{(Eq. 2.41)}$$

$$A_{s,max} = 0.04A_c \quad \text{(Eq. 2.42)}$$

Where

- N : Design axial compression force
- f : Design yield strength of the longitudinal reinforcement

For joint reinforcements,

$$A_s = 0.09sb_{ch}\frac{f_c'}{f_{yh}} \quad \text{(Eq. 2.43)}$$

And not less than;

$$A_{sh} = 0.3sb_{ch}\left(\frac{A_g}{A_{ch}} - 1\right)\frac{f_c'}{f_{yh}} \quad \text{(Eq. 2.44)}$$

$$S_{cl,max} = \min\left(20\emptyset_{l,min}; b; 400mm\right) \quad \text{(Eq. 2.45)}$$

2.4.6.2. Shear verification

Just like the beam, the procedure goes same. Provisions given by the Eurocode 2 requires a minimum diameter of 6mm or one quarter of the maximum diameter of the longitudinal bars. The maximum spacing of the transverse reinforcement is given by the equation 2.45.

Where:

- $\emptyset_{l,}$: Minimum diameter of the longitudinal bars
- b: Lesser dimension of the column

The factor of 0.6 is used to reduce the maximum spacing in sections within a distance equal to the larger dimension of the column bars.

2.4.6.3. Slenderness verification

The need for slenderness verification arises from whether or not second order effects are to be accounted for. Eurocode 2 recommendations are outlined below in equation 2.46.

$$\lambda_{lim} = 20.A.B.C/\sqrt{n} \quad \text{(Eq. 2.46)}$$

With:

- $A = \frac{1}{1+0.2\varphi_{ef}}$ (φ_{ef}: is the effective creep ratio; If not known, A=0.7)
- $B = \sqrt{1+2\omega}$ ($\omega = A_s f_{yd}/A_c f_{cd}$: mechanical reinforcement ratio)
- C=1.7−r_m (r_m =M_{01}/M_{02}: the moment ratio; equal to 1 for unbraced system)
- n=$N_{Ed}/A_c f_{cd}$: relative normal force

The equation 2.47 is the one used for the estimation of slenderness.

$$\lambda = l_0/i \quad \text{(Eq. 2.47)}$$

Where:

- l_0: Effective length of the element (l_0 =0.7l)
- i : The gyration radius of the uncracked concrete given by equation 2.48

$$i = \sqrt{\frac{I}{A}} \quad \text{(Eq. 2.48)}$$

Where I: Moment of inertia and A is the area of the section.

2.4.7. Foundation design

Two types of foundations are designed namely the isolated and the combined footings. The solicitations are obtained through the finite element method using the Winkler approach of soil structure interaction. The admissible bearing pressure of the soil considered for this study is 3 bars.

2.4.7.1. Soil structure interaction

The footings are designed as plate thick elements. The footings will be modelled in SAP2000 as plates resting on Winkler's springs. The stiffness of the springs is obtained from the modulus of

subgrade reaction of the soil times the area of the meshing square using equation 2.49. The modulus of subgrade reaction is obtained using the figure presented in Annex A5

$$k = C \times A_m \quad \text{(Eq. 2.49)}$$

Where:

- C is the modulus of subgrade reaction of the soil
- A_m is the mesh area

2.4.7.2. Design of the isolated footing

The design involves a preliminary design, a geotechnical design and a structural design.

(a) Preliminary design

The section of footings is obtained using equation 2.50.

$$S = \frac{N}{\sigma adm} = AxB \quad \text{(Eq. 2.50)}$$

Where:

- N is the total vertical load arriving at the foundations
- σ_{adm} is the admissible bearing pressure of the soil
- S is the section of the footing
- A is the shorter side of the footing
- B is the longer side of the footing

The depth of the footing is obtained using equation 2.51.

$$h = \max\left(\frac{A-a}{4}; \frac{B-b}{4}\right) \quad \text{(Eq. 2.51)}$$

Where:

- h is the depth of the footing
- a is the shorter side of the column
- b is the longer side of the column

(b) Geotechnical design

The pressure developed by the total vertical load of applied on the footing should be less than the allowable pressure of the soil as expressed in relation 2.52 as:

$$\sigma = N / A \leq \sigma_{adm} \quad \text{(Eq. 2.52)}$$

Where:

- σ is the contact pressure
- σ_{adm} is the admissible bearing pressure on the soil
- N is the total vertical load arriving at the foundations

(c) Structural design

The quantity of steel reinforcements in both directions are obtained using the equation 2.7.

2.4.7.3. Design of the combined footing

The section and depth of the footing are obtained using equations 2.50 and 2.51 respectively. To obtain the section, the value of the vertical load is the sum of all the vertical loads acting on the combined footing.

The procedures for the geotechnical and structural designs are similar to those of the isolated footing as shown in sections 2.4.7.2(b) and 2.4.7.2(c) respectively.

2.5. Crack analysis methodology

The finite element analysis (FEA) of the cracking propagation in the beam specimen is performed in a nonlinear static analysis format. A beam in a structure under static loading is subjected to bending and a displacement based method is used to express the effects. The finite element analysis software used for the crack analysis in this study is Abaqus. This is a software suite for finite element analysis and computer-aided engineering. The core product, eventually known as ABAQUS/Standard which is an implicit finite element solver, was complemented by other software packages including ABAQUS/Explicit, a dynamic explicit analysis package, and ABAQUS/CAE, a finite element pre- and post-processing package released. For this study, ABAQUS/CAE will be the chosen package.

2.5.1. Analysis approach

Constitutive behaviour of concrete is very difficult to capture by using elastic damage models or elastic plastic laws. In elastic damage model irreversible strains cannot be captured. It can be seen in figure 2.9(b) that a zero stress corresponds to a zero strain which makes damage value to be overestimated. On the other hand when elastic plastic relation is adopted the strain will be overestimated since the unloading curve will follow the elastic slope (figure 2.9(c)). Concrete Damage Plasticity (CDP) model which combines these two approaches can capture the constitutive

behaviour of experimental unloading (figure 2.9(a)) (Jason et al., 2004). So, this study is carried out using concrete damage plasticity approach.

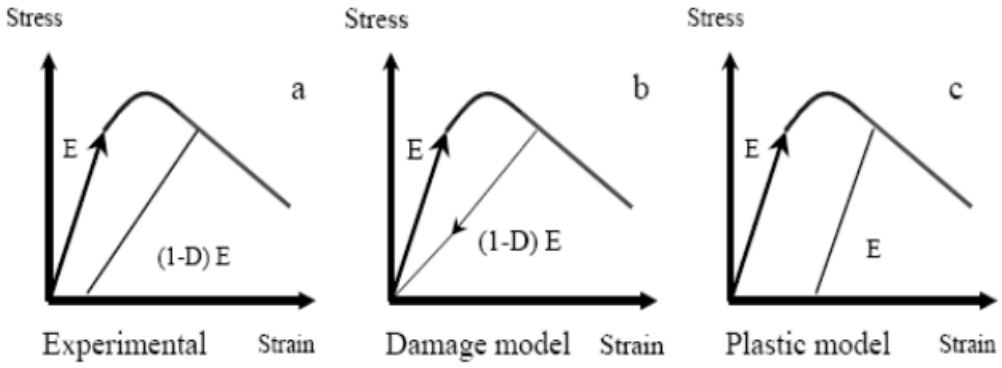

Figure 2.9. Elastic plastic damage law (Jason et al., 2004).

In this model two main failure mechanisms are assumed: tensile cracking and compressive crushing of the concrete. The evolution of the yield surface is controlled by tensile and compressive equivalent plastic strains.

Numerical models for the constituent material properties are described in this section.

2.5.2. Concrete model

There are three main domains that categorize the compressive behavior of concrete which are; the linear-elastic branch which continues to reach the stress level of σ_{co}. The second domain presents the hardening part of the concrete uniaxial compressive stress-strain behavior. This represents the ascending branch of the stress-strain relationship reaching to the peak load at the corresponding strain level ε_o. The third domain is representative of the attributes to the post-peak softening behaviour and therefore represents the initiation and progression of compressive damage in the concrete material until the ultimate compressive strain ε_u.

The tensile behavior of concrete comprises two parts the first of which is a linear elastic behavior and the second part initiates together with crack occurrence and its propagation in concrete material under tension, demonstrating a descending branch in the uniaxial tensile stress-strain diagram.

CDP is one of the possible constitutive models to predict the constitutive behaviour of concrete. It describes the constitutive behaviour of concrete by introducing scalar damage

variables. The tensile and compressive response of concrete can be characterized by CDP in figure 2.10.

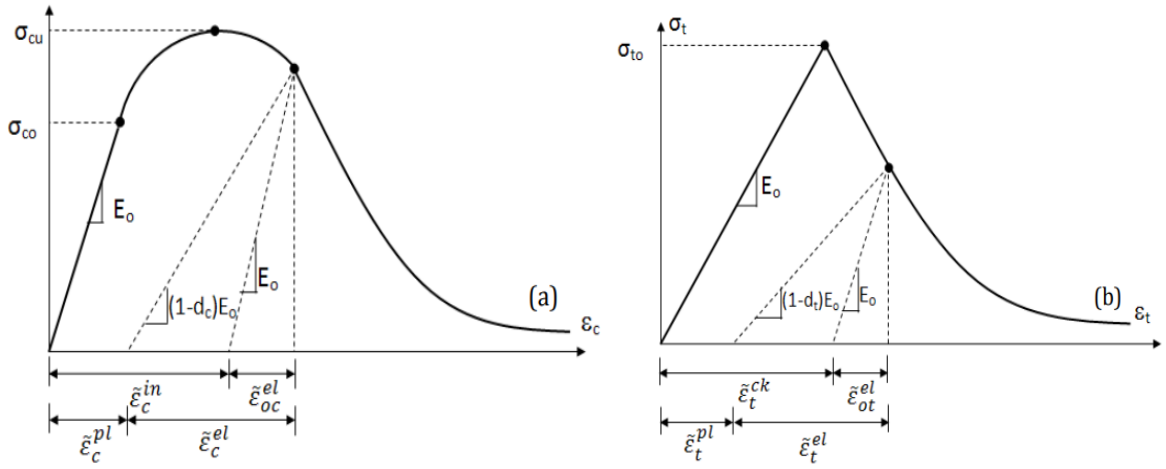

Figure 2.10. Behaviour of concrete under uniaxial compressive (a) and tension (b) strength (Abaqus User Manual, 2008).

As shown in figure 2.10, the unloaded response of concrete specimen seems to be weakened because the elastic stiffness of the material appears to be damaged or degraded. The degradation of the elastic stiffness on the strain softening branch of the stress-strain curve is characterized by two damage variables, d_t and d_c, are the tensile and compressive damage in concrete respectively and can take values from zero to one. Zero represents the undamaged material where one represents total loss of strength (Abaqus User Manual, 2008). E_0 is the initial (undamaged) elastic stiffness of the material and $\tilde{\varepsilon}_c$, $\tilde{\varepsilon}_t^{pl}$, $\tilde{\varepsilon}_c^{in}$, $\tilde{\varepsilon}_t^{in}$ (or ε_t^{ck}) are compressive plastic strain, tensile plastic strain, compressive inelastic strain and tensile inelastic strain respectively. The stress-strain relations under uniaxial tension and compression are taken into account in equations 2.53 and 2.54 respectively.

$$\sigma_t = (1 - d_t) \cdot E_0 \cdot (\varepsilon_t - \tilde{\varepsilon}_t^{pl}) \qquad \text{(Eq. 2.53)}$$

$$\sigma_c = (1 - d_c) \cdot E_0 \cdot (\varepsilon_c - \tilde{\varepsilon}_c^{pl}) \qquad \text{(Eq. 2.54)}$$

$$d_t = 1 - \frac{\sigma_t}{\sigma_{to}} \qquad \text{(Eq. 2.55)}$$

$$d_c = 1 - \frac{\sigma_c}{\sigma_{cu}} \qquad \text{(Eq. 2.56)}$$

Interface behaviour between rebar and concrete is modelled by implementing tension stiffening in the concrete modelling to simulate load transfer across the cracks through the rebar. Tension stiffening also allows to model strain-softening behaviour for cracked concrete. Thus it is necessary to define Tension stiffening in CDP model. From CDP perspective, ABAQUS automatically calculates both plastic displacement values using the equations 2.57 and 2.58.

$$\varepsilon_t^{\sim pl} = \varepsilon_t^{ck} - d_t \cdot \sigma_t / ((1-d_t) \cdot E_0) \qquad \text{(Eq. 2.57)}$$

$$\varepsilon_c^{\sim pl} = \varepsilon_c^{\sim in} - d_c \cdot \sigma_c / ((1-d_c) \cdot E_0) \qquad \text{(Eq. 2.58)}$$

From these equations "effective" tensile and compressive cohesion stresses ($\bar{\sigma}$, $\bar{\sigma_c}$) are defined in equations 2.59 and 2.60.

$$\bar{\sigma_t} = \sigma_t / (1-d_t) = E_0 \cdot (\varepsilon_t - \varepsilon_t^{\sim pl}) \qquad \text{(Eq. 2.59)}$$

$$\bar{\sigma_c} = \sigma_c / (1-d_c) = E_0 \cdot (\varepsilon_c - \varepsilon_c^{\sim pl}) \qquad \text{(Eq. 2.60)}$$

The effective cohesion stresses determines the size of the yield (or failure) surface (see figure 2.11).

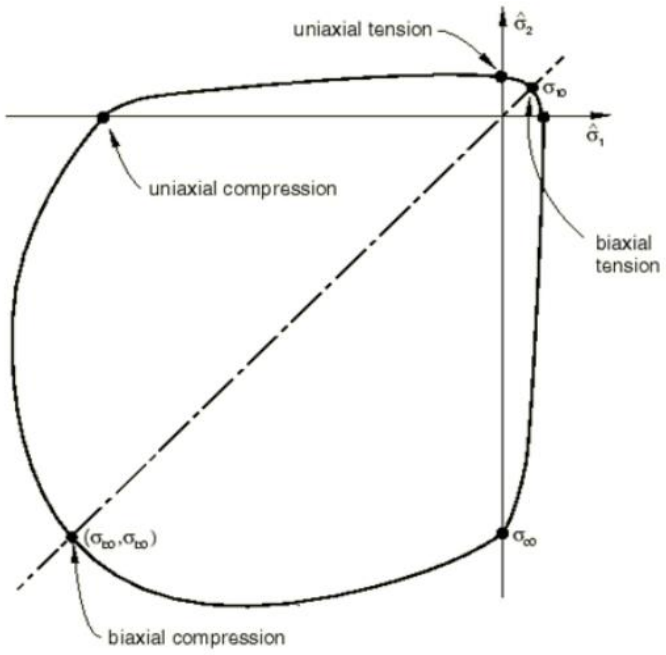

Figure 2.11. Biaxial yield surface in CDP Model (Abaqus User Manual, 2008).

In Abaqus the parameters required to define the yield surface consists of some constitutive parameters. The Poisson's ratio controls the volume changes of concrete for stresses below the

critical value which is the onset of inelastic behaviour. Once the critical stress value is reached concrete exhibits an increase in plastic volume under pressure (Chen, 1982). This behaviour is taken into account by defining a parameter called the angle of dilation. In CDP model ψ is the dilation angle measured in the p-q plane at high confining pressure. ϵ is an eccentricity of the plastic potential surface. The ratio of initial biaxial compressive yield stress to initial uniaxial compressive yield stress, σ_{b0}/σ_{c0}, with values in the range from 1.10 to 1.16. Finally Kc is the ratio of the second stress invariant on the tensile meridian to compressive meridian at initial yield with default value of 2/3 (Abaqus User Manual, 2008). The parameter Kc should be defined based on the full triaxial tests of concrete, moreover biaxial laboratory test is necessary to define the value of σ_{b0}/σ_{c0}.

2.5.3. Steel model

The assumption that the uniaxial tensile stress-strain behavior of reinforcement was made with conventional Young's modulus and Poisson's ratio. The plastic behavior is also modeled including yield stress and corresponding plastic strain.

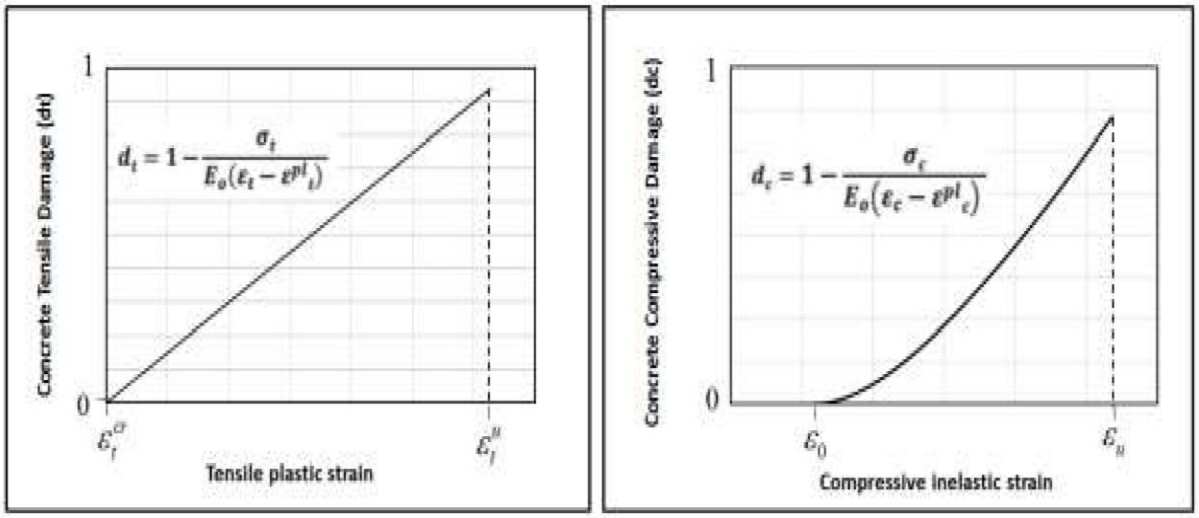

(a) Uniaxial tensile damage (b) Uniaxial compressive damage

Figure 2.12. Definition of damage parameter in CDP model

The cracking strain is calculated as the difference between the total strain and the elastic strain corresponding to the undamaged material as given in the equations 2.61 and 2.62.

$$\tilde{\varepsilon}_t^{ck} = \varepsilon_t - \varepsilon_{ot}^{el} \qquad \text{(Eq. 2.61)}$$

$$\varepsilon_{ot}^{el} = \sigma_t / E_0 \qquad \text{(Eq. 2.62)}$$

Conclusion

In this chapter, the European design code (Eurocode) was presented. Particular attention was given to Eurocodes 0, 1, 2 and 7, outlining the procedures recommended by these codes for beams, columns and foundations design and verifications. A brief description of the finite element method analysis software Abaqus/CAE was done, also talking about the concrete damage plasticity constitutive model used by this software. The following chapter will be mainly be concerned with the presentation of the case study and the implementation of the procedures discussed in this chapter to carry out a linear static analysis on a selected beam, column and footing using the structural analysis software SAP 2000 version 22. Also, the results and interpretations of the non-linear finite analysis whose procedure were as well described in this chapter will also be presented.

CHAPTER 3: PRESENTATION AND INTERPRETATION OF RESULTS

Introduction

The methodology presented previously is applied on a case study and the results are highlighted here. This chapter will consist in a preliminary part in the presentation of the case study and the different loads and material properties considered for its analysis. The solicitation parameters (moments, shear forces and axial forces) as well as the stresses in the constitutive materials are determined after the static analysis is performed. These data give indication on the choice of the characteristics (geometric and mechanical) of the structural elements The structural elements, once they are designed, can now be used to model the reinforced concrete frame in ABAQUS/CAE for an analysis to study the crack pattern. The results of the numerical method (FEM) will be compared with those of the experimental methods to investigate the correspondence between the experimental results and the FEM results.

3.1. General presentation of the site

Here, we present the study area through its location, geology, relief, climate, hydrology, population and socio-economic activities.

3.1.1. Geographic location

Yaoundé, the political capital of Cameroon, is the chief town of the Center region and of the Mfoundi department. Yaoundé is located between 3°45 'and 4°00' north latitude and between11°00' and 11°30' east longitude at the edge of the savannah and the great rainforest of South Cameroon (Djocgoue, 2012). Figure 3.1 shows a map of the city of Yaoundé.

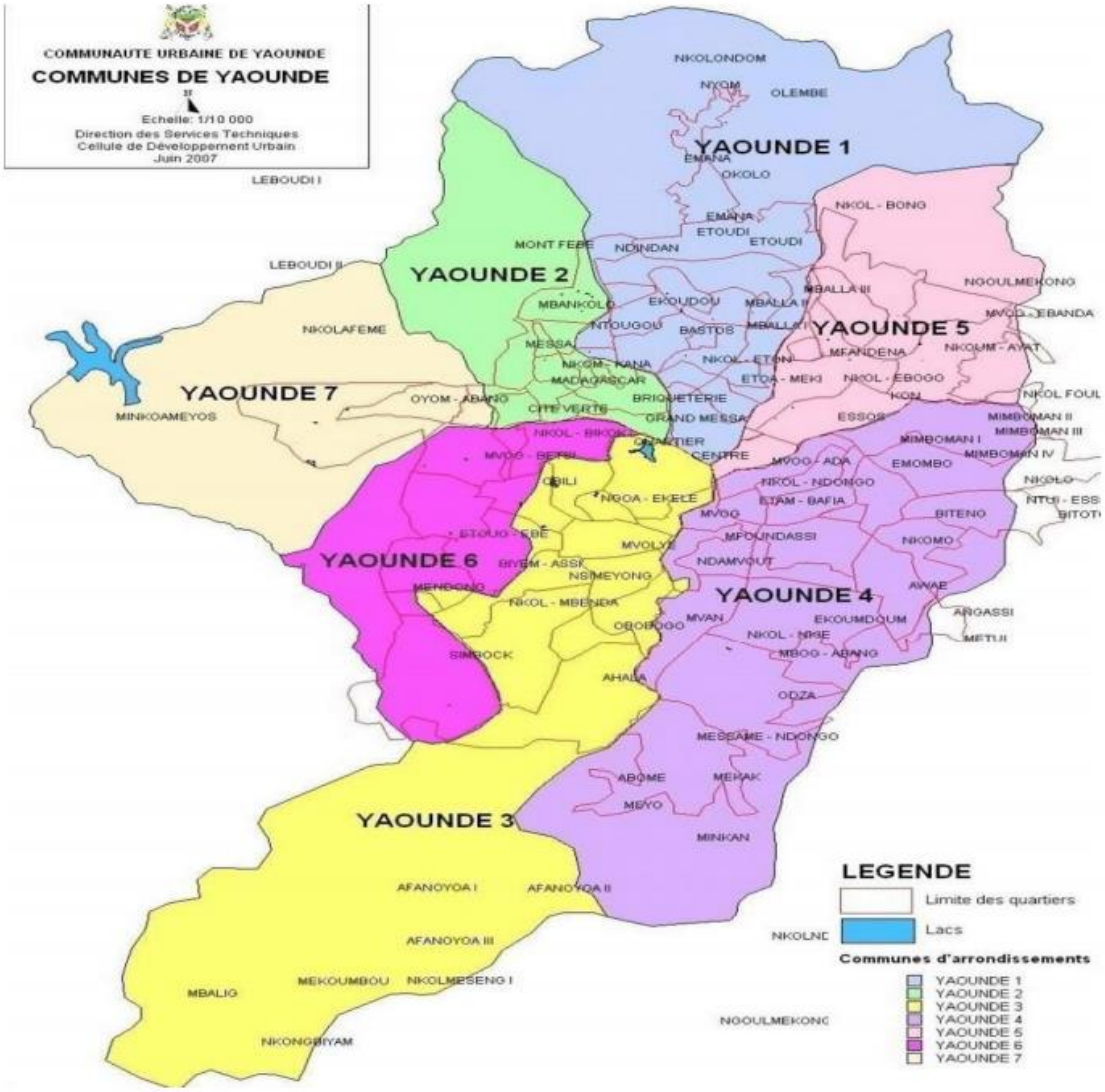

Figure 3.1. Geographic map of Yaounde

3.1.2. Climate

Yaoundé features a tropical wet and dry climate, with record high temperatures of 36ºC, an average of 23.8ºC and a record low temperature of 14ºC. Primarily due to the altitude, temperatures are not as high as would have been expected for a city located near the equator. The town of Yaoundé features a lengthy rainy season covering a nine-month span between March and November. However, there is a noticeable decrease in precipitation within the rainy season, observed during the months of July and August, giving the city the appearance of having two rainy

and two dry seasons. The average precipitation is 1650mm of rain per year and average humidity is 80%.

3.1.3. Geology

The bedrock in Yaoundé is mainly composed of gneiss. This rock is neither porous nor soluble, but it is its discontinuities (faults, diaclases) that give fissure permeability to the formation. The hydrogeology is characterized by continuous aquifers, approximately exploitable overlying water bearing fissures or fracture aquifers in the bedrock; these types of aquifers are superimposed or isolated.

3.1.4. Relief

Concerning the relief, the land rises gently in escarpments from the southwestern coastal plain before joining the Adamawa Plateau via depressions and granite massifs. The field is characterized by rolling, forested hills, the tallest of which have bare, rocky tops.

3.1.5. Hydrology

The hydrographic network of Yaoundé is very dense and composed permanent rivers such as the Mfoundi river which crosses the city from North to South, a few creeks and lakes. Yaoundé is part of the western sector of the Southern Cameroon Plateau. The area is characterized by gentle rolling chains of hills, and numerous valleys and wetlands; this varied physical landscape permits a combination of streams, hydromorphic soils and a great variety of plants and Fauna.

3.1.6. Population

Yaoundé has a total population estimated at 3.8 million in 2019. The city of Yaoundé being a cosmopolitan city, there is a considerable portion of population coming from several other region of the country (west, far north etc.).

3.1.7. Socio-economic activities

Most of Yaoundé's economy is centered on the administrative structure of the civil services and the diplomatic services. Due to these, Yaoundé has a higher standard of living and security than the rest of Cameroon. However, Yaoundé is a tertiary city and there are a few industries: breweries, sawmills, carpentry, tobacco, paper mills, machinery and building materials.

3.2. Physical description of the site

The case study is located in the NASPW Yaounde and is going to serve as an administrative building. In the school campus, it is surrounded by other school facilities such as classrooms; administrative buildings, laboratories, libraries and gymnasium. Out of the campus, we have a dense traffic mostly caused by the presence of a nearby market and hospital. Figure 3.2 shows a picture of our case study.

Figure 3.2. New administrative building of the NASPW Yaounde

3.3. Presentation of the project

The case study, is made up of three reinforced concrete building blocks frames (block A, block B and block C), separated by a rupture joints. Blocks A and B are made up of six-storeys for office use while block C consists of 5 storeys and contains an emergency staircase.

3.3.1. Geometrical data

The formwork plan of the whole building is shown in figure 3.3.

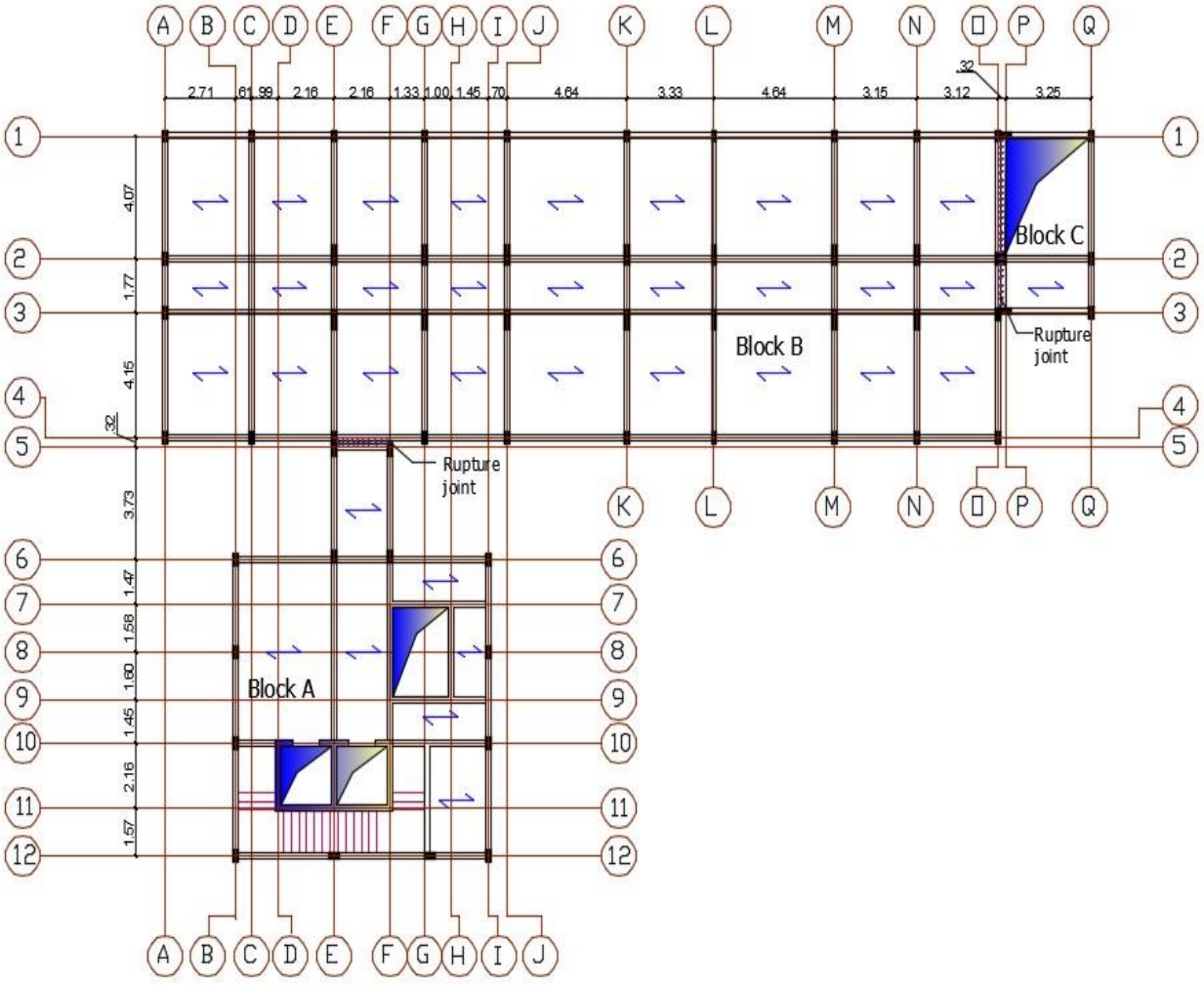

Figure 3.3. Formwork plan of the building

Since the different building blocks are separated by rupture joints, they can be studied separately. This work is focused on building block B. It is a rectangular floor, with its length being 32.18m and the width 10.19m. The slab is assumed to be a reinforced concrete slab with hollow blocks of thickness 20cm. The height of every floor is 3.2m making a total height of 19.2m for the building. The formwork plan and a cut sections of building block B are shown in figures 3.4 to 3.6 figure. Beams on the same floor do not have the same design. They have the same sections but not the same influence areas, and this is the case in either directions (x-direction and y-direction). The

structure has identical floor plan as from level one to level six but a different floor plan for level 7 as can be seen on the 3D model. The formwork plan of the building block B is shown in figure 3.4.

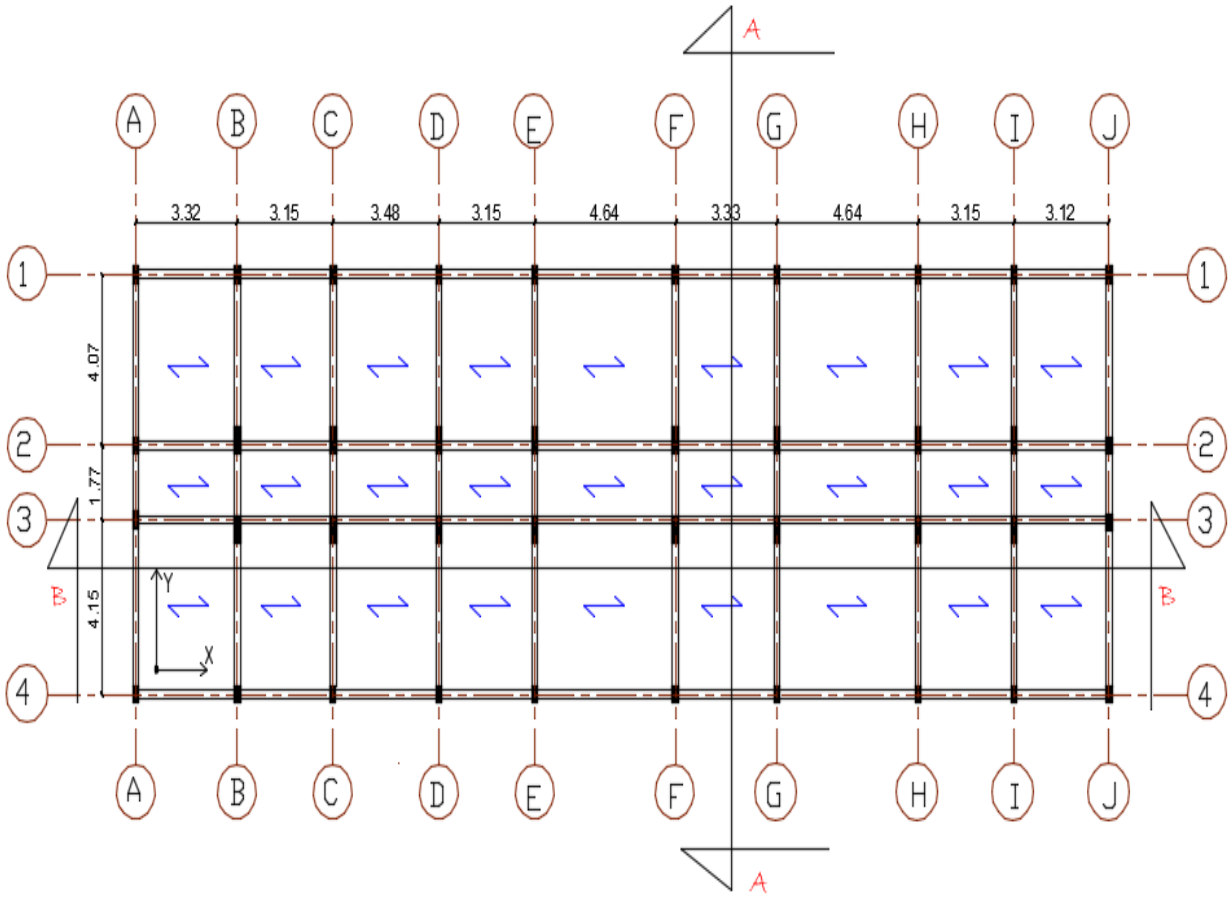

Figure 3.4. Formwork plan of the building block B

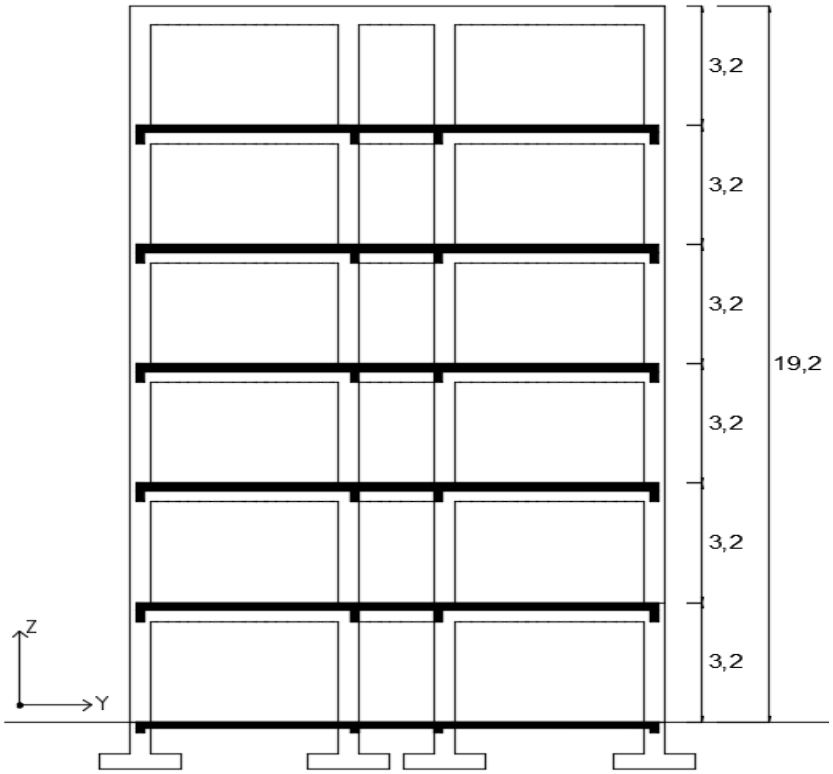

Figure 3.5. Section A-A of the building block B

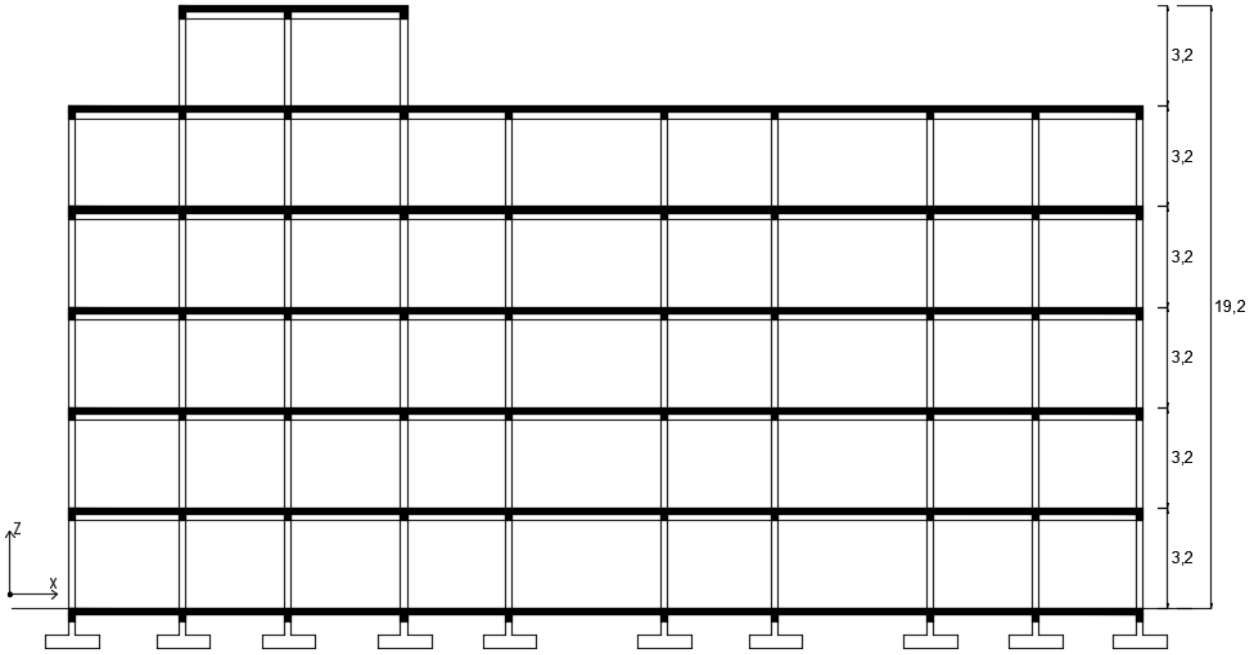

Figure 3.6. Section of the building block B

3.3.2. Material properties

The concrete class chosen is C25/30 and the longitudinal steel reinforcement is FE400. We consider a characteristic yield strength of 235 Mpa for the transversal reinforcement. Table 3.1 below shows the main characteristics of concrete and table 3.2 that of steel used as reinforcement for linear analysis and design of the structure.

Table 3.1. Concrete characteristics.

Property	Value	Unit	Definition
Class	C25/30	-	Concrete class
$f_{ck,cube}$	30	Mpa	Characteristic cubic compressive strength
f_{ck}	25	Mpa	Characteristic compressive strength of concrete at 28 days
$f_{cm} = f_{ck} + 8$	33	Mpa	Mean value of concrete cylinder compressive strength
γ_c	1.5	-	Partial factor for concrete
$f_{ctm} = 0.3 \times (f_{ck})^{\frac{2}{3}}$	2.56	Mpa	Mean value of axial tensile strength of concrete
$f_{ctd} = 0.7 \times \frac{f_{ctm}}{\gamma_c}$	1.2	Mpa	Design resistance in traction
$E_{cm} = 22000 \times (f_{cm}/10)^{0.3}$	31476	Mpa	Secant modulus of elasticity
ν	0.2	-	Poisson's ratio
G	13115	Mpa	Shear modulus
γ	25	KN/m^3	Specific weight of the concrete

Table 3.2. Longitudinal reinforcement characteristics

Property	Value	Unit	Definition
Class	FE400	-	Steel class
f_{yk}	400	Mpa	Characteristic yield strength
γ_s	1.15	-	Partial safety factor for steel
γ	78.5	Mpa	Specific weight of the steel
ν	0.3	-	Poisson's ratio

3.4. Linear static design results of the project

Static design is done for vertical static actions on the building. This implies considering only permanent and imposed loads.

3.4.1. Determination of actions on the building

The building is subjected to vertical (gravity) loads. The loads are either permanent or variable and are combined in various ways in order to study the various effects and to determine the most unfavorable (worst loading case) situation.

3.4.1.1. Permanent actions

There are two categories of permanent loads acting on the structure which are the permanent structural loads and the permanent non-structural loads. Both are presented in Table 3.3 and 3.4 below.

Table 3.3. Structural loads of building

Nature	Description	Value	Unit
G_{1K}	Hollow block slab (16+4 cm)	2.85	kN/m^2

Table 3.4. Non-structural loads of the building

Nature	Description	Value	Unit
G_{2k}	Tiles	0.44	kN/m^2
G_{2k}	Cement coating(1.5 cm thick)	0.33	kN/m^2
G_{2k}	Partition wall (15 cm thick)	1.35	kN/m^2
G_{2k}	Alucobond	0.08	kN/m^2
Total G_{2k}		**2.2**	**kN/m^2**

3.4.1.2. Variable actions

The building, because of its function is classified as category B building for which the imposed load is in the range 2.0 to 3.0 kN/m^2. In this work we consider an imposed load of 2.5 kN/m^2.

3.4.2. Determination of the load combinations

The load combination in the equations 3.1 and 3.2 provides for the verification of the structure at Ultimate Limit State.

$$1.35G_k + 1.5Q_k \quad \text{(Eq. 3.1)}$$

$$G_k = G_{1k} + G_{2k} \quad \text{(Eq. 3.2)}$$

For non-reversible Serviceability Limit State (SLS), the verification is done using the equation 3.3.

$$G_k + Q_K \quad \text{(Eq. 3.3)}$$

3.4.3. Determination of concrete cover

Considering a concrete structural class S4 and the exposure class XC1 together with the provisions of the Eurocode 2 outlined in section 2.4.3, the minimum concrete cover obtained is given by:

C_{min} = max (16; 15; 10) = 16mm

From Eq. 2.3, $C_{nom} = 16+10 = 26mm$

So, we will consider a concrete cover, c = 30mm.

3.4.4. Modeling of the project

The slab loads are applied directly to the beams as distributed loads. In the same way is applied the loads of the walls as they are considered being carried by the slab. Beams and columns are modelled as frame elements having their connections (beam-column joints) ensured by the insertion of joints between two or more elements. To ensure rigidity of every floor above ground level, a diaphragm constraint is assigned to each node of the structure from the first to the last storey. And finally, the foundations are modelled considering the soil structure interaction. Figure 3.7 shows the 3D structural model of the building.

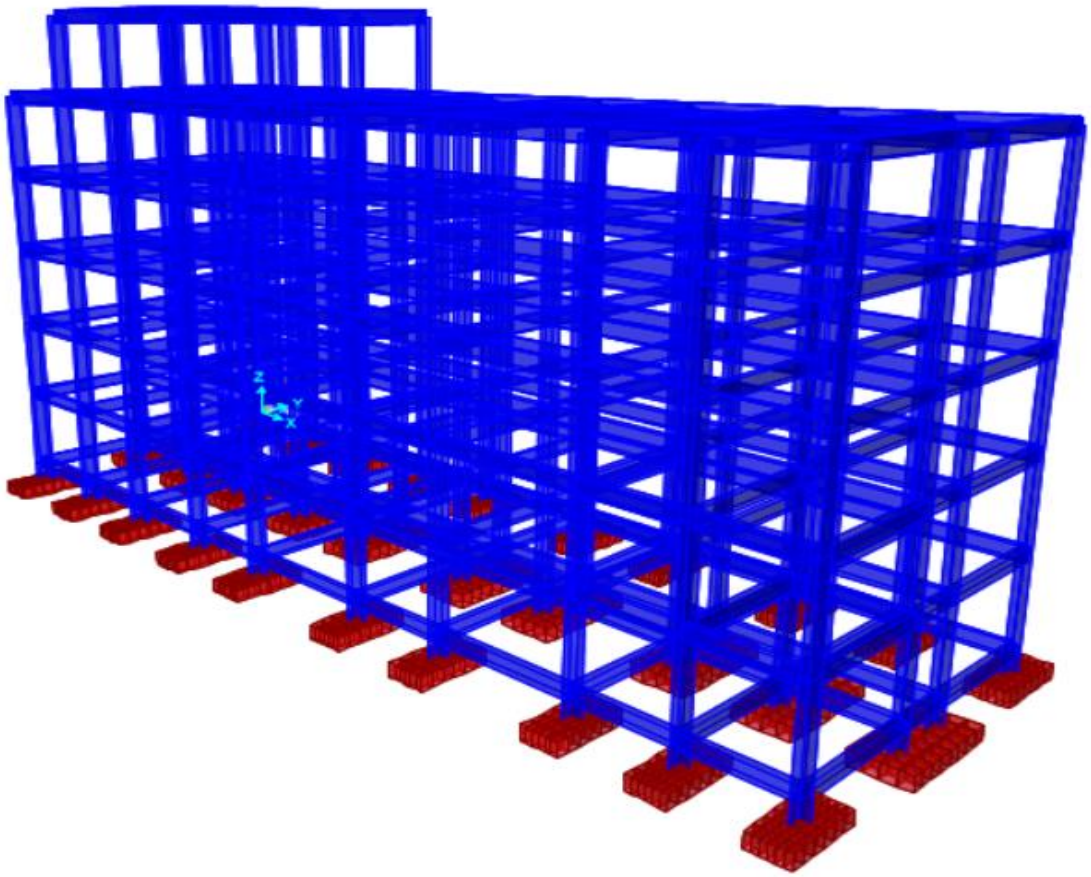

Figure 3.7. 3D structural model of building block B

3.4.5. Horizontal structural element design results

The principal and secondary beams constitute the horizontal structural elements. Principal beams are those which support the slab and transfer the loads to the columns.

3.4.5.1. Preliminary design

Figure 3.8 shows the choice of the beam under study.

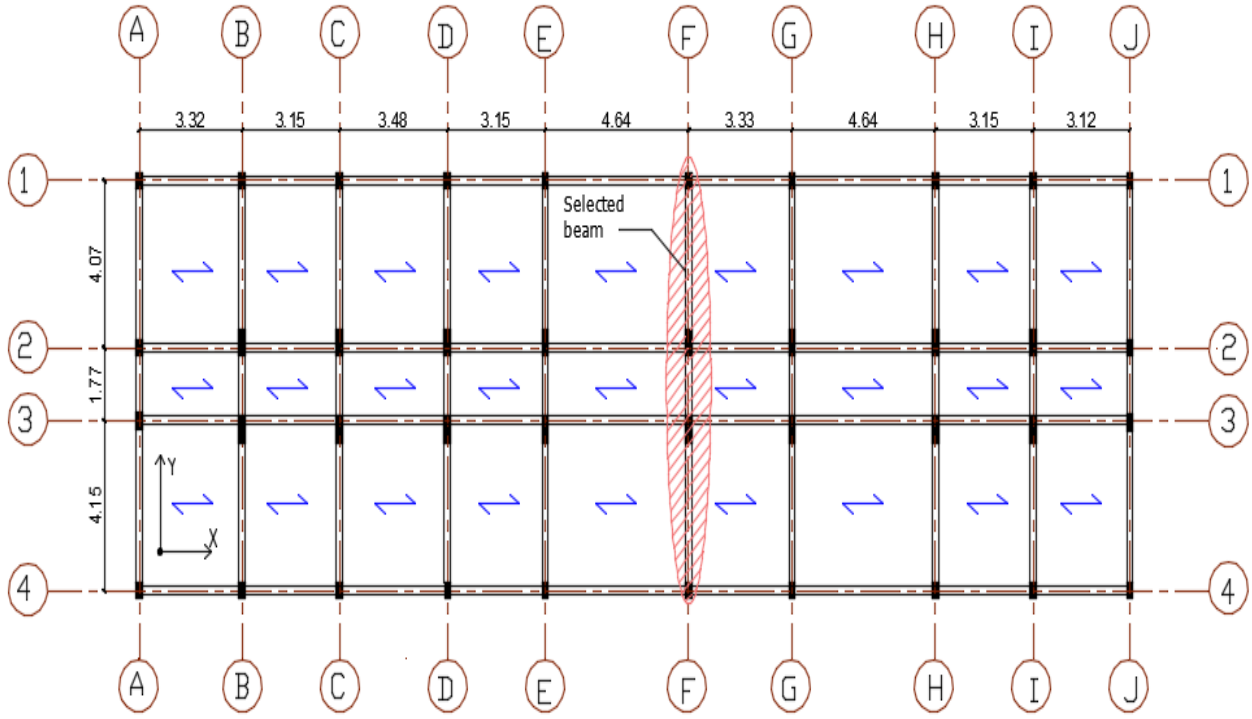

Figure 3.8. Selected beam for design

For the design of the above horizontal element, the loads arrangements from which design solicitation parameters are determined are shown in Figure 3.9.

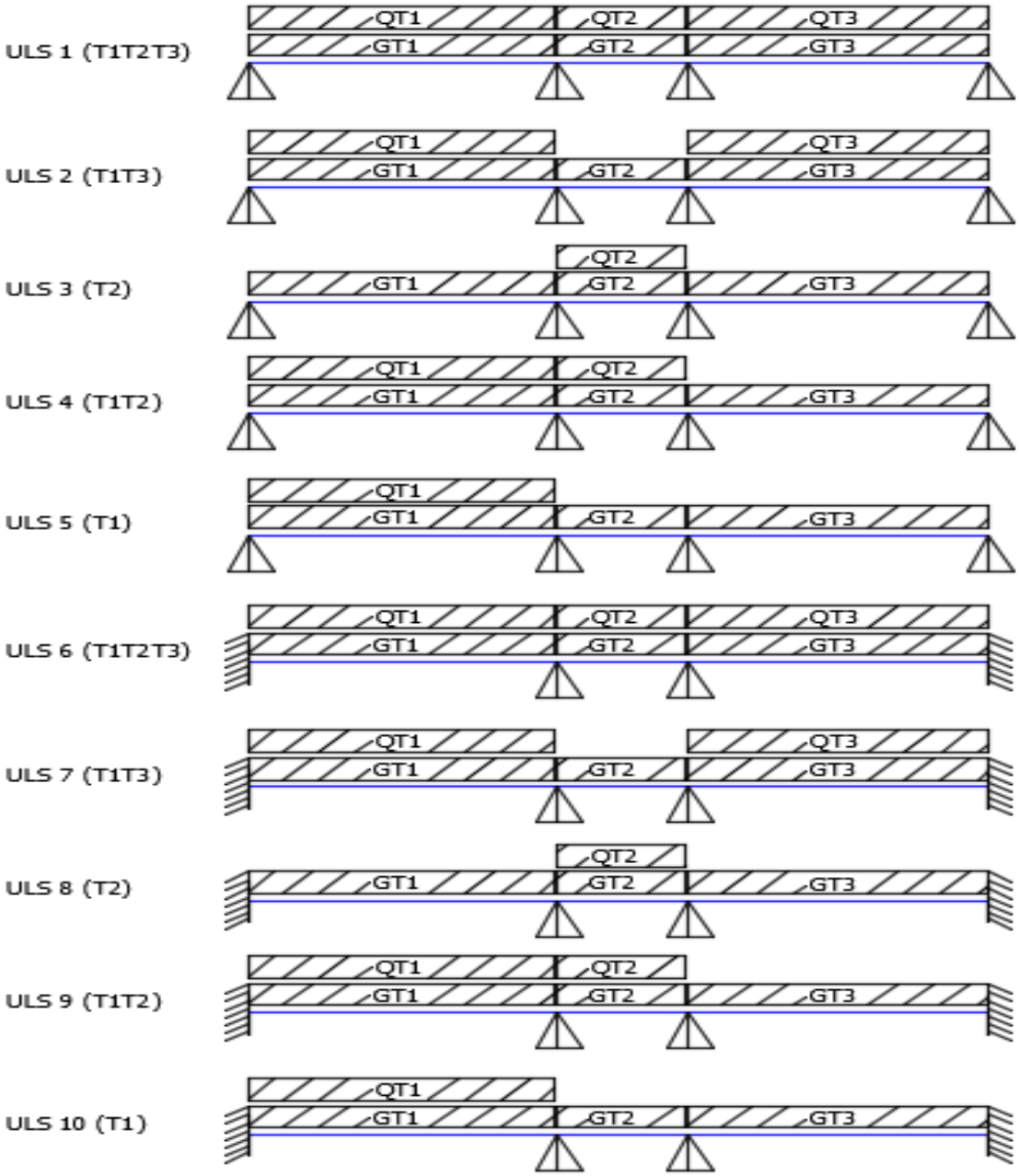

Figure 3.9. Load combinations at ULS

The dimensions b (width) and h (depth) are the geometric characteristics of the beam section. On the site the values measured are b=200 mm and h=500 mm as represented in figure 3.10.

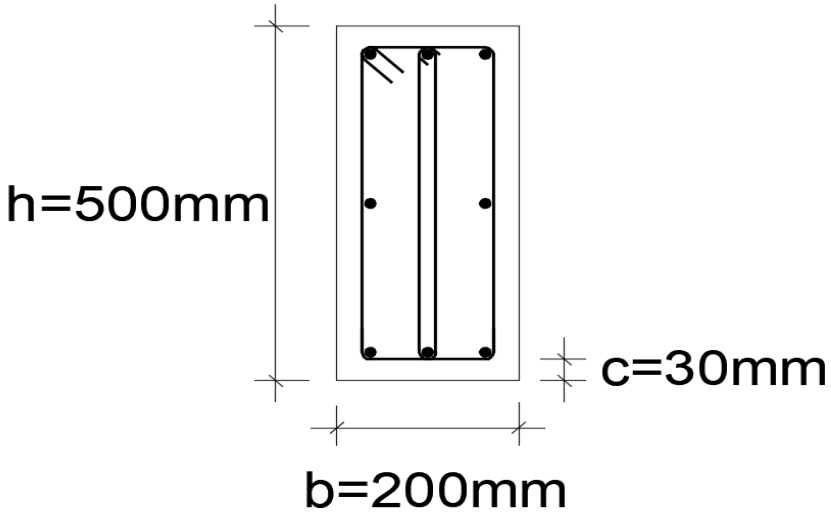

Figure 3.10. . Dimensions of the beam section

End supports of the beam are modelled with simple support for maximum positive bending moment at mid-spans illustrated in figure 3.11(a) and fixed supports for maximum negative bending moment illustrated in figure 3.11(b).

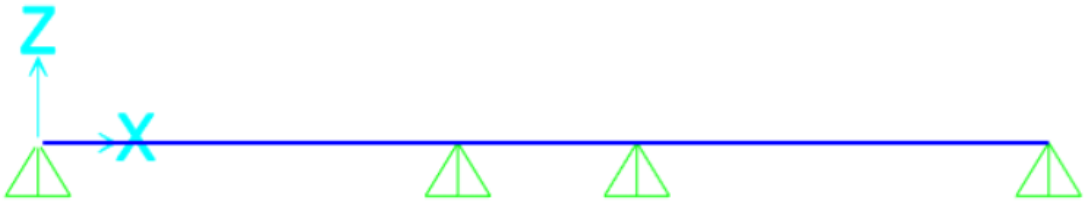

(a) Beam model with simply supported end supports

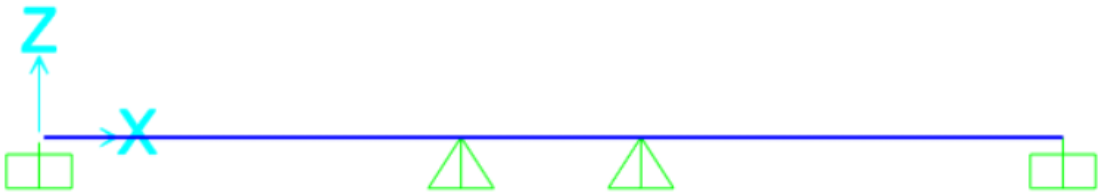

(b). Beam model with fixed end supports

Figure 3.11. Beam model

The analysis from SAP 2000 V22 generates results which presents the solicitation parameters at ULS and SLS. The design and verifications can thus be performed.

3.4.5.2. Ultimate Limit State design

The curves in figure 3.12 and figure 3.13 show the solicitations for bending moment and shear forces respectively for the beam obtained from the results of the analysis drawn using excel.

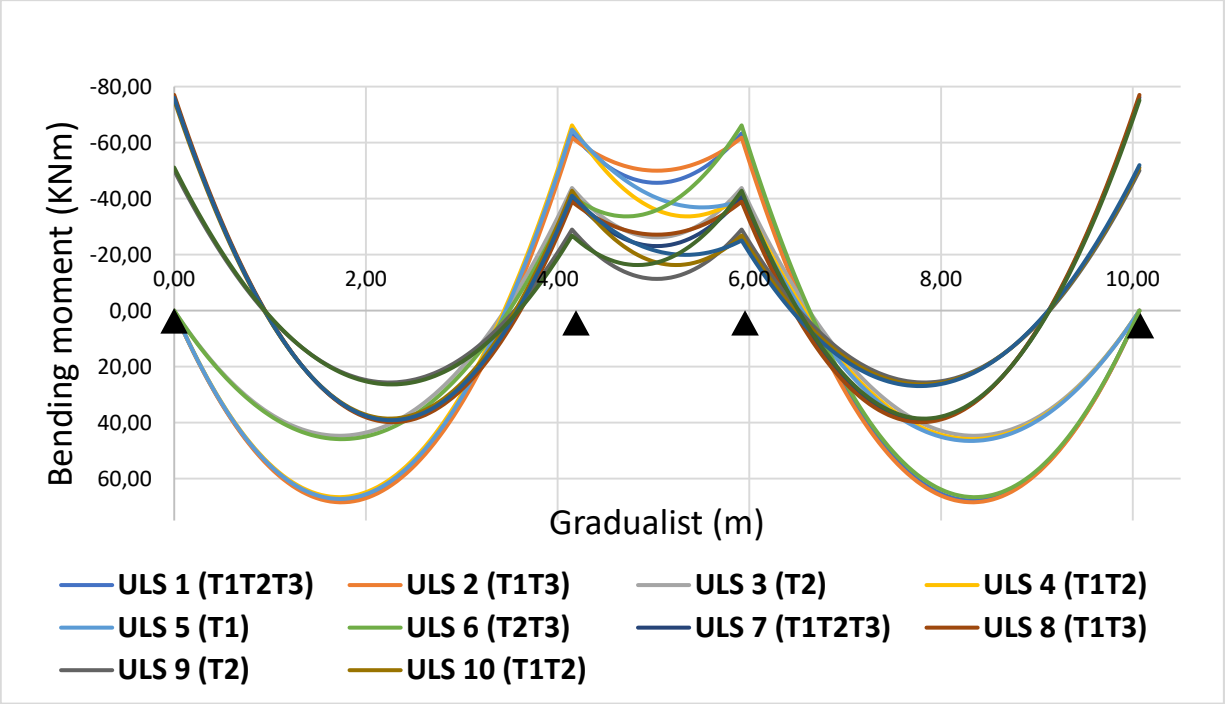

Figure 3.12. Bending moment solicitation curves of the beam

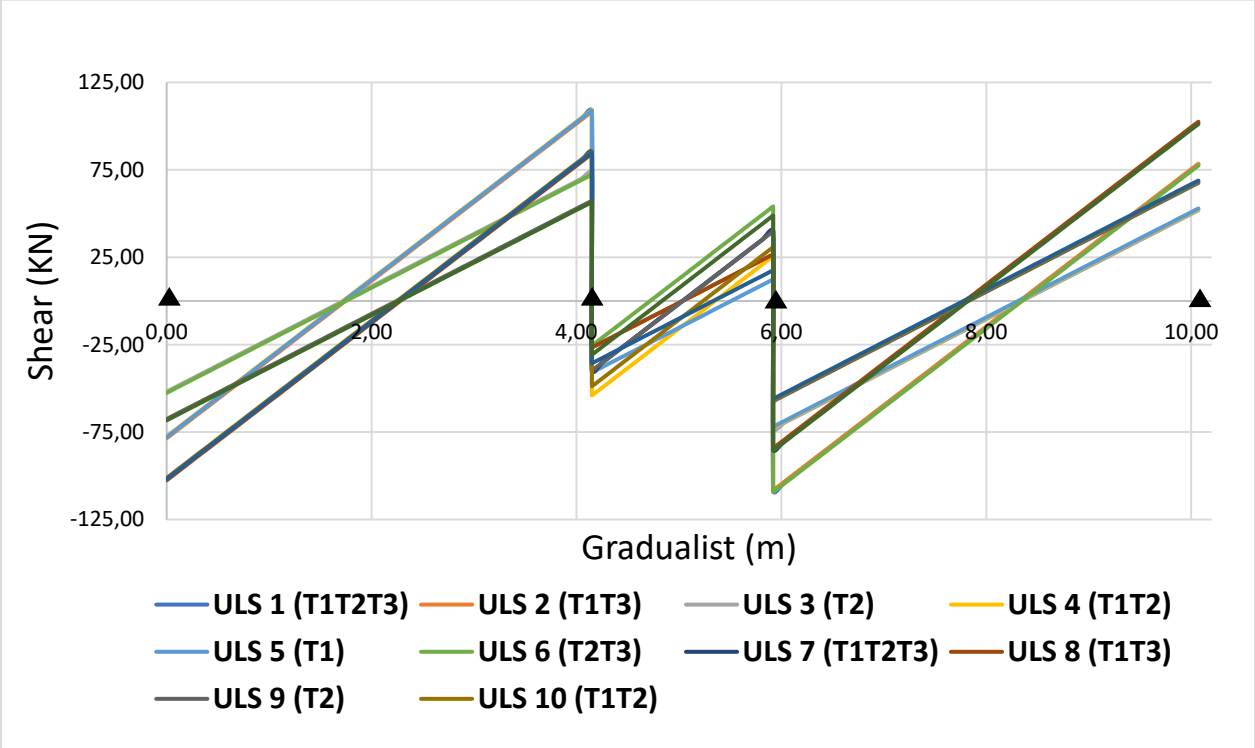

Figure 3.13. Shear solicitation curves on the beam

The design is done using the greatest values of moments and shears in each section. These values corresponds to the maximum of the positive values and the minimum of the negative values. From the curves in figure 3.12 and figure 3.13 above, these values extracted to obtain the envelope curve of both bending moment and shear forces respectively. The envelope curves are represented in figure 3.14 and figure 3.15.

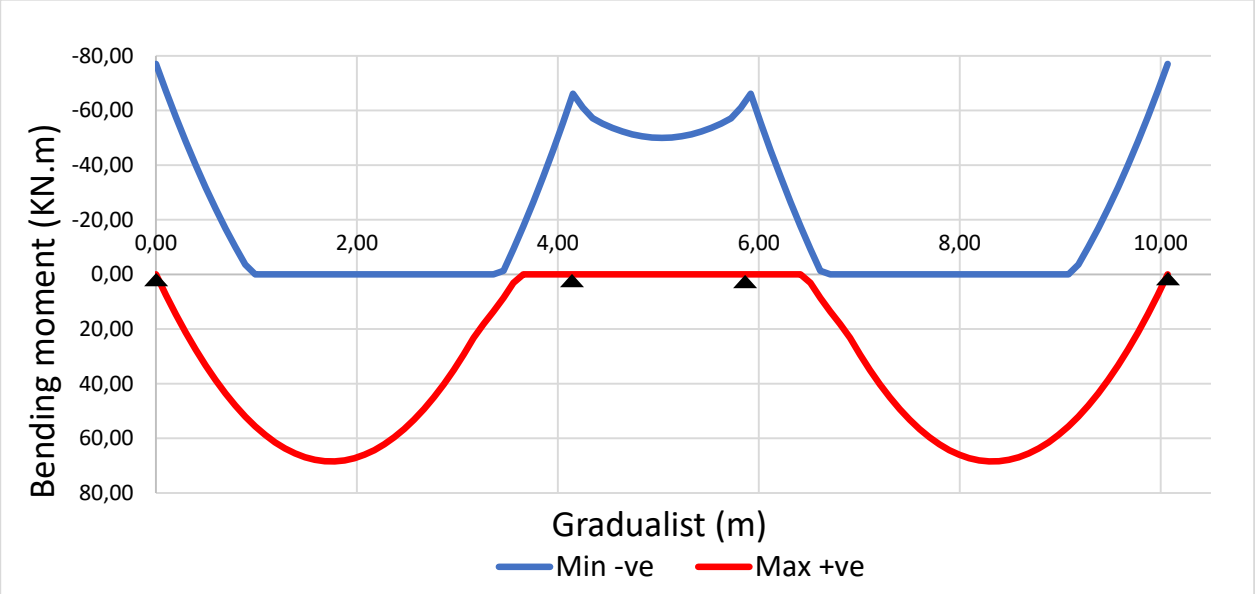

Figure 3.14. Envelope curve for bending moment

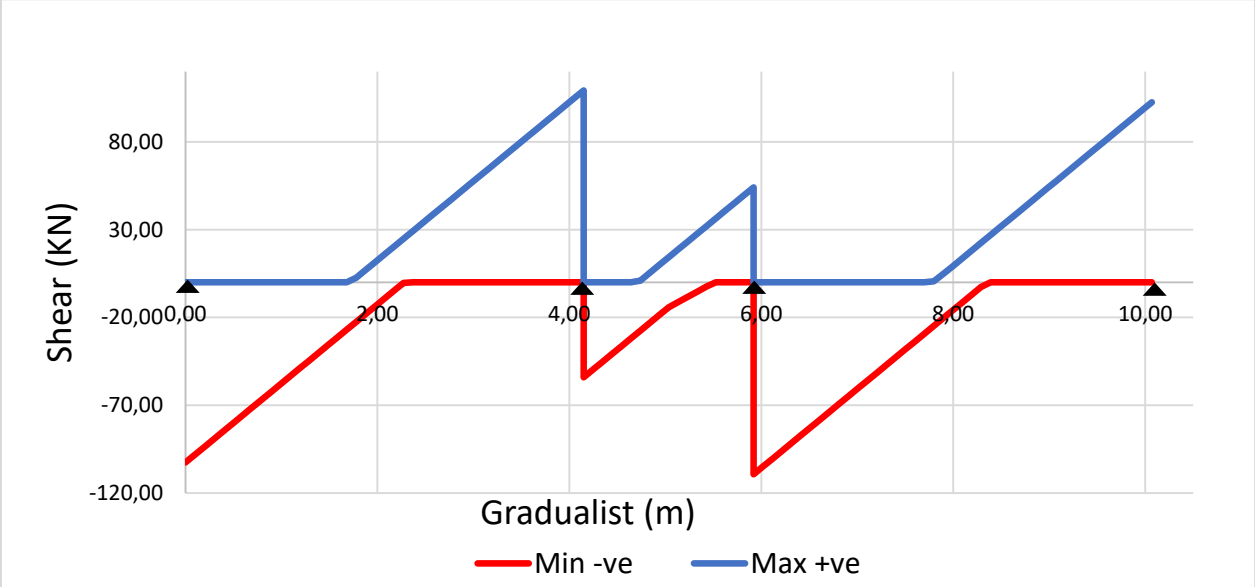

Figure 3.15. Envelope curve for shear solicitation

From the envelope curve of the bending moment presented in figure 3.14, we apply the procedure detailed on the section 2.4.5.1(a) to obtain the final solicitation curve presented in figure 3.16.

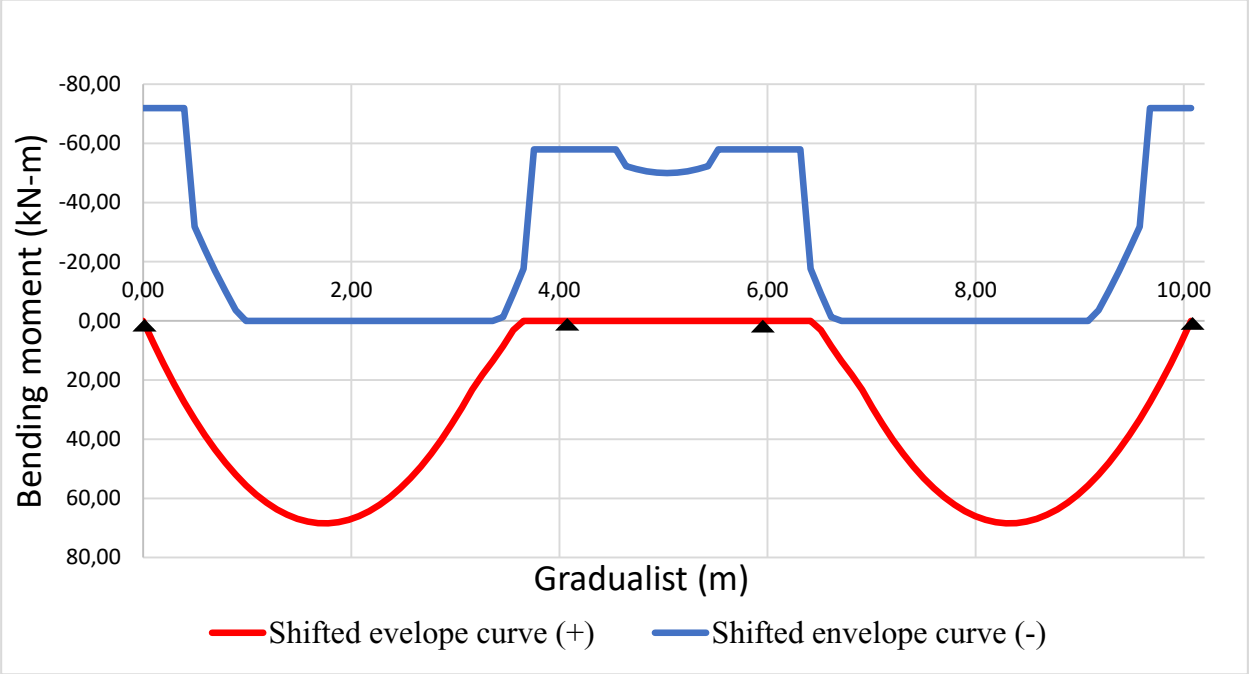

Figure 3.16. Shifted envelope curve for bending moment

The steel reinforcements are computed using Eq. 2.7. The verifications are performed for the detailing of the horizontal structural element using equations 2.8 and 2.9. Finally, the steel section is verified for a beam section of $200\times500\ mm$. Below in Figure 3.17 are the reinforcements obtained from the previous computations.

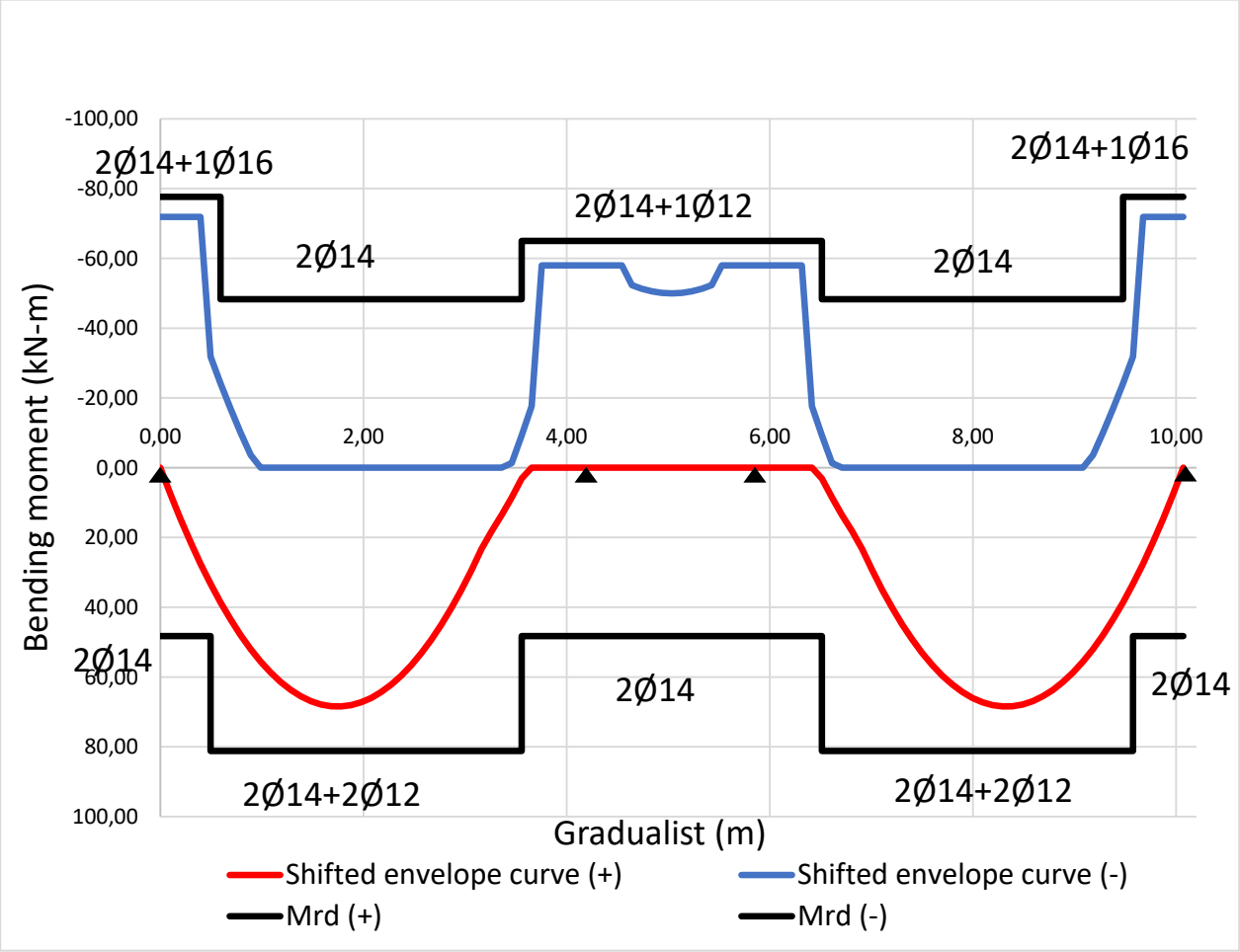

Figure 3.17. Recapitulative curve for bending moment verification of the beam

For the transversal reinforcement, considering a diameter of 6mm, the design procedure presented on the section 2.4.5.1(b) enables to obtain the spacing of the stirrups necessary to resist to the envelope of the shear solicitations. Figure 3.17 presents a recapitulative of these stirrups spacing along the beam.

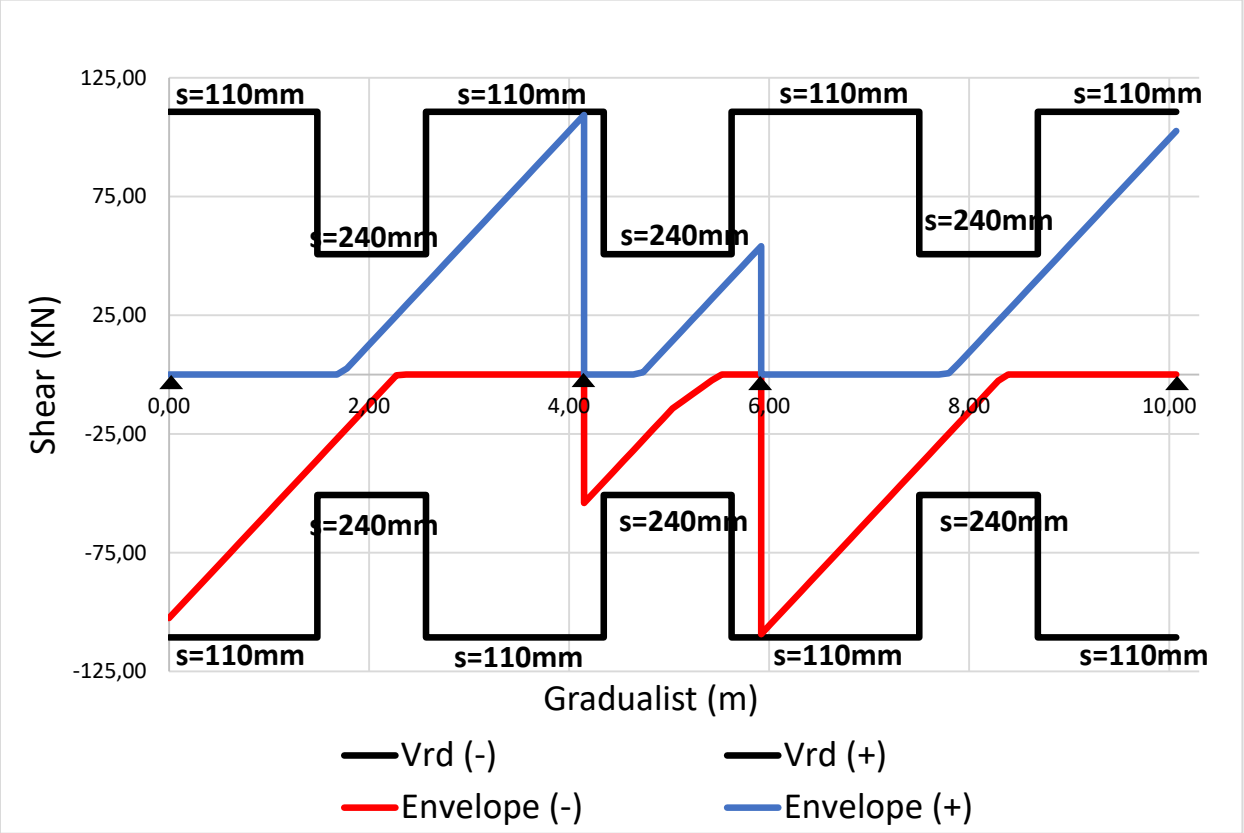

Figure 3.18. Recapitulative curve for shear verification of the beam

3.4.5.3. Stress limitation and deflection control in serviceability limit state

For the same 10 load arrangements of the beam, we obtain the solicitation curves for SLS by using the SLS load combination detailed in section 2.4.5.2, and the results of the bending moments solicitations for each load combination are shown in figure 3.19.

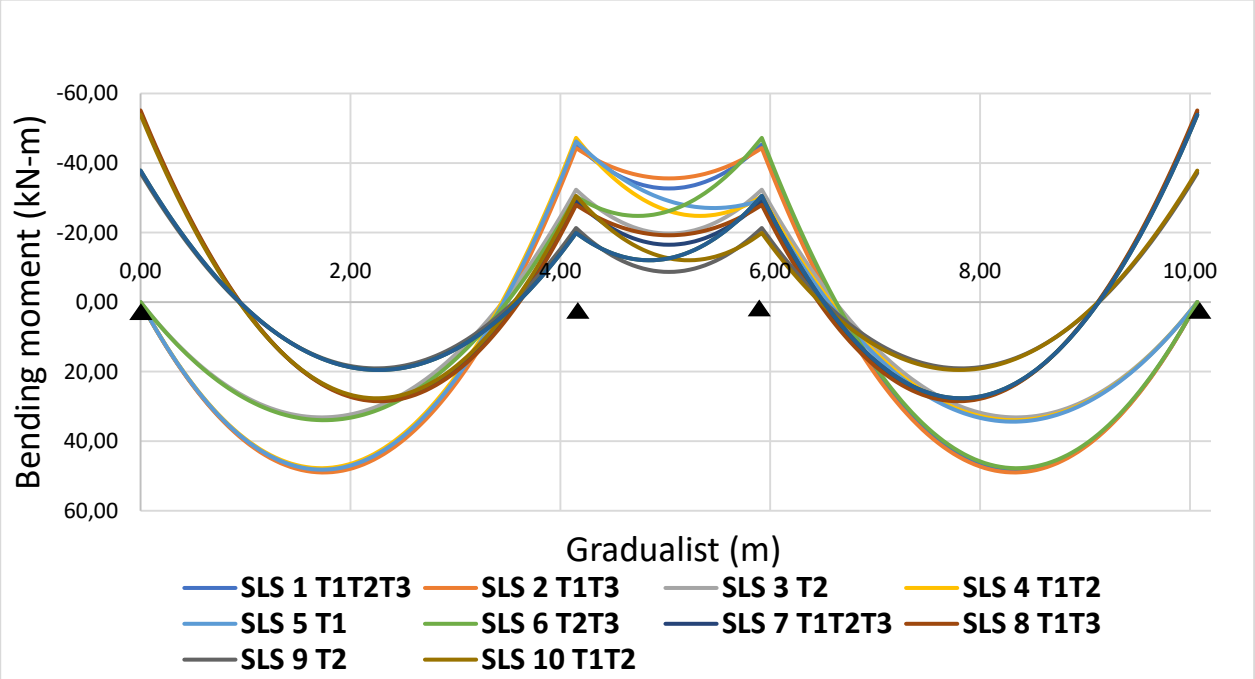

Figure 3.19. Bending moment solicitation curves for the beam at SLS

These solicitations enables to obtain the envelope curve presented in the figure 3.20.

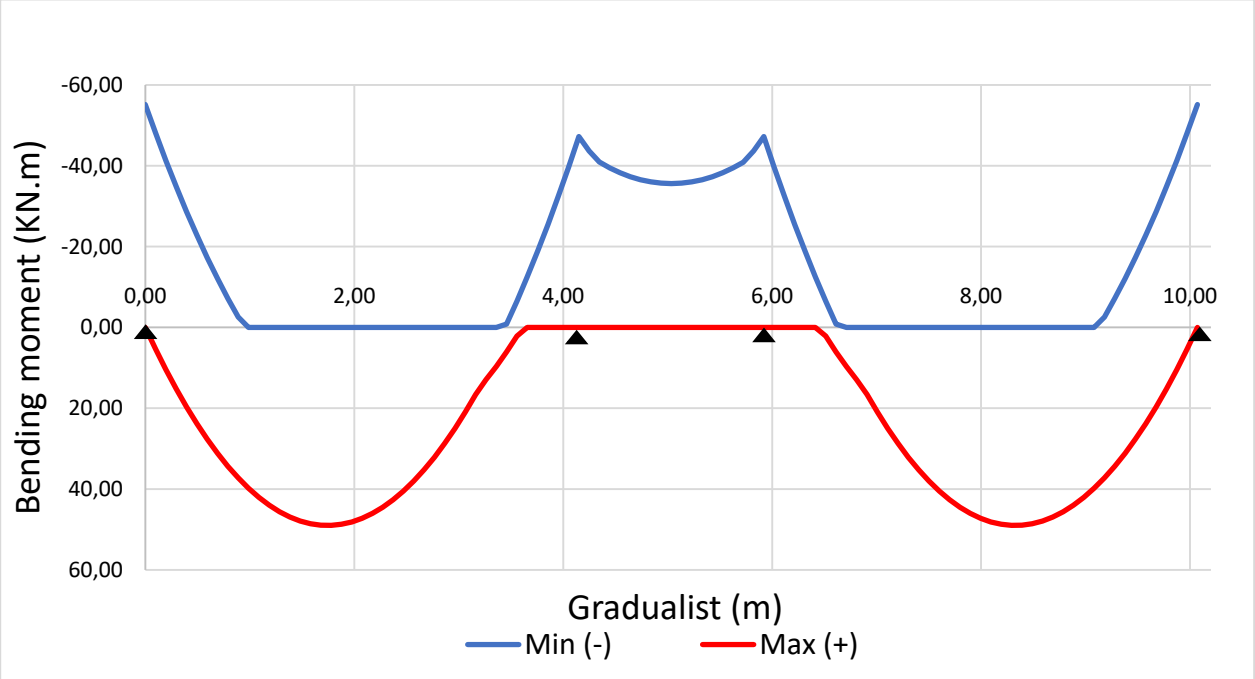

Figure 3.20. Envelope curve for bending moment at SLS

With this envelope curve for bending moment at serviceability limit state the stress in the concrete and in the reinforcement are obtained using the equations 2.22 and 2.23 respectively. The limit values on the stresses are evaluated from the equations 2.24 and 2.25 using the recommended values of the Eurocode 2. Figure 3.21 shows the respective curves for the stress verification in both concrete (a) and steel (b).

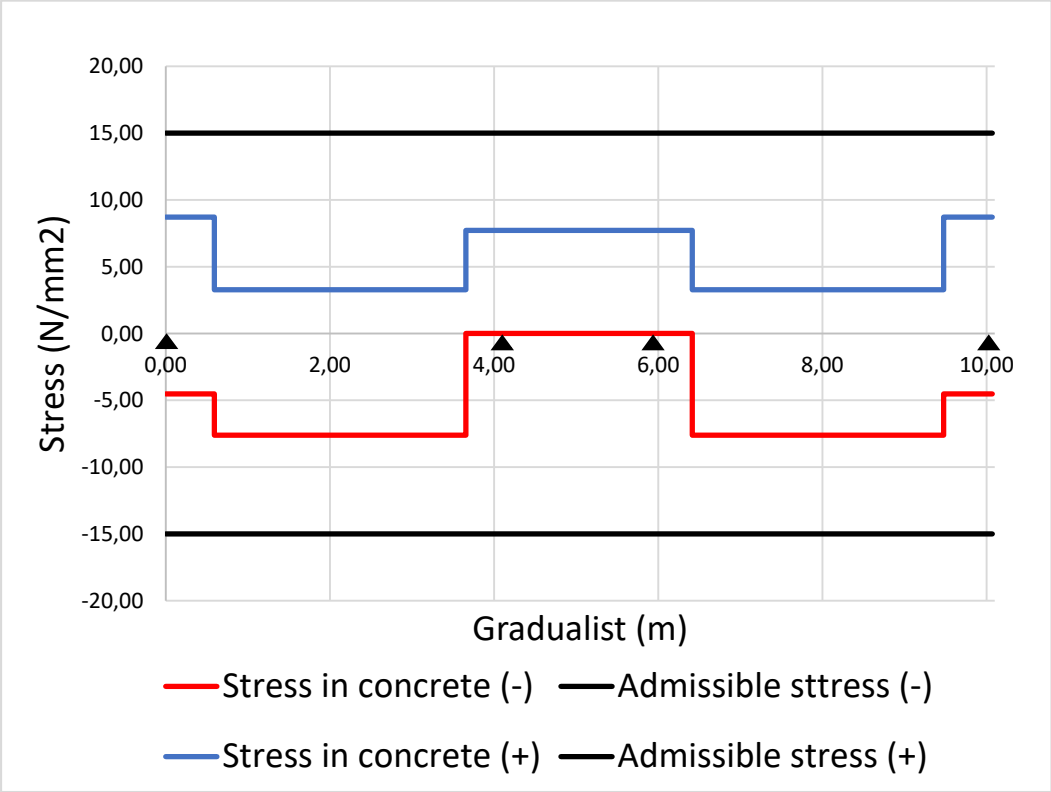

(a) Stress verification in concrete

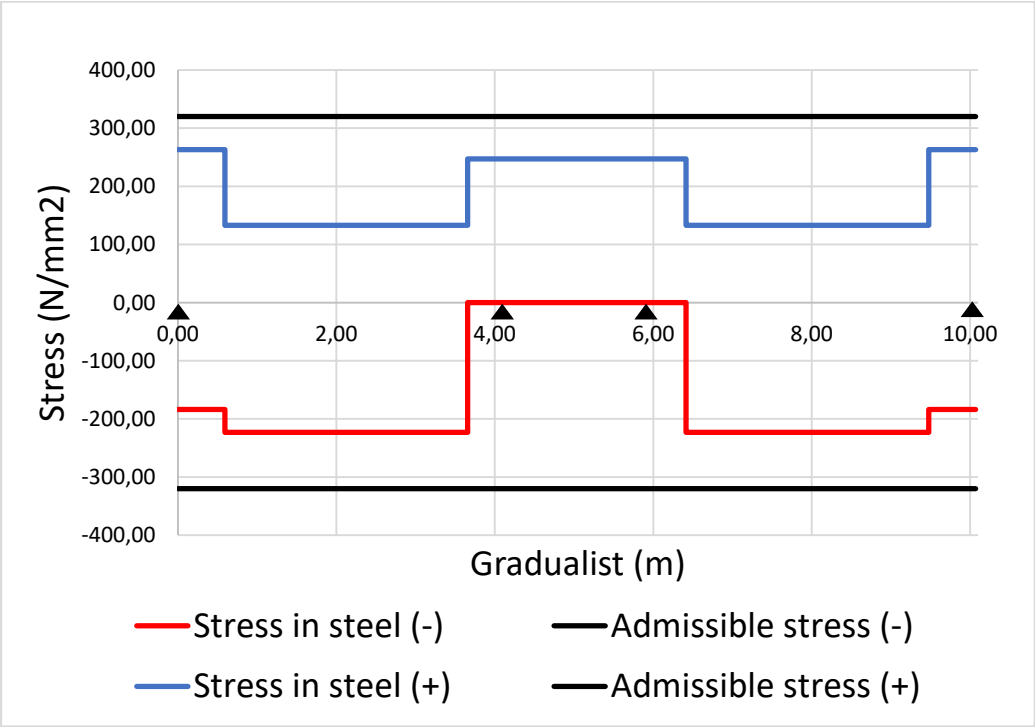

(b) Stress verification in steel

Figure 3.21. Recapitulative curve of the stress verification of the beam

The computation of the deflection control is done according to procedures detailed in section 2.4.5.2(b). The different results of this computation are presented in Table 3.5.

Table 3.5. Deflection at pre-cracking and cracked phase

PRE-CRACKING PHASE	
Inertia moment I_1	2351666218 mm^4
Deflection, f_1	1.32 mm
CRACKING PHASE	
Neutral axis, X_2	73 mm
Inertia moment, I_2	27436215.2 mm^4
Deflection, f_2	5.27 mm
First cracking moment, M_{cr}	21.5 kNm
Moment at SLS, M	47.23 kNm
Deflection, f	4.45 mm
Maximum deflection, L/250	16.6 mm
Since f < L/250, then deflection is verified	

Figure 3.22 shows the details of the designed beam.

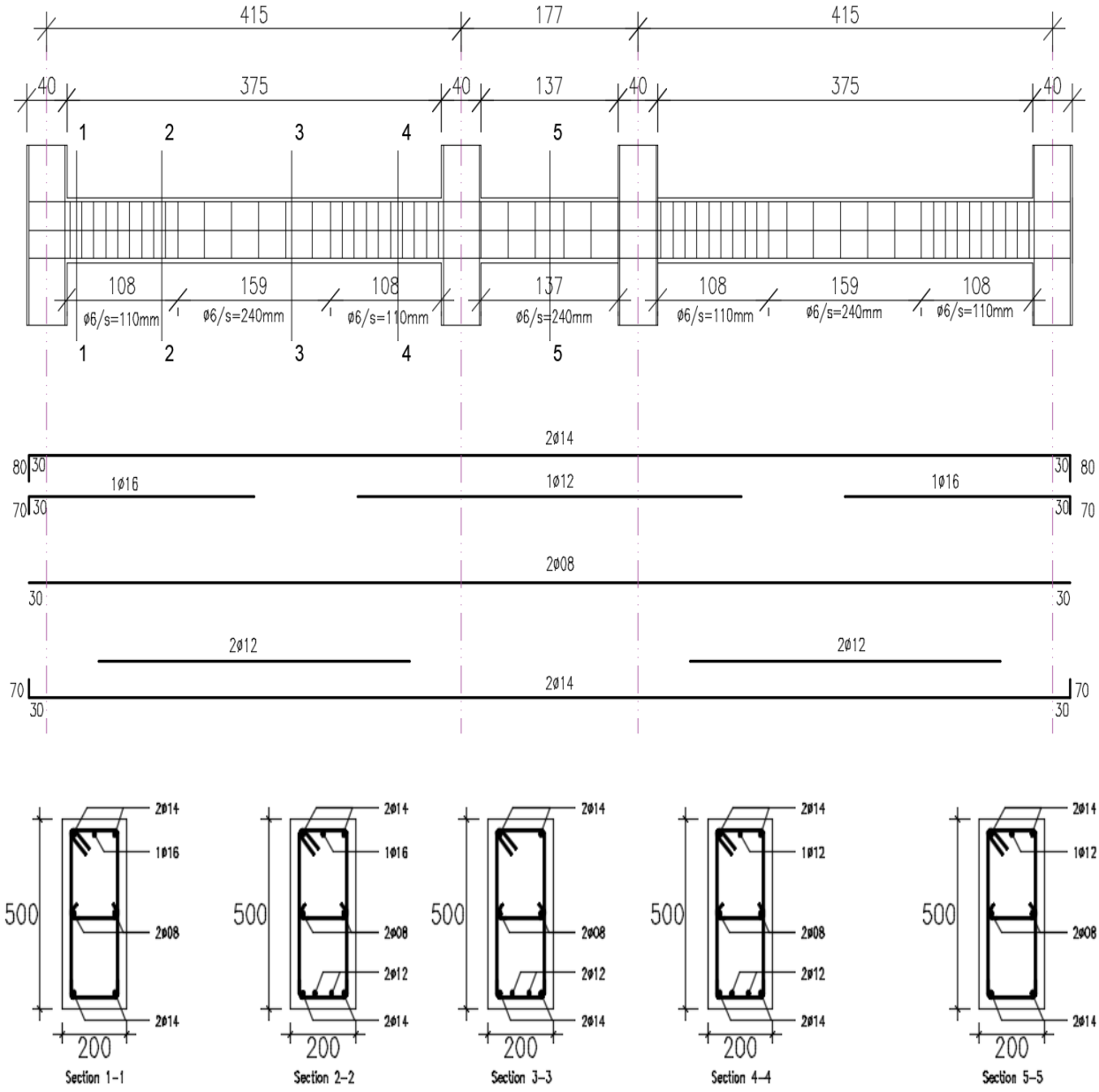

Figure 3.22. Recapitulative of the beam detailing

3.4.6. Vertical structural element design results

A column line corresponding to the most loaded one is selected and designed to represent the other column lines.

3.4.6.1. Preliminary design

The column chosen for the design is the column corresponding to row F2 presented in figure 3.23.

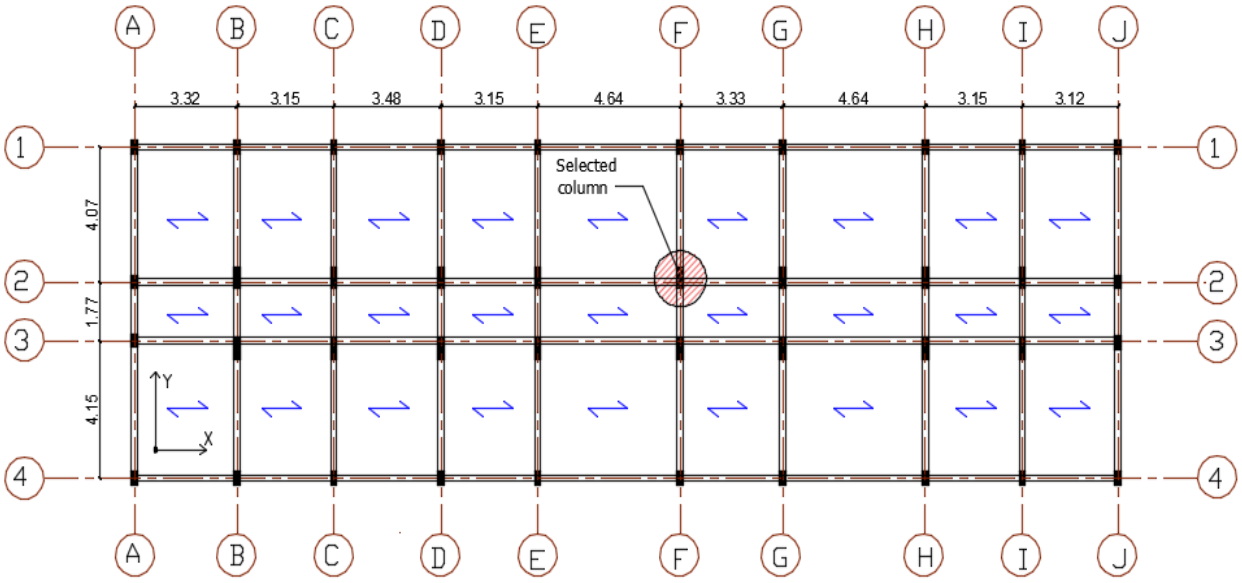

Figure 3.23. Choice of the studied column

The combination of the principal beams loads arrangements and the secondary beams loads arrangements leads to seven (07) load arrangements for the columns.

The dimensions b (width) and h (depth) are the geometric characteristics of the column section. On the site the values measured are b=200 mm and h=400 mm as represented in figure 3.24. This section of column goes from the first to the last floor.

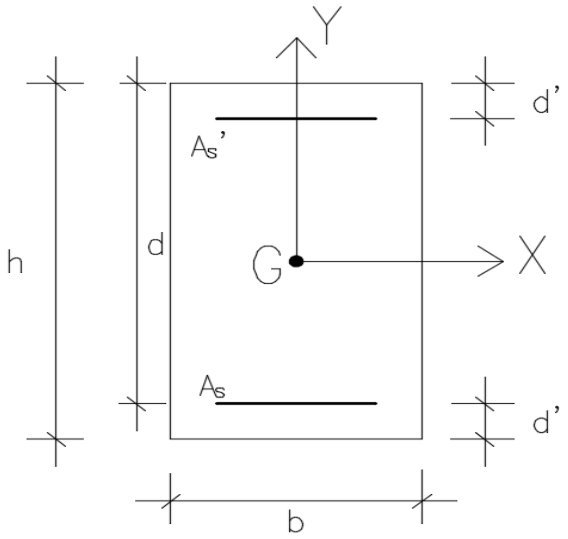

Figure 3.24. Dimensions of the beam section

3.4.6.2. Bending moment-axial force design verification

The load combinations considered for the principal and secondary beams of the building generate the following solicitation curves for bending moment presented in figure 3.25 and axial force presented in Figure 3.26.

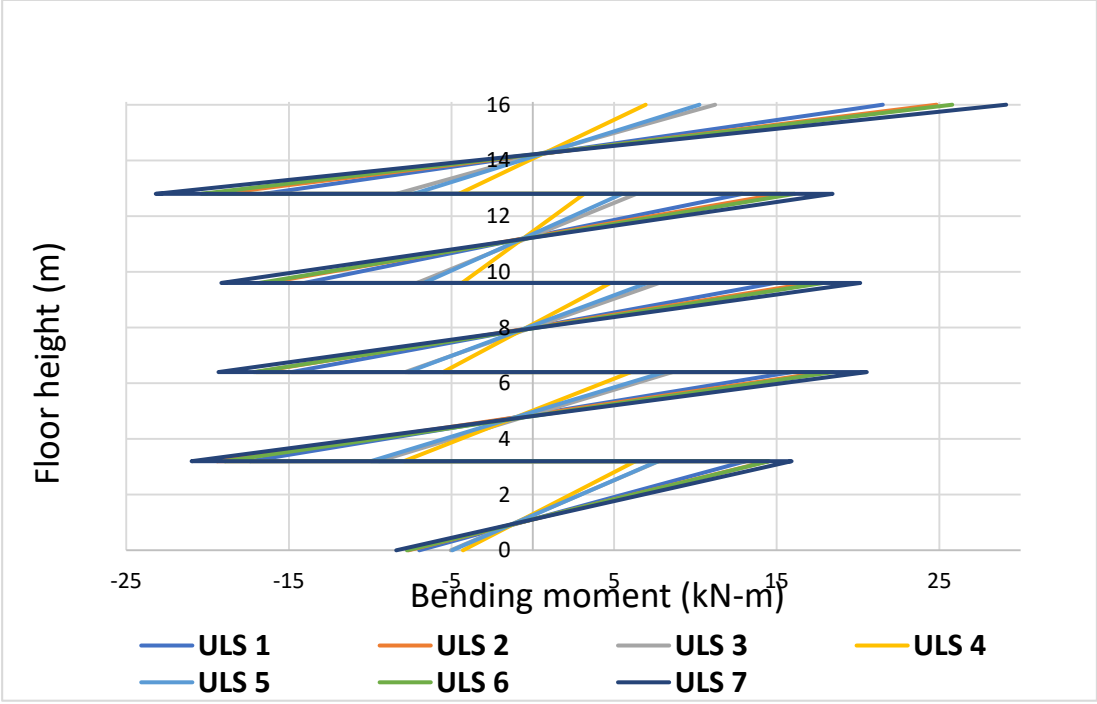

(a) Bending moment solicitation curves in the x-direction

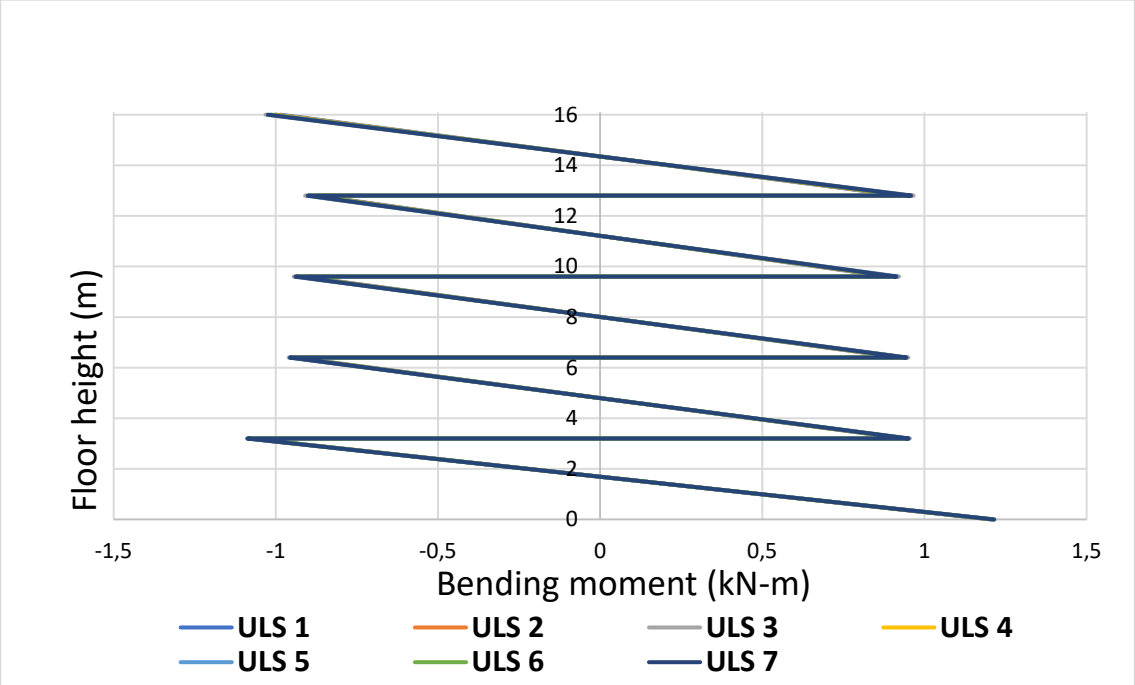

(b) Bending moment solicitation in the y-direction

Figure 3.25. Bending moment solicitation curves on the columns

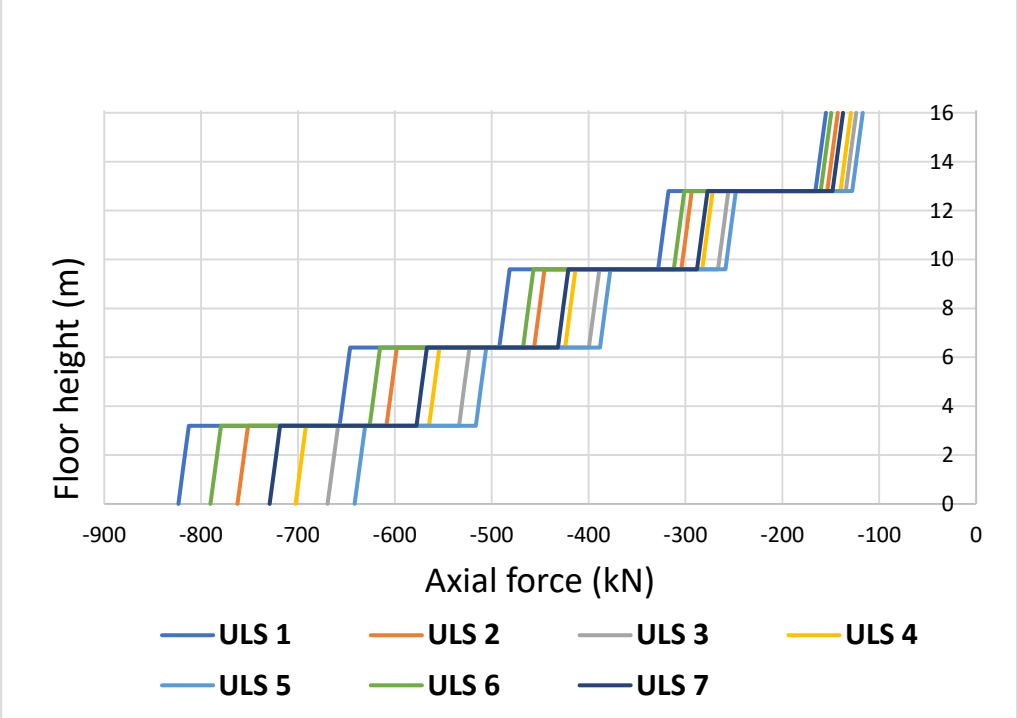

Figure 3.26. Axial load solicitation curve on the column

Similarly to the beam design, the maximum of the positive values and the minimum of the negative values are extracted from the curves in figure 3.25 and figure 3.26 above to obtain the envelope curve for both bending moment and axial forces respectively. The envelope curves are presented in figure 3.27 and figure 3.28.

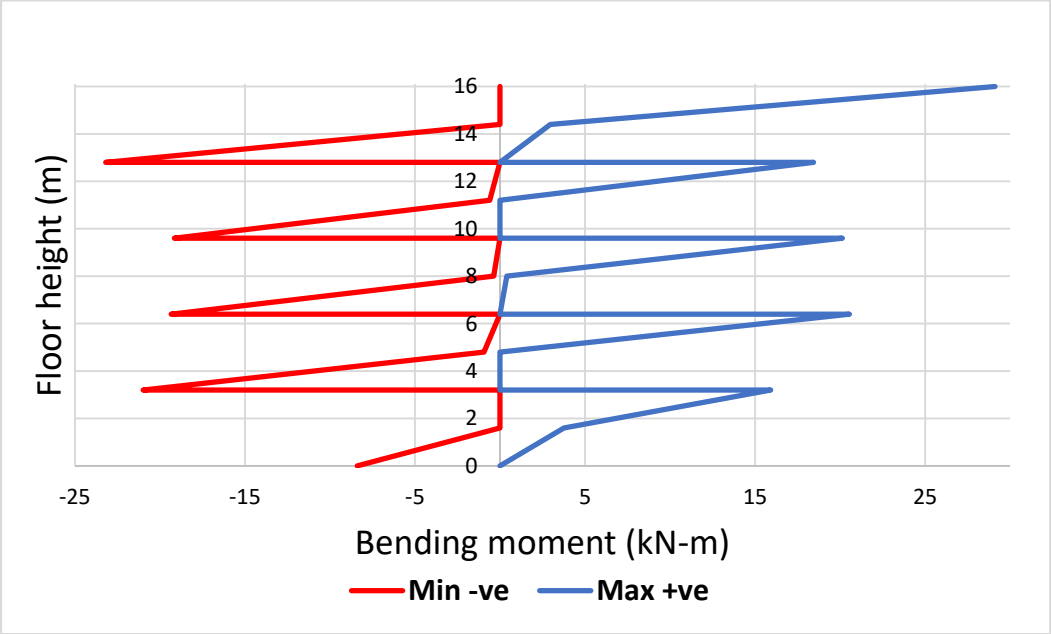

(a) Bending moment envelope curve on the x-axis

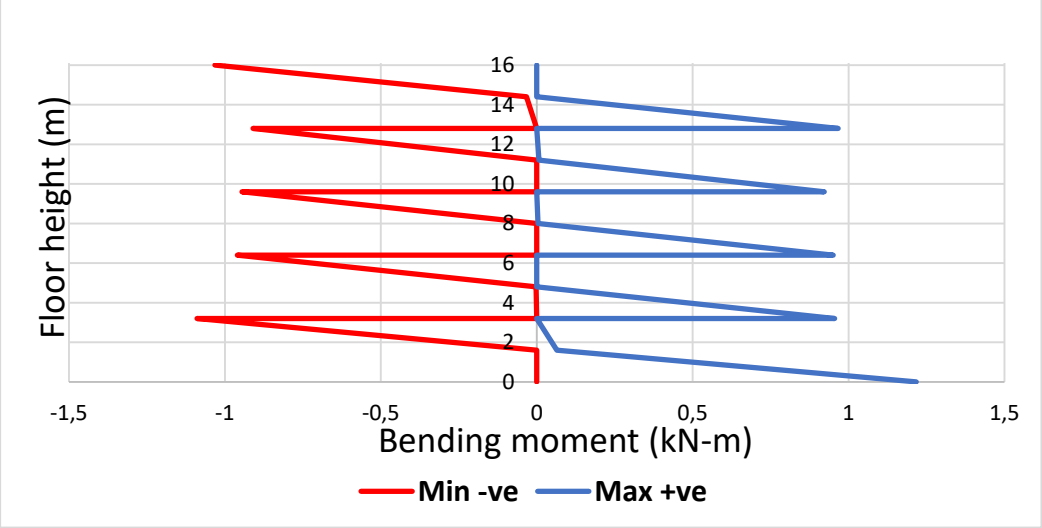

(b) Bending moment envelope curve on the y-axis

Figure 3.27. Envelope curve of bending moment on the column

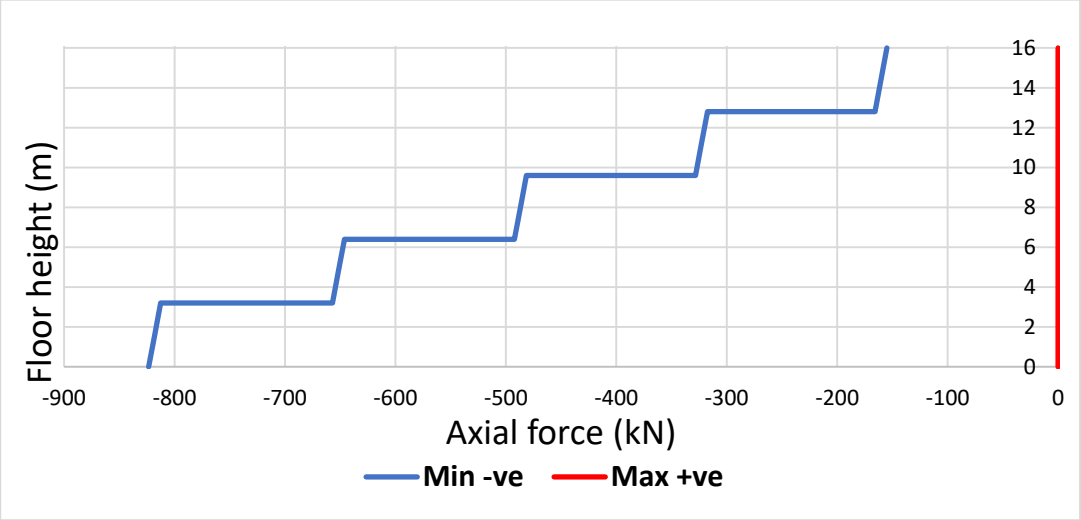

Figure 3.28. Envelope curve of axial load on column

The column verification can be assessed by calculating moment-axial load interaction diagram. Tension is assumed negative, whereas compression is considered positive. According to section 2.6.3.2 we obtain that $237mm^2 \leq A_s \leq 5600\ mm^2$. Therefore, we select 4 Ø14 and 2 Ø10 (A_s = 772.44 mm^2) and a concrete cover, c = 30 mm.

This column section can be verified by calculating moment-axial load interaction diagram in both X and Y directions. Tension is assumed negative, whereas compression is considered positive. The M-N diagram for the columns are presented in figure 3.29 and figure 3.30 for x-direction and y-direction respectively.

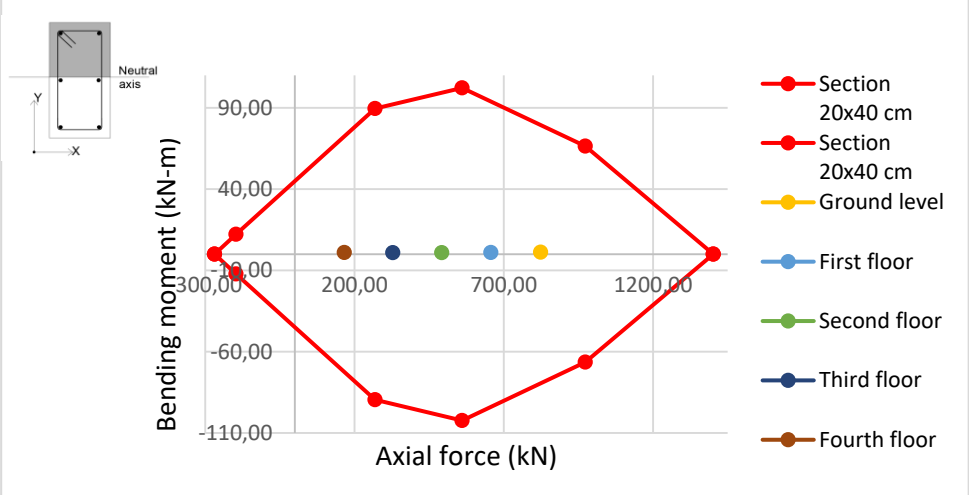

Figure 3.29. Interaction diagram of the column F2 in the x-direction

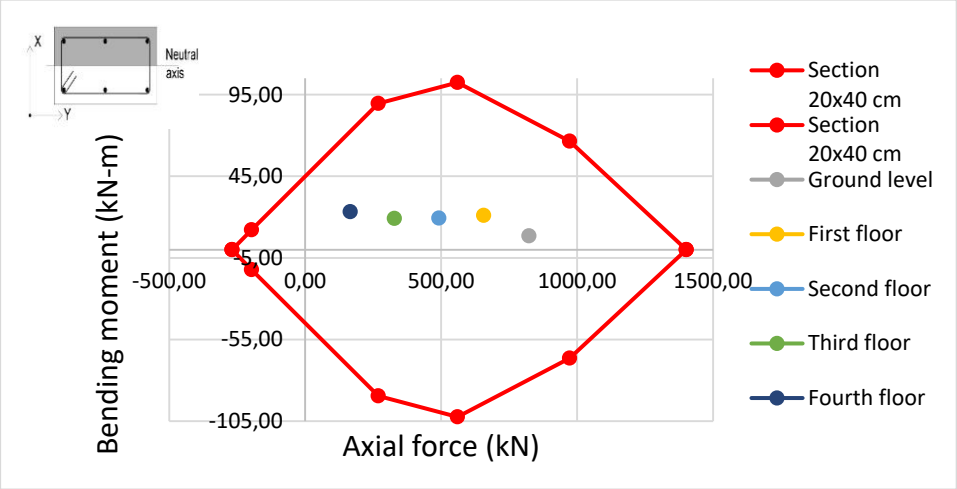

Figure 3.30. Interaction diagram of the column F2 in the y-direction

From the construction of the interaction diagram of the column, it is possible to observe that the acting forces on the element fell inside the diagram and, therefore, the column is able to withstand them.

3.4.6.3. Shear verification

The solicitation curves for shear from the load arrangements are obtained for both x and y directions as presented in figure 3.31.

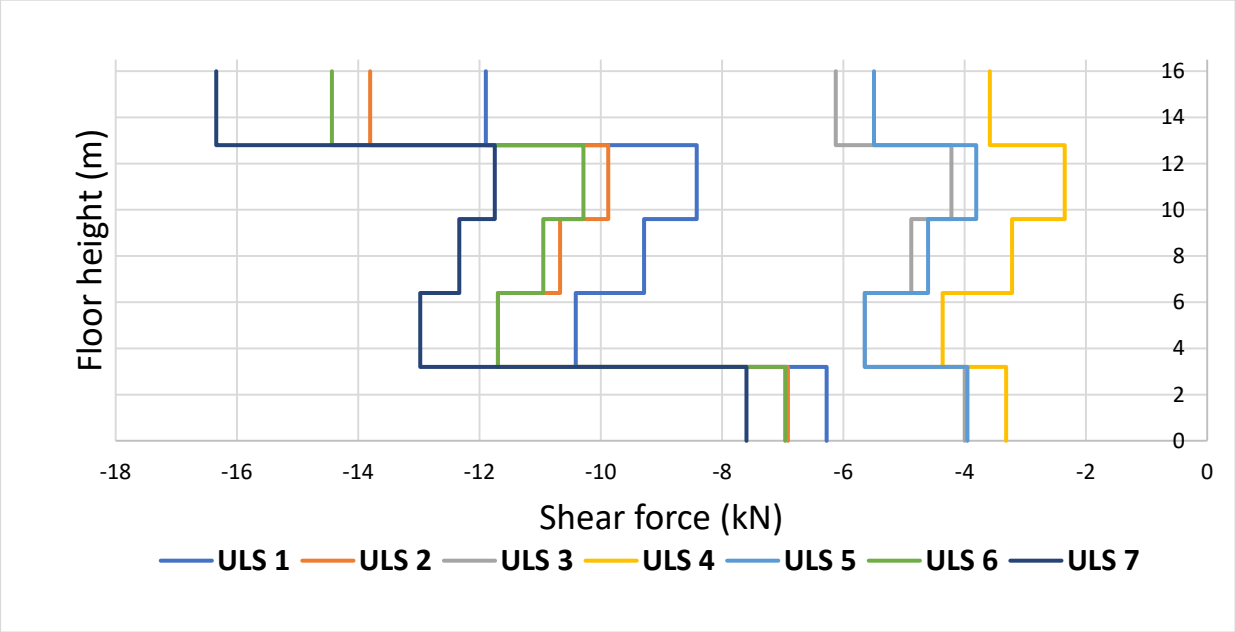

(a) Shear force solicitation curves in the x-direction

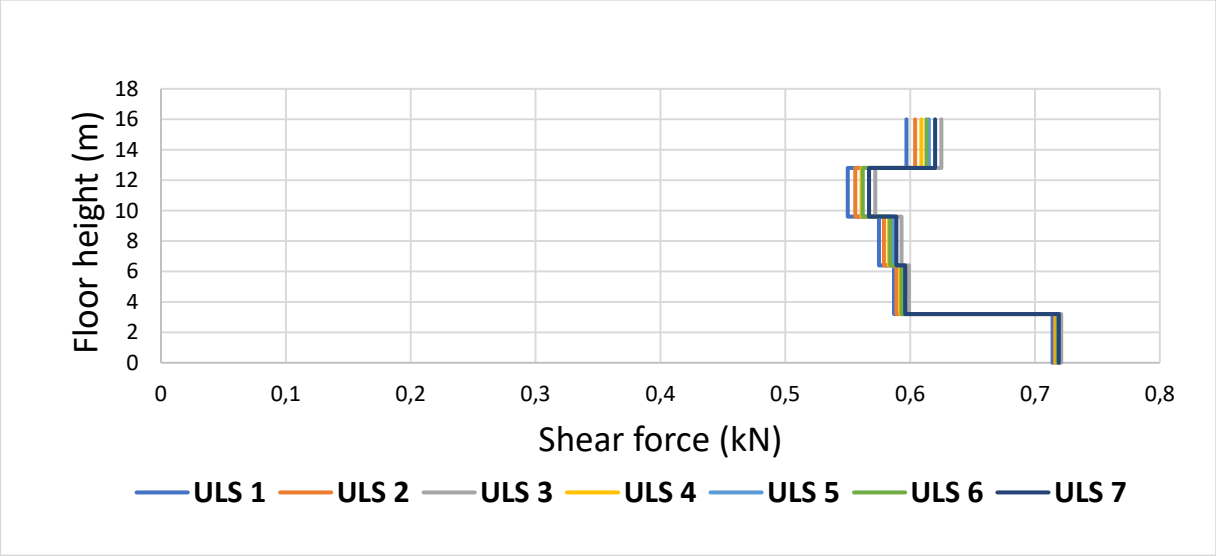

(b) Shear force solicitation curves in the y-direction

Figure 3.31. Shear force solicitation curve on the column

The envelope curves obtained from figure 3.31 are shown in figure 2.32.

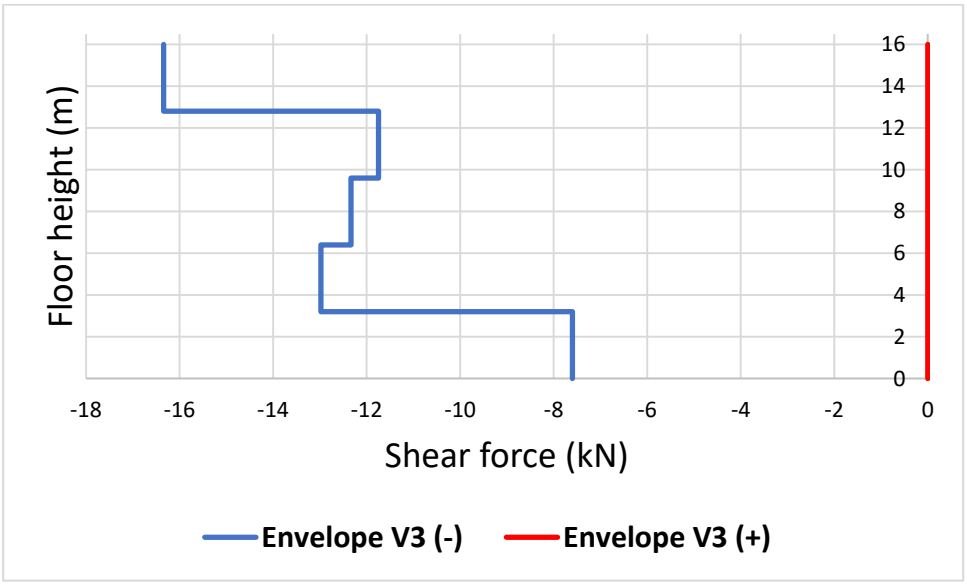

(a)Shear force envelope curve in the x-axis

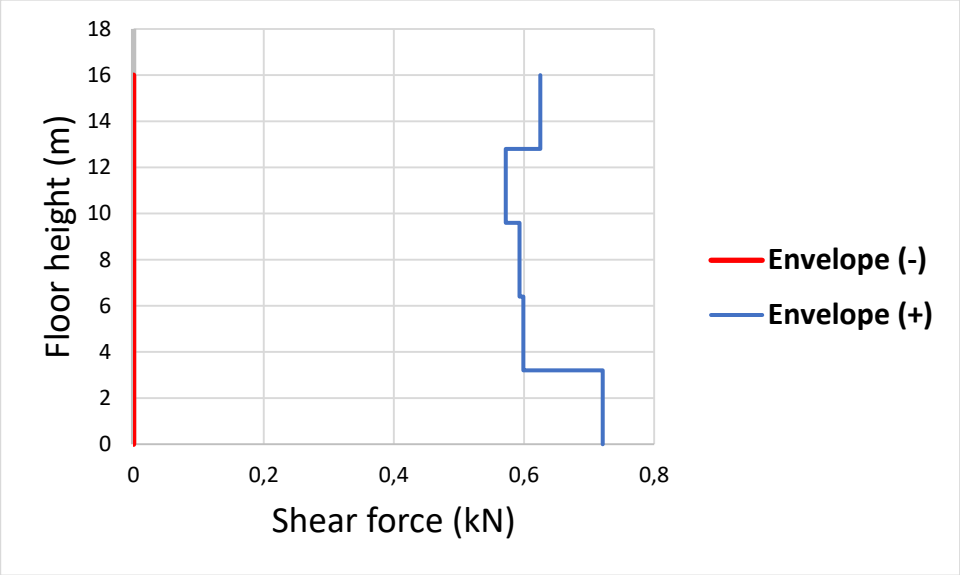

(b) Shear force envelope curve on the y-axis

Figure 3.32. Shear force envelope on the column

Applying the procedure presented in the section 2.4.5.1(b) and 2.4.6.2, we observe that the shear resistance of the section without shear reinforcement ($V_{rd,c}$ = 47.16kN) is greater than the maximum shear solicitation on the column. So we can apply the maximum spacing. If we consider a diameter of $6mm$ as stirrups, the maximum spacing of the transverse reinforcement is given by:

$S_{cl,max} = \min(280; 200; 400) = 200mm$

So, we obtain a spacing of the shear reinforcement of:

- 12 cm within 0.4 m above and below the beam
- 20 cm along the rest of the column section

3.4.6.4. Slenderness verification

Following the procedure presented on the section 2.4.6.3, the different parameters are evaluated and presented in table 3.6.

Table 3.6. Parameter for the computation of λ_{lim}

A	B	C	n
0.7	1.38	1.7	0.73

The limit value of the slenderness obtained is: $\lambda_{lim} = 27.99$

The slenderness of an element is evaluated using the equation 2.40. So, $\lambda = l_o/i$

The application of the equation 2.41 permits to evaluate the gyration radius of the section and we obtain: $i = 0.115\ m$

For a column height of 3.2m, we have the slenderness $\lambda = 19.48 < \lambda_{\text{lim}}$. So the slenderness is verified for the column. Figure 3.33 shows the details of the designed column.

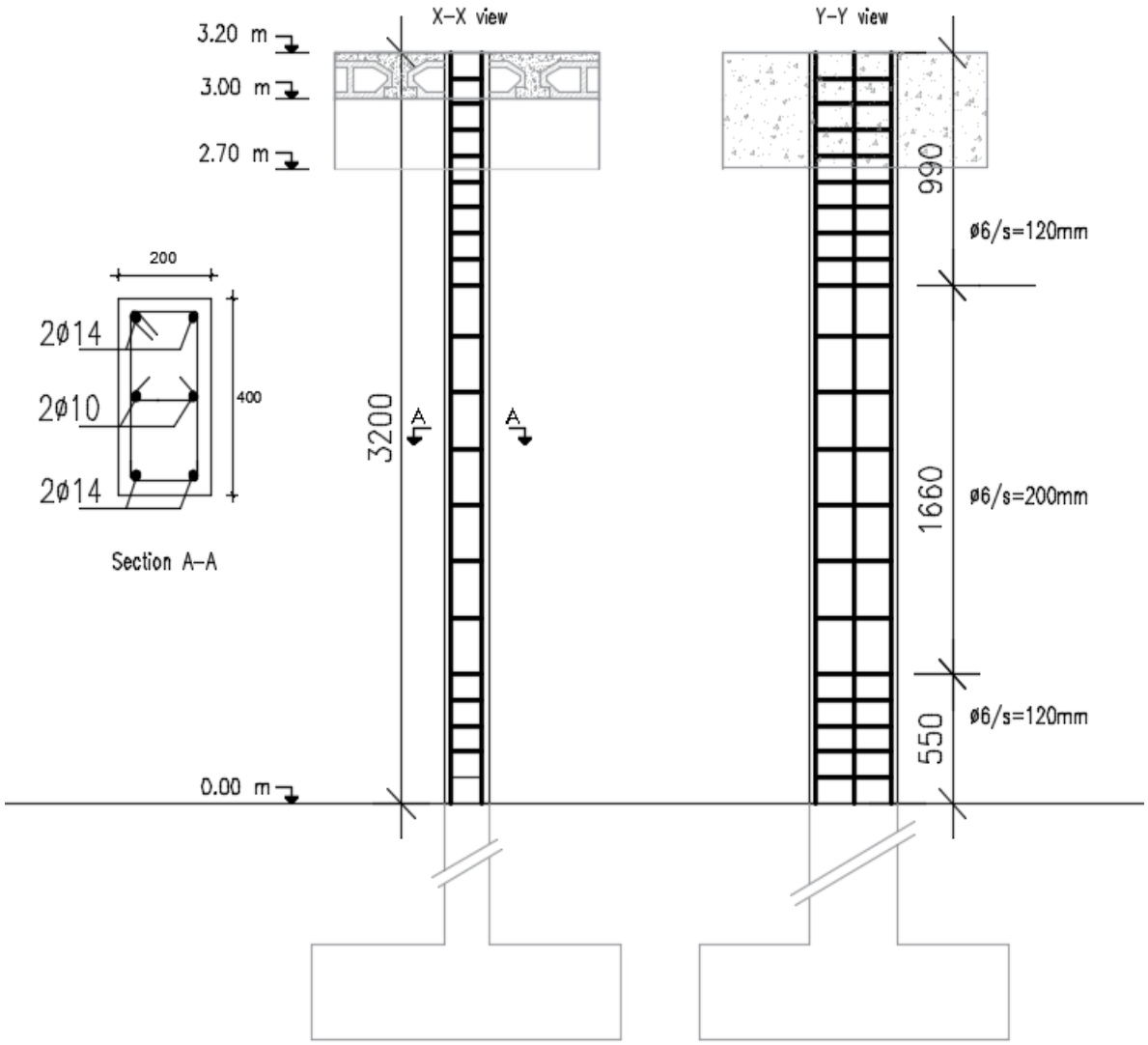

Figure 3.33. Recapitulative of the column detailing

3.4.7. Foundation design results

Here all the results obtained after the footings design using soil structure interaction are presented.

3.4.7.1. Soil-structure interaction

The soil considered for this study is medium gravel with fine sand with a modulus of subgrade reaction of value 100000 kN/m^3.

3.4.7.2. Isolated footing design results

The most loaded isolated footing is selected and this serves as a representative of the other footings.

(a) Preliminary design

The selected footing for the design is shown in figure 3.34.

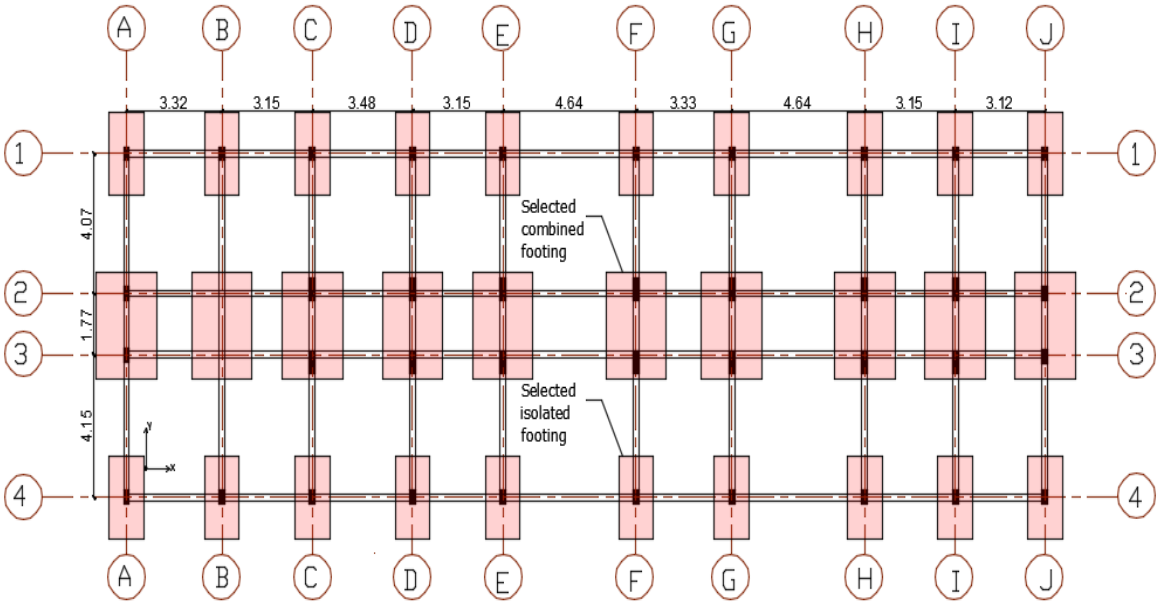

Figure 3.34. Selected footings for the design

The section and depth obtained for the footing are presented in table 3.7

Table 3.7. Section and depth of the isolated footing

Designations	Values	Units
Axial load at SLS, N_{SLS}	823.443	kN
Admissible stress, σ_{adm}	0.3	N/mm^2
Area, S	$2.88x10^6$	mm^2
Depth, h	500	mm

(b) Geotechnical design

The maximum value of the soil pressure beneath the footing is 0.298 N/mm^2 which is less than the admissible soil pressure (0.3 N/mm^2).

(c) Structural design

The values obtained for the section of the longitudinal reinforcement are presented in table 3.7.

Table 3.8. Moment and reinforcement sections of the isolated footing

Designations	Values	Units
Moment in the x-direction, M_x	148,6741	kNm/m
Moment in the y-direction, M_y	257,1538	kNm/m
Area of steel in the x-direction, $A_{s,x}$	1055,391	mm^2/m
Area of steel in the y-direction, $A_{s,y}$	1825,454	mm^2/m

3.4.7.3. Combined footing design results

The most loaded combined footing is selected and this serves as a representative of the other footings.

(a) Preliminary design

The selected footing for the design is shown in figure 3.34. The section and depth obtained for the footing are presented in table 3.8.

Table 3.9. Section and depth of the combined footing

Designations	Values	Units
Axial load at SLS, N_{SLS}	1646.886	kN
Admissible stress, σ_{adm}	0.3	N/mm^2
Area, S	$6.3x10^6$	mm^2
Depth, h	500	mm

(b) Geotechnical design

The maximum value of the soil pressure beneath the footing is 0.274 N/mm^2 which is less than the admissible soil pressure (0.3 N/mm^2).

(c) Structural design

The values obtained for the section of the longitudinal reinforcement are presented in table 3.9.

Table 3.10. Moment and reinforcement sections of the combined footing

Designations	Values	Units
Moment in the x-direction, M_x	181,359	kNm/m
Moment in the y-direction, M_y	173,479	kNm/m
Area of steel in the x-direction, $A_{s,x}$	1287,411	mm^2/m
Area of steel in the y-direction, $A_{s,y}$	1231,469	mm^2/m

3.5. Crack analysis modelling and results interpretations

The literature review suggested that use of a finite element package to model reinforced concrete beams was indeed feasible. The geometric properties used in the model including the detail reinforcement are obtained from the design of the horizontal and vertical elements. The model consists of the 3 spans of the beam and half of the height of the columns supporting this beam to simulate real beam-column connection.

3.5.1. Crack analysis modelling

The main units are: Newton (N) for the force, millimeters (mm) for the distance, $tons/mm^3$ for the density.

3.5.1.1. Parts

Nine parts have been created in the part module of the software and they are:

- **Beam part**: This part was model as a 3d deformable solid. The section of the beam is 200mm of width and 500mm of height and the length is 10470mm.
- **Beam PHI 16 part**: These are longitudinal bars for beams modelled as wire elements with line shape of 10410mm.
- **Beam PHI 14 part**: These are longitudinal bars for beams modelled as wire elements with line shape of 10410mm.
- **Beam PHI 12 part**: These are longitudinal bars for beams modelled as wire elements with line shape of 10410mm.
- **Beam PHI 08 part**: These are longitudinal bars for beams modelled as wire elements with line shape of 10410mm.
- **Beam PHI 06 part:** These are stirrups also modelled as wire element with rectangular shape. Taking into account the concrete cover of 30mm, the rectangle is 440mm long and 140mm wide.
- **Column part**: This part was model as a 3d deformable solid. The section of the beam is 200mm of width and 400mm of height and the length is 1500mm.
- **Column PHI 14 part**: These are longitudinal bars for beams modelled as wire elements with line shape of 1940mm.
- **Column PHI 06 part:** These are stirrups also modelled as wire element with rectangular shape. Taking into account the concrete cover of 30mm, the rectangle is 340mm long and 140mm wide.

The various dimensions are shown in Figure 3.32.

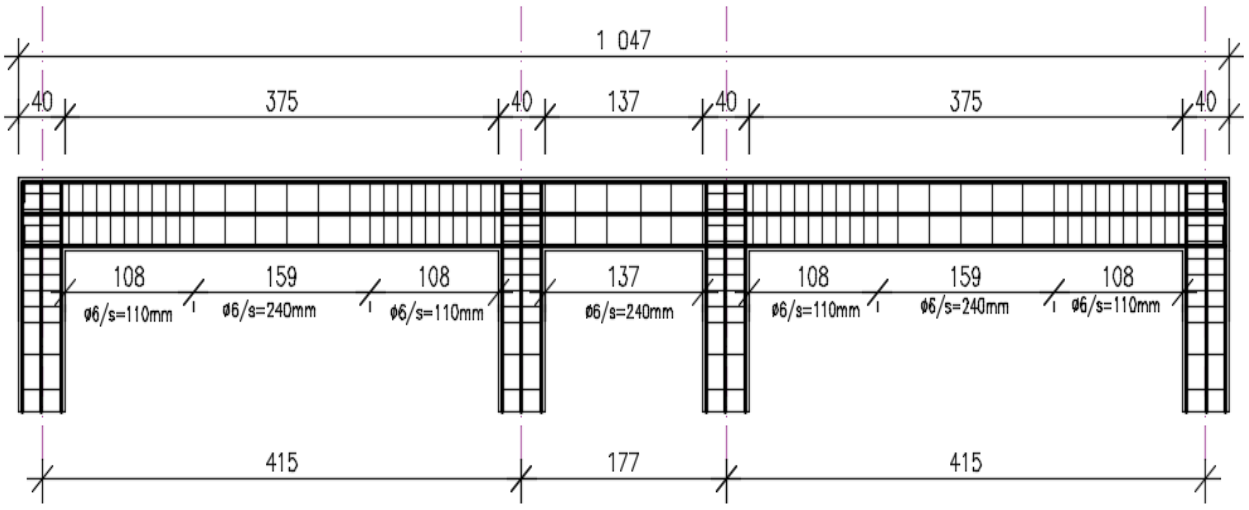

Figure 3.35. Details of drawn model

3.5.1.2. Materials Properties

The concrete material and the steel reinforcements (both for longitudinal and transversal) are modelled in ABAQUS/CAE.

Concrete parameters are shown in table 3.11.

Table 3.11. Concrete elastic properties

Elastic properties				
Density		**Young modulus**	**Poisson's ratio**	
2.5E-5		31476	0.2	
Plasticity				
Dilation angle	**Eccentricity**	**fb0/fc0**	**K**	**Viscosity parameter**
35	0.1	1.12	0.667	0.0005
Compressive behaviour				
Yield stress		**Inelastic strain**		
10.2		0		
25		0.0025615		
3.4		0.011		
Concrete compression damage				
Damage parameter		**Inelastic strain**		
0		0		
0.9		0.011		
Tensile behaviour				
Yield Stress		**Cracking strain**		
1.35		0		
1.92		0.001604		
0.02		0.002086		
Tensile damage				
Yield Stress		**Cracking strain**		
0		0		
0.99		0.002		

Where:

- fb0/fc0: Stress ratio
- K: Shape factor

Steel parameters are shown for longitudinal bars and transversal bars in table 3.12 and table 3.13 respectively.

Table 3.12. Steel longitudinal bars parameters

Elastic properties		
Density	**Young modulus**	**Poisson's ratio**
7.75E-06	210000	0.3
Plastic properties		
Yield stress	**Plastic strain**	
400	0	
405	0.000111905	
410	0.00167857	
413	0.00223809	

Table 3.13. Steel transversal bars parameters

Elastic properties		
Density	**Young modulus**	**Poisson's ratio**
7.75E-06	210000	0.3
Plastic properties		
Yield stress	**Plastic strain**	
235	0	
237	0.000111905	
240	0.00167857	
243	0.00223809	

3.5.1.3. Assembly

All the parts are assembled using the module Assembly of Abaqus to produce the reinforced concrete beam and the supporting columns model. The assembled parts are presented in figures 3.36 to 3.38.

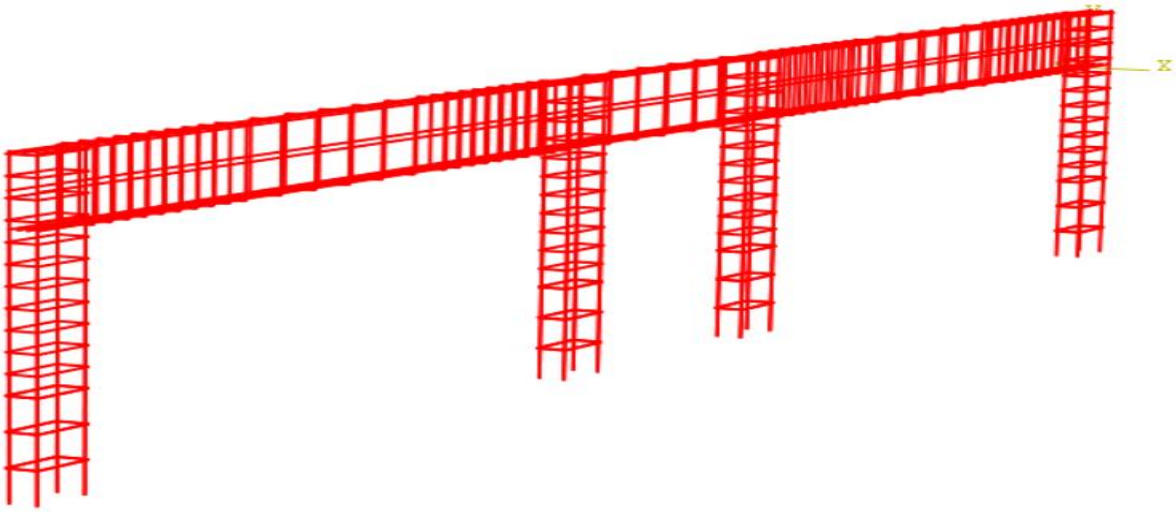

Figure 3.36. Assembly of steel reinforcement parts

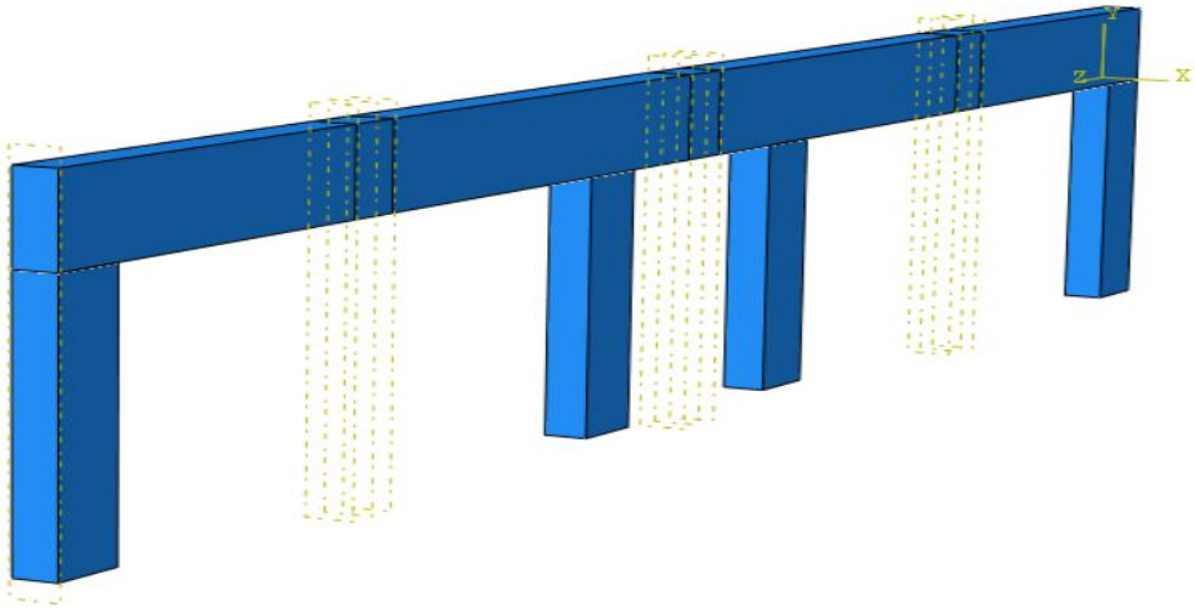

Figure 3.37. Assembly of concrete beam and columns parts

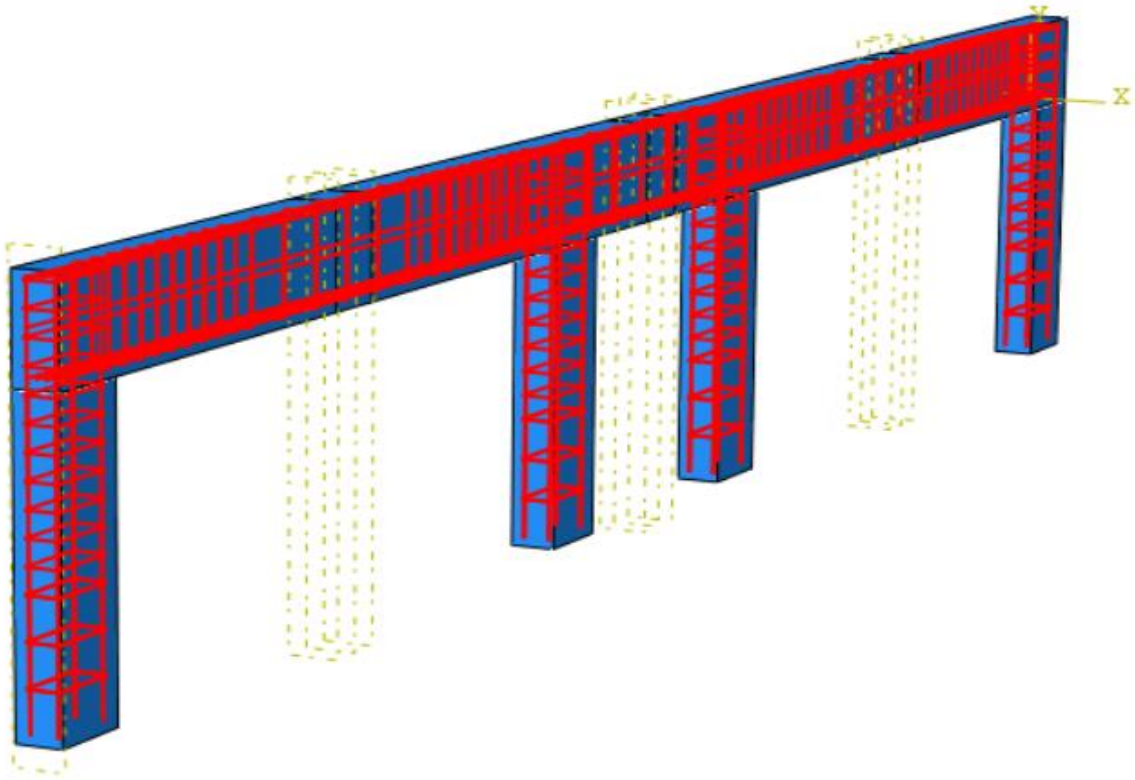

Figure 3.38. Assembly of parts of the study beam and columns with reinforcements

3.5.1.4. Steps

The time period used is 1 and two steps were created: initial and dynamic explicit step.

3.5.1.5. Interactions

The two types of interactions used are the embedded region constraint type and the tie constraint type. These constraints are used to simulate the real interaction between reinforcing steel and concrete and between the concrete beam and concrete columns respectively. Figure 3.39 is shows these applied interactions.

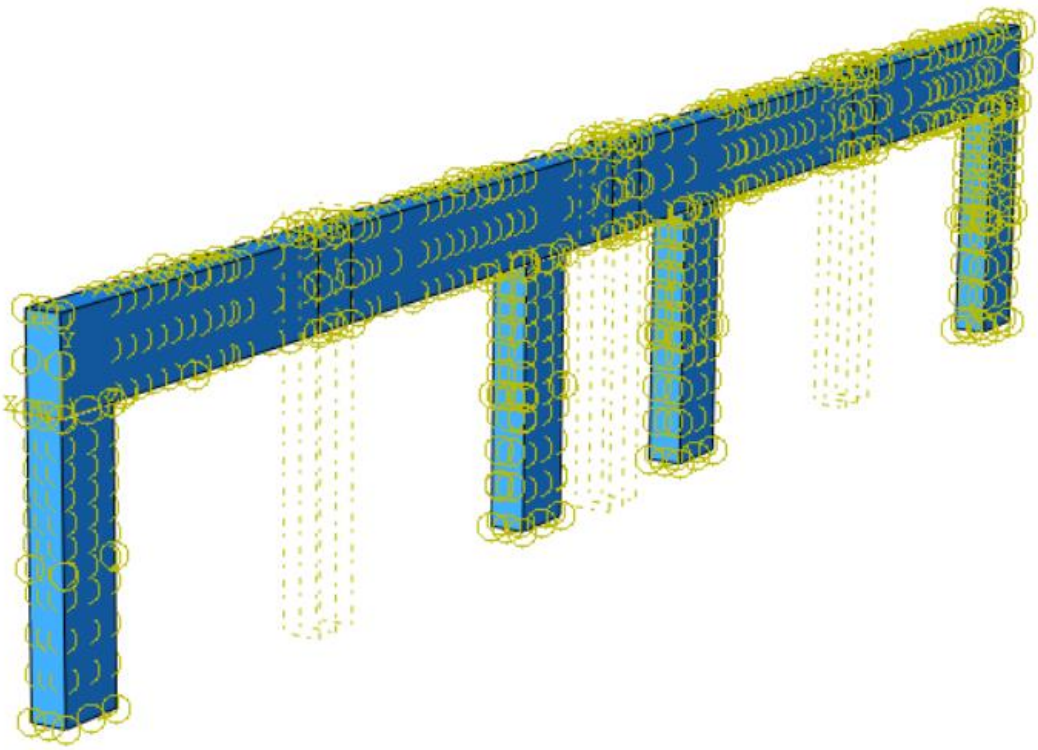

Figure 3.39. Interactions in beam and columns.

3.5.1.6. Boundary conditions

At the bottom surfaces of the columns were defined restraints of type pinned (U1=U2=U3=0) which prevents translation in the three axes. Also, two displacements spaced at 300mm (150mm on each opposite sides of the different spans) and of values 30mm each were imposed at the top middle of each span of our beam in the negative y-direction according to the axis orientation as can be seen in figure 3.40. This is to simulate a static loading condition that causes the reinforced structural model to arrive its plastic phase and present crack patterns and damaged areas.

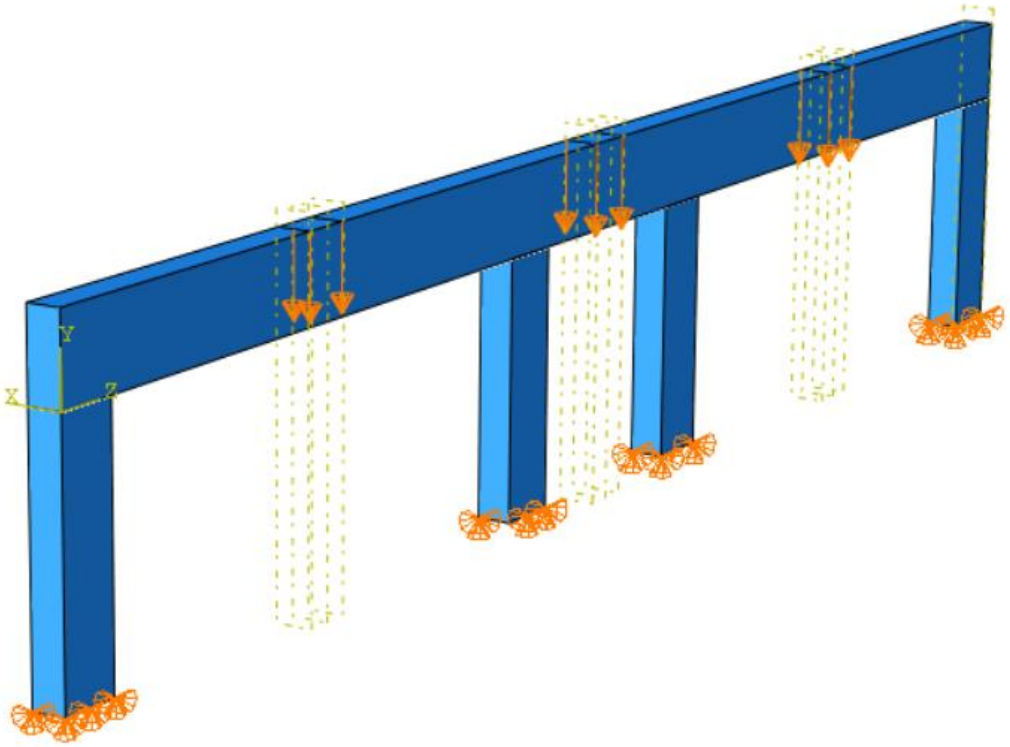

Figure 3.40. Boundary conditions applied on the studied model

3.5.1.7. Meshing

The mesh size of 50 mm is chosen for the concrete elements over the whole geometry of the beam and columns while the mesh size of 25mm is adopted for steel longitudinal bars and stirrups. The meshing can be seen in Figure 3.41.

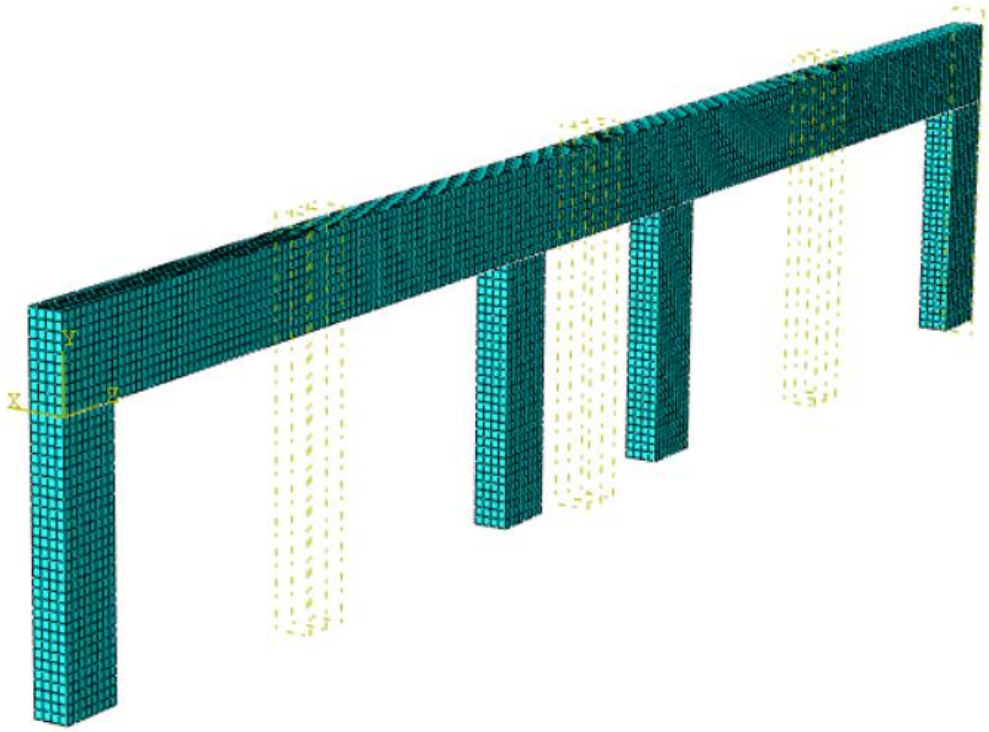

Figure 3.41. Meshing of the model

3.5.2. Crack analysis results interpretations

The finite element analysis of the model was set up to examine what happens before initial cracking and the crack propagation mechanism till failure of the beam due to a maximum displacement of 30mm imposed on the beam. The application of the displacements up to failure was done incrementally. This enables us to predict regions of weaknesses and failure mechanism of the beam which can be an important knowledge during forensic engineering investigations.

3.5.2.1. Results of the analysis

The presentation of the results will be made in two main axes. Firstly, it will be the presentation of the results on the reinforced concrete frame (deflections and cracking initiation and propagation observed in the beam element with time), then the results on the tension stresses in the steel reinforcements in the beam.

(a) Results on the reinforced concrete frame

Results on the reinforced concrete frame are presented as the evolution of damage observed on the concrete at different time intervals.

(i) At initial step, t=0s

Initially, when the step time, t is at 0s no displacement is applied on the beam and so no crack caused by tensile stresses and no crack caused by compressive stresses are observed in the beam as can be shown by figures 3.42 and 3.43 respectively.

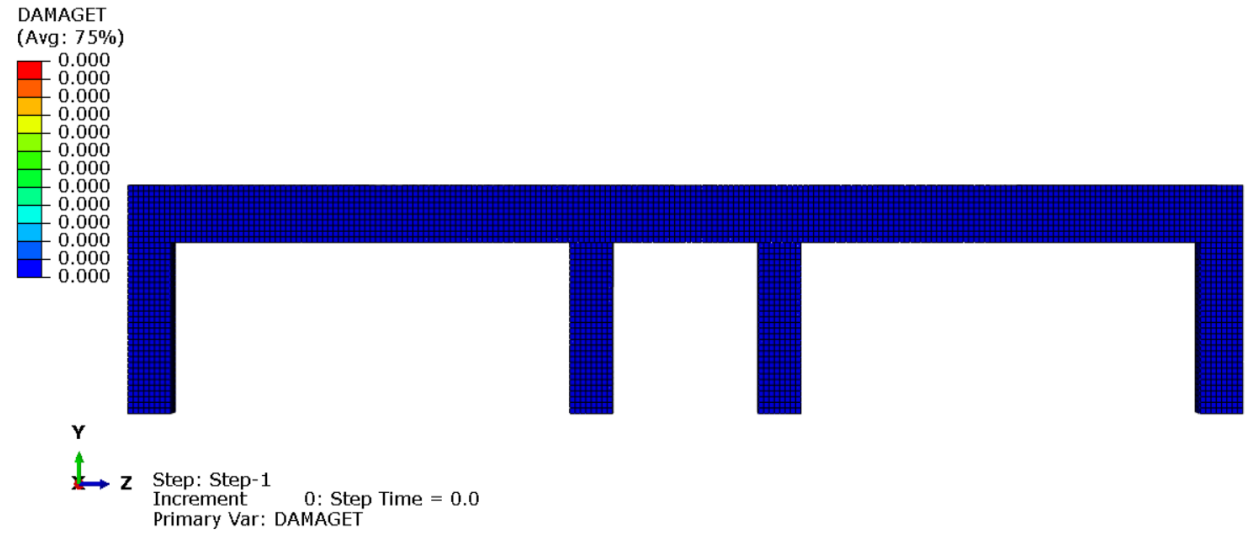

Figure 3.42. Tensile crack patterns in the frame at time t=0s

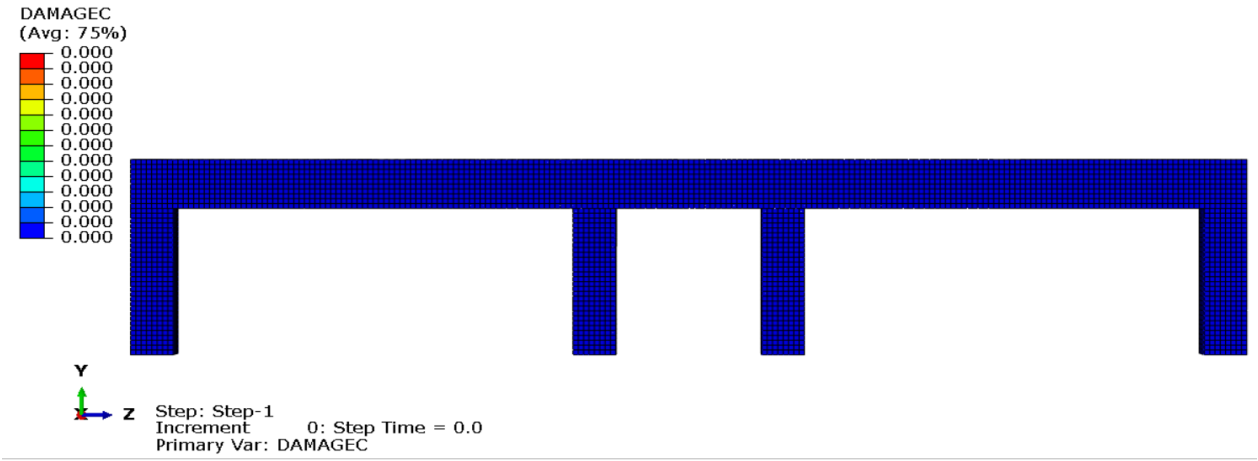

Figure 3.43. Compressive crack patterns in the frame at time t=0s

(ii) At time t= 0.1s

The increment at the end of each step corresponds to the displacement applied. For this step the increment is 1481 referring to a displacement, U2 in the negative y-direction of 1.481mm

applied to the beam. We notice the appearance of the first crack contours caused by both tensile and compressive stresses in the beam as can be shown by figures 3.44 and 3.45 respectively.

Tensile stresses are set in the lower fibres of the mid spans which are caused by high bending moments. It is observed that flexural cracks in the concrete starts appearing in these regions since concrete has a negligible resistance to tensile stresses. So the longitudinal steel reinforcements starts resisting the tensile stresses at these points as will be shown in section 3.5.2.1(b).

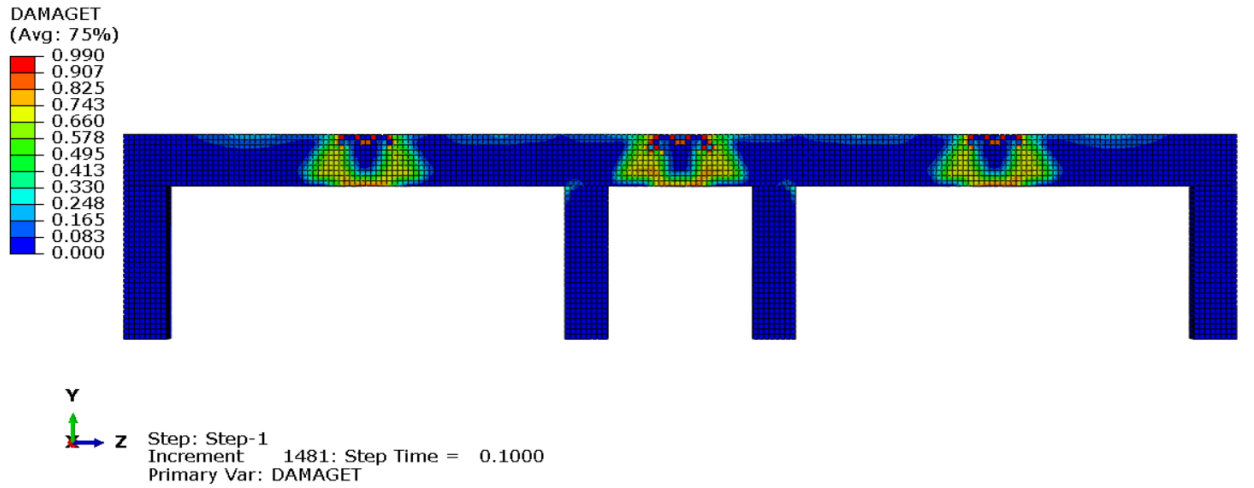

Figure 3.44. Tensile crack patterns in the frame at time t=0.1s

In accordance with Kachlakev, compressive failures initiates at the point of applications of the load as can be seen in figure 3.45.

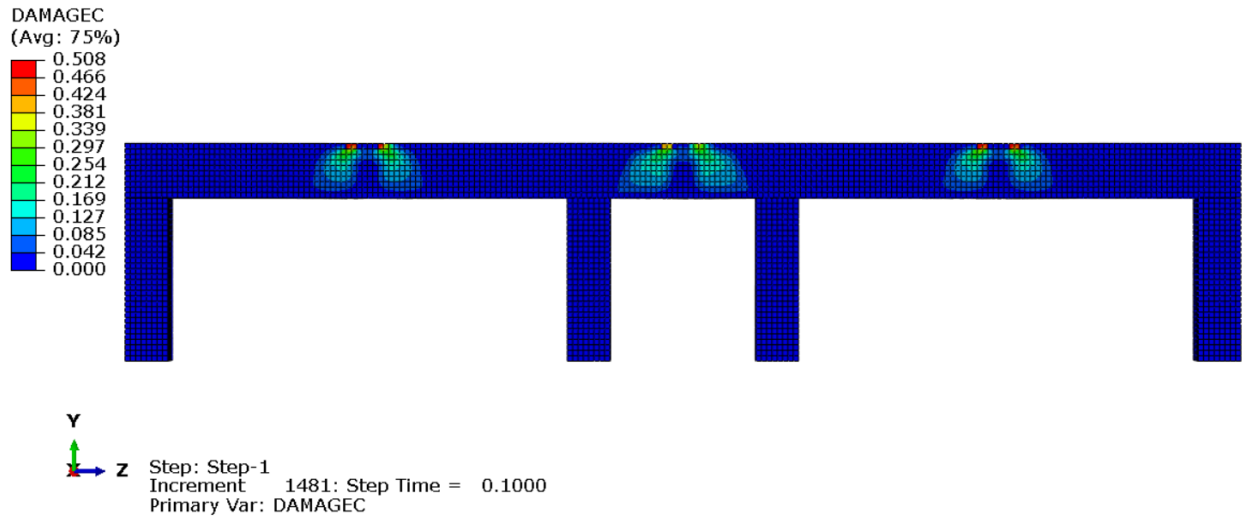

Figure 3.45. Compressive crack patterns in the frame at time t=0.1s

(iii) At time t= 0.15s

Subsequent flexural cracking occurs as more load is applied to the beam. Cracking increases in the lower parts of the mid spans, and the beam begins cracking out towards the supports and up towards the neutral axis. New cracks contours appear at the upper fibers of the beam near the supports which also corresponds to regions subjected to high bending moments in the beam as can be seen in figure 3.46.

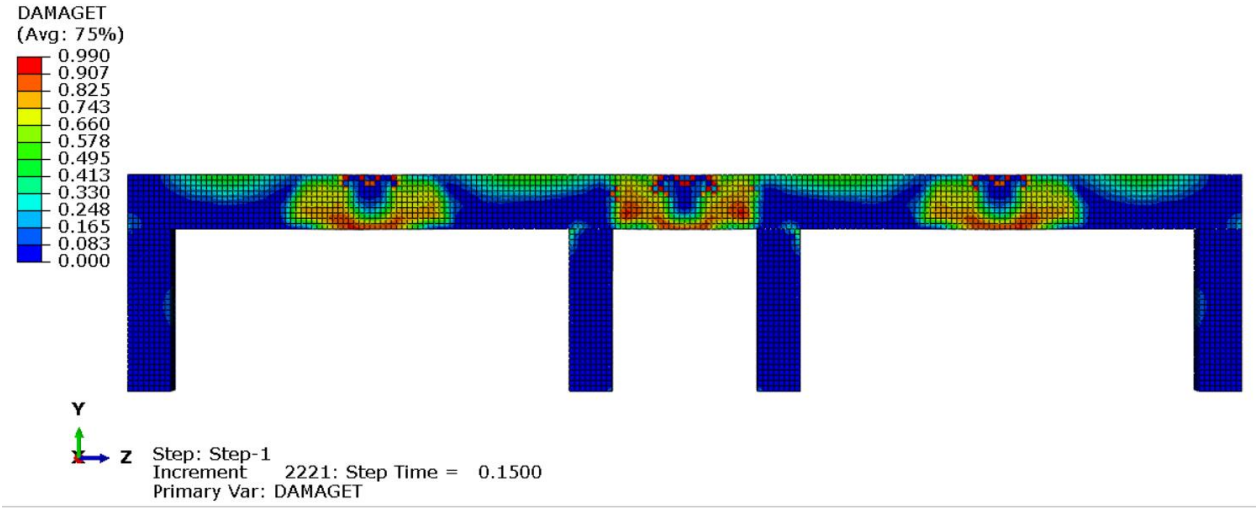

Figure 3.46. Tensile crack patterns in the frame at time t=0.15s

Compressive failures propagates downward through the concrete struts of the beam almost inclined at 45°, but they clearly appear to be lesser than cracks due to tensile stresses as shown by figure 3.47. The reason being that concrete resists very much better to tension than to compression.

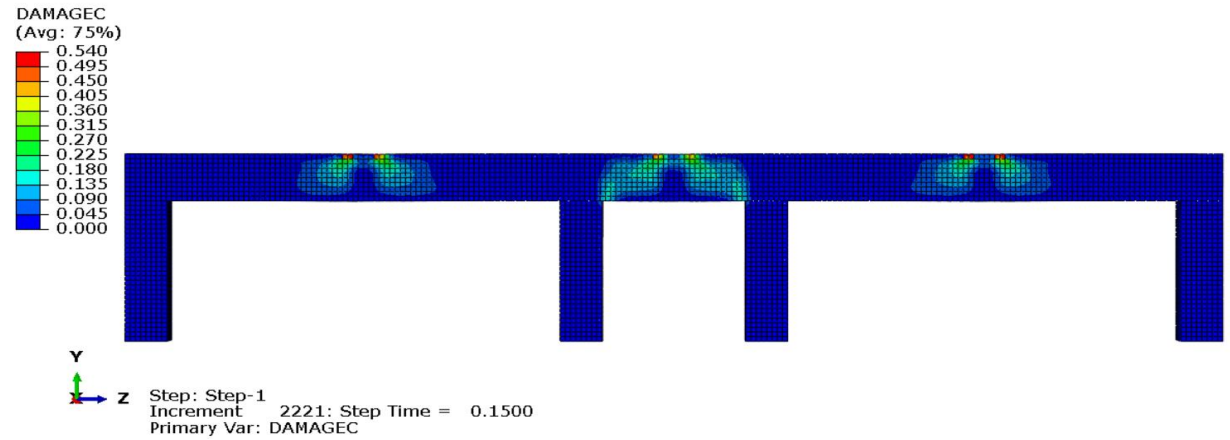

Figure 3.47. Compressive crack patterns in the frame at time t=0.15s

The shorter middle span shows a greater rate of cracks propagation (both under tension and compression) as compared to the other two spans.

(iv) At time t= 0.2s

The lower fibers of the mid span already indicates complete damage shown by the red zones in figure 3.48. Cracking propagation sideward towards the supports and upward towards the neutral axis continues at an increasing rate. Cracks at the upper fibers of the beam near the supports extends towards the mid spans. Some cracks also starts appearing at the beam-column joints.

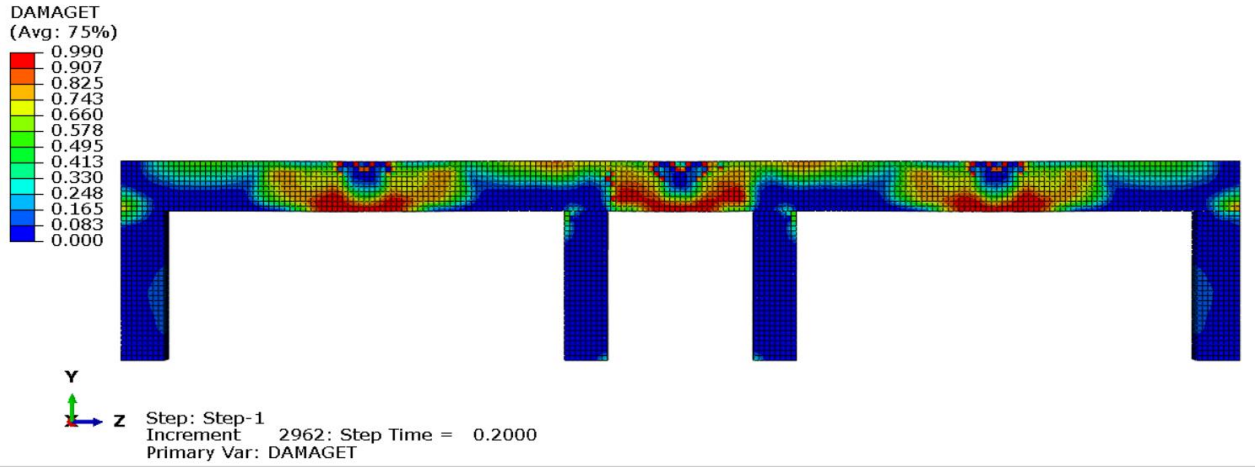

Figure 3.48. Tensile crack patterns in the frame at time t=0.2s

Compressive failures continues its evolution downward through the concrete struts of the beam still almost inclined at 45°. It still appears to be greater in the middle span (see figure 3.49).

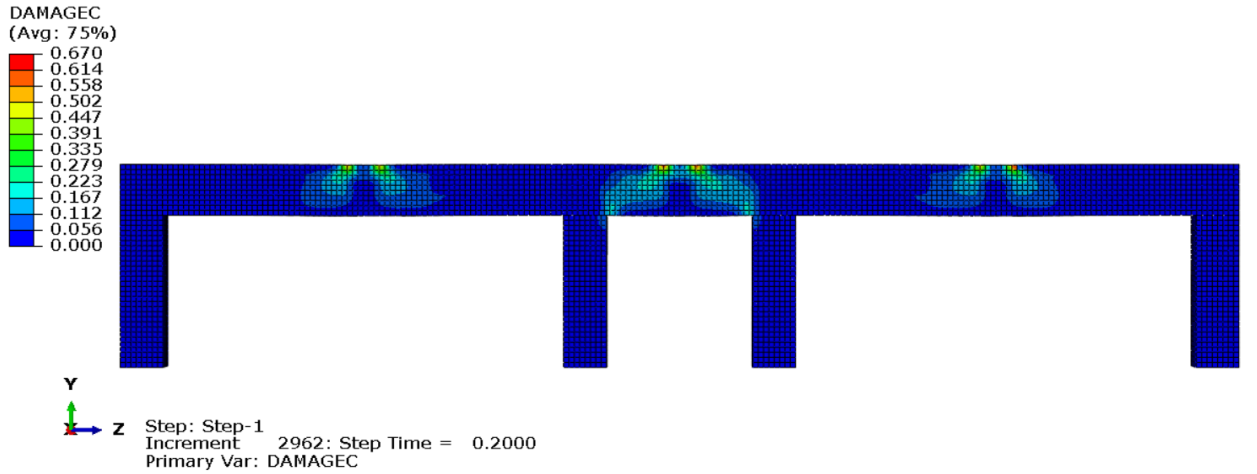

Figure 3.49. Compressive crack patterns in the frame at time t=0.2s

(v) At time t= 0.35s

At this point in the response, the displacements of the beam begin to increase at a higher rate as more load is applied. Therefore, greater deflections occurs at the beam mid spans.

The ability of the beam to distribute load throughout the cross-section has diminished greatly. The beam has increasing flexural cracks and diagonal tension cracks. Also, more cracks have now formed in the mid spans almost reaching the top of the beam. At the middle span, cracking has reached the top of the beam, and failure is soon to follow as seen in figure 3.50.

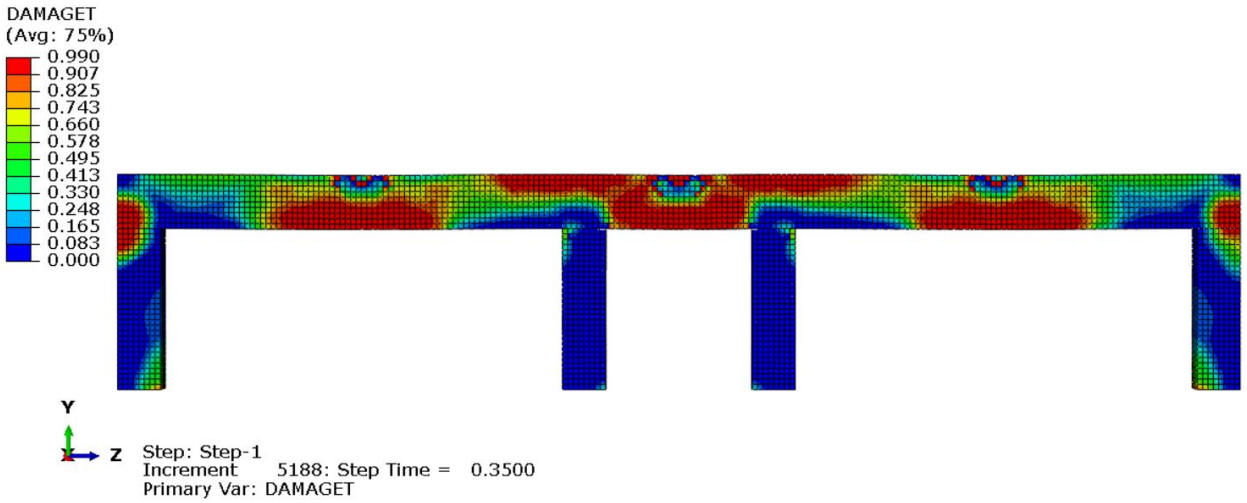

Figure 3.50. Tensile crack patterns in the frame at time t=0.35s

Compressive failure continues its propagation but slower than tensile failures (figure 3.51).

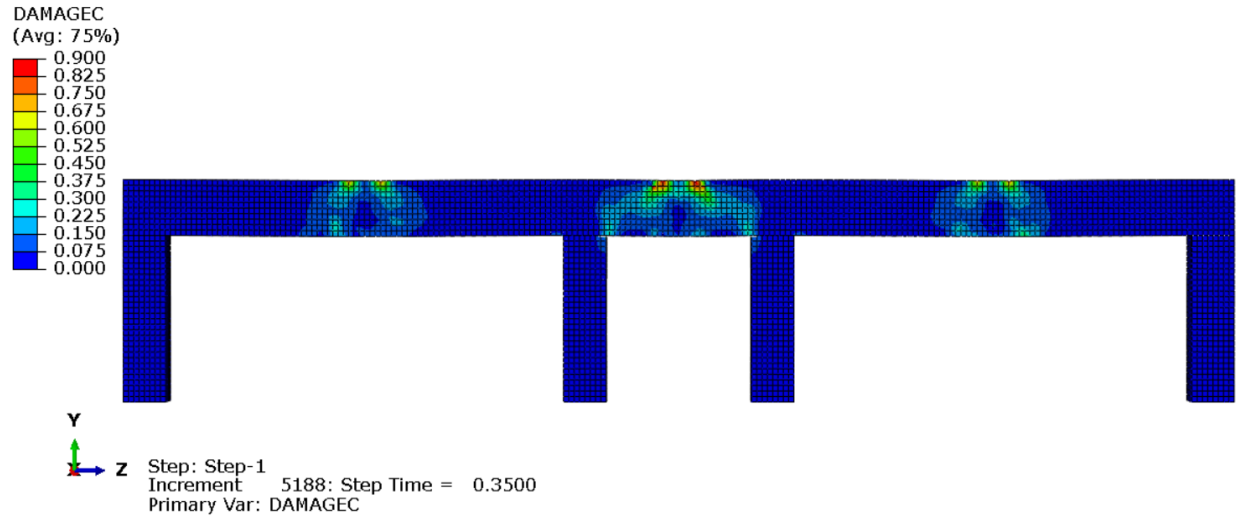

Figure 3.51. Compressive crack patterns in the frame at time t=0.35s

(vi) At time t= 0.55s

The beam has increasing flexural cracks, and diagonal tension cracks. Severe cracking throughout the entire constant moment region occurs. At the middle span, failure has occurred. Cracking has reached the top of the end spans, and failure is soon to follow. Columns starts being damaged as beam-column joints are almost failing.The beam no longer can support additional load as indicated by an insurmountable convergence failure as shown by figure 3.52.

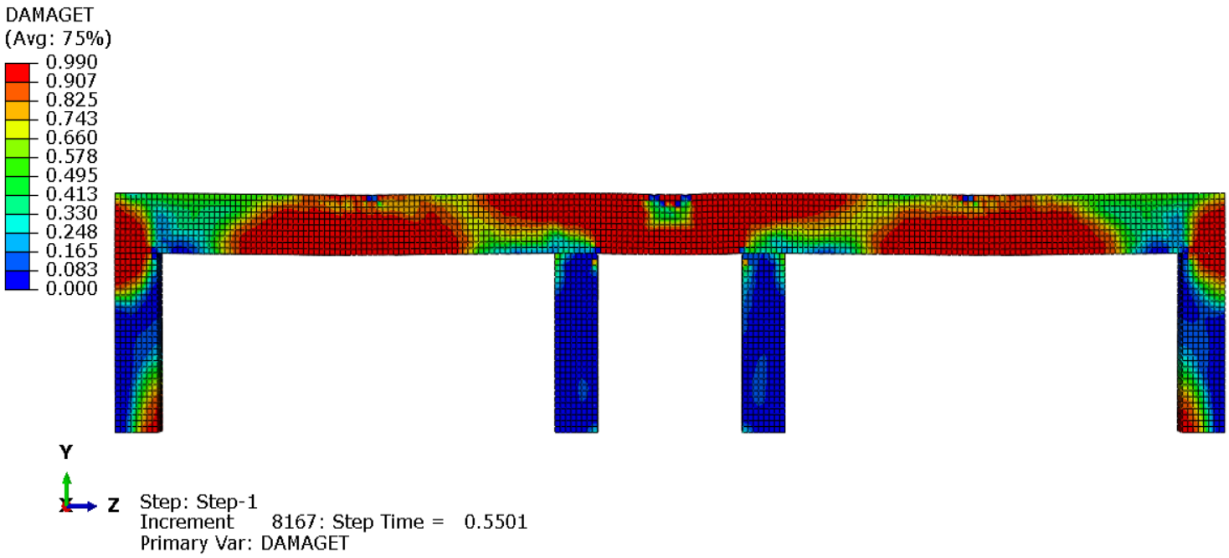

Figure 3.52. Tensile crack patterns in the frame at time t=0.55s

Compressive failure will soon occur in the mid spans as crushing in the concrete reaches the bottom of the beam (figure 3.53).

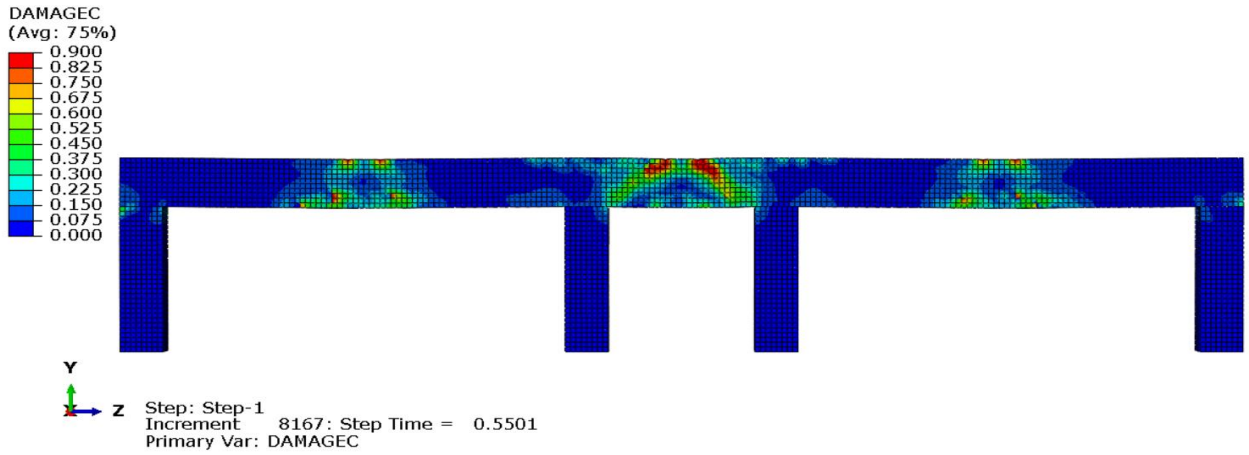

Figure 3.53. Compressive crack patterns in the frame at time t=0.55s

(vii) At time t= 0.75s

Complete failure of the beam is noticed and external columns will soon follow (figure 3.54 and 3.55).

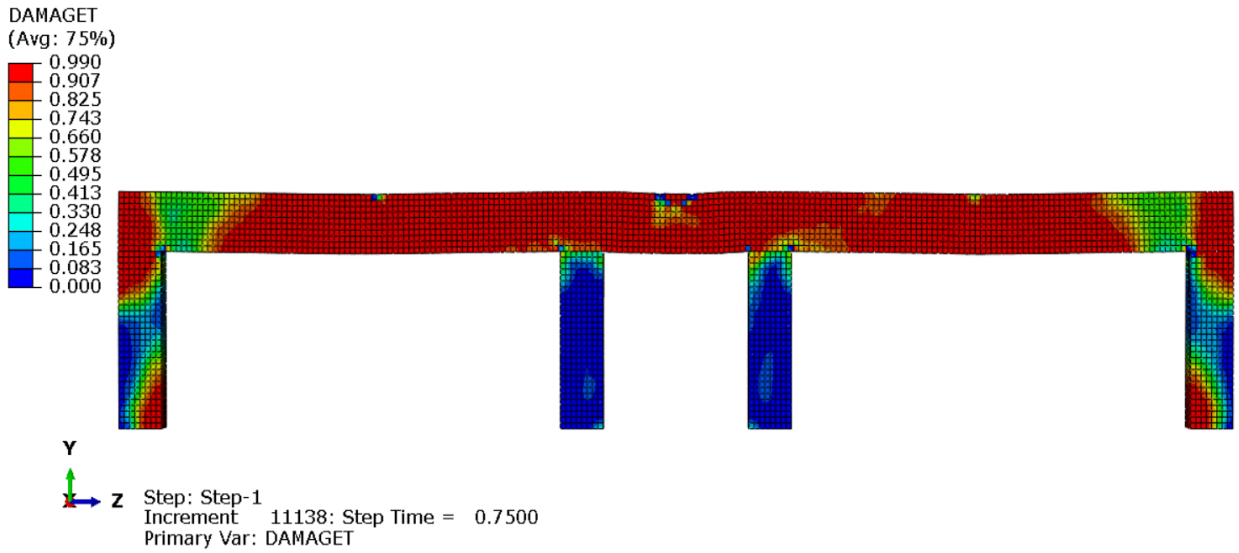

Figure 3.54. Tensile crack patterns in the frame at time t=0.75s

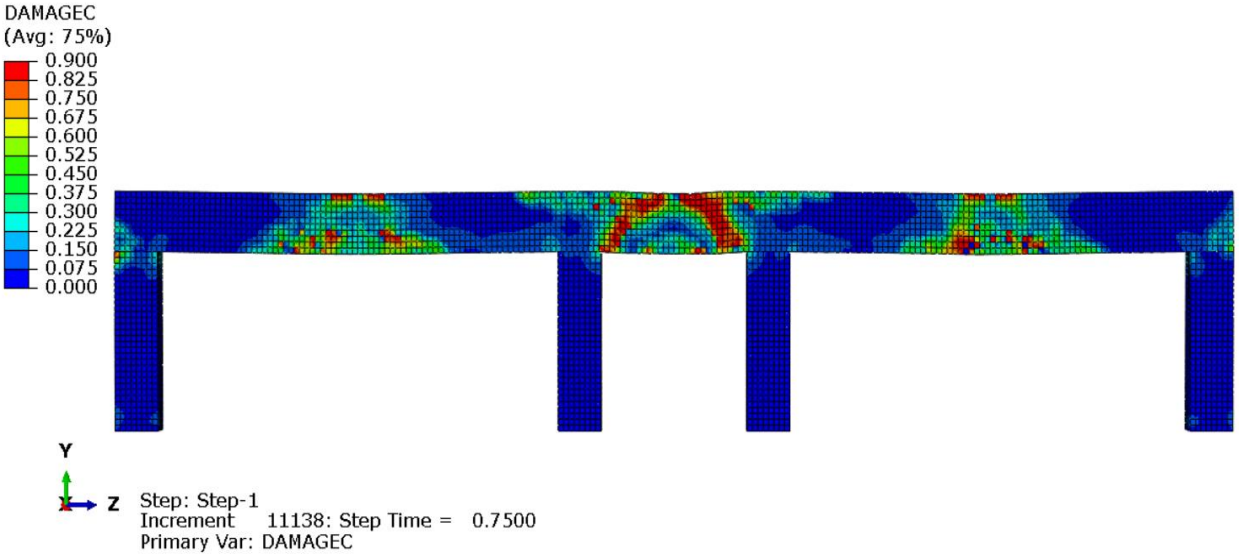

Figure 3.55. Compressive crack patterns in the frame at time t=0.75s

(viii) At time t= 1s

At the end of the simulation, the whole beam damaged with tensile failure all over the beam (figure 3.56) and compressive failure at mid spans and joints (figure 3.57).

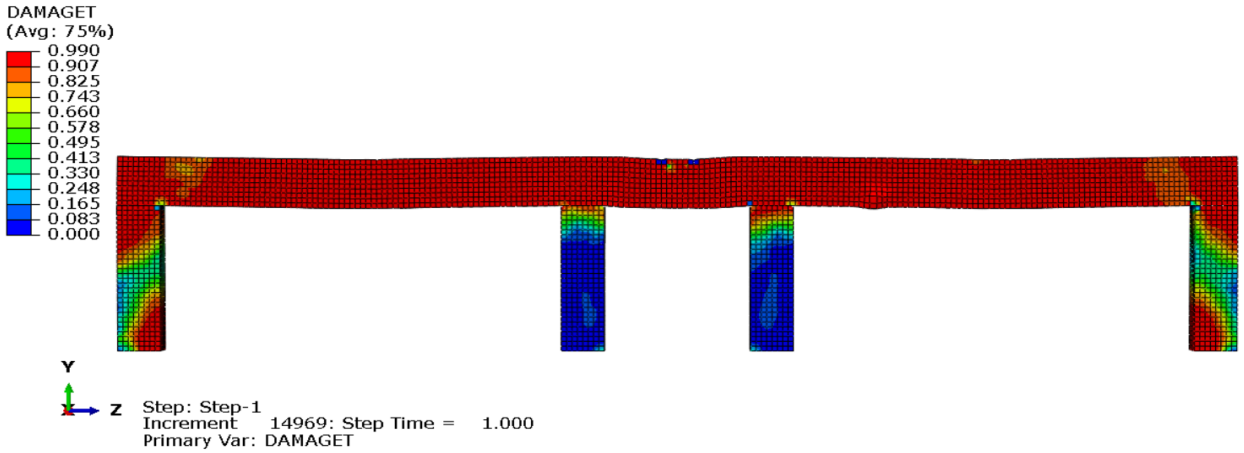

Figure 3.56. Tensile crack patterns in the frame at time t=1s

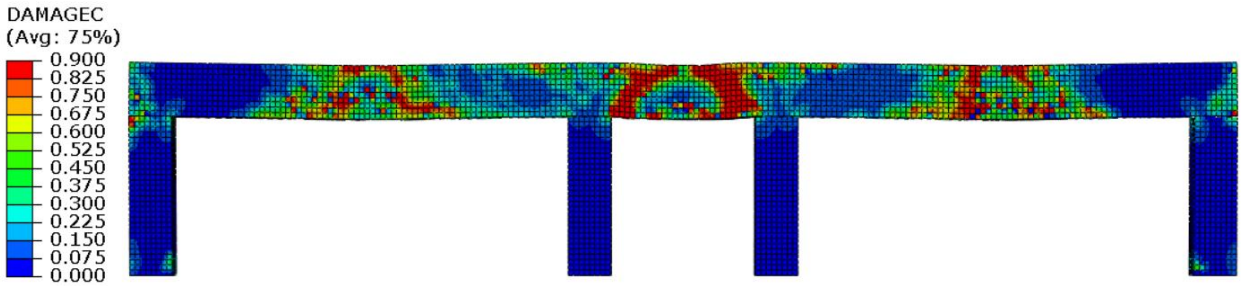

Figure 3.57. Compressive crack patterns in the frame at time t=1s

To illustrate graphically these results, 7 critical elements on the meshed beam have been chosen as shown in figure 3.58. Due to perfect symmetry of the frame, elements 1 and 7, 2 and 6 and 3 and 5 behaves similarly. So only 4 elements can be plotted to perfectly illustrate crack patterns in these critical points.

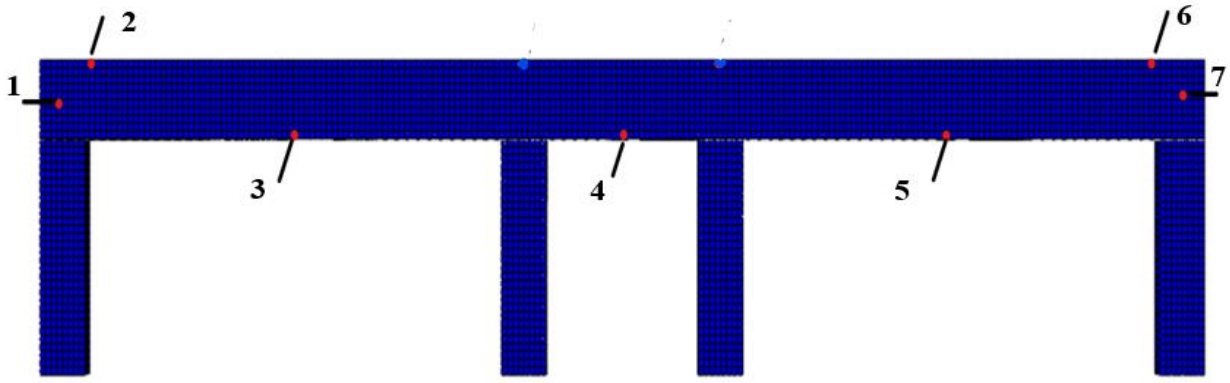

Figure 3.58. Regions of high cracking activity

The damages recorded in these points are plotted against time in figure 3.59 and figure 3.60.

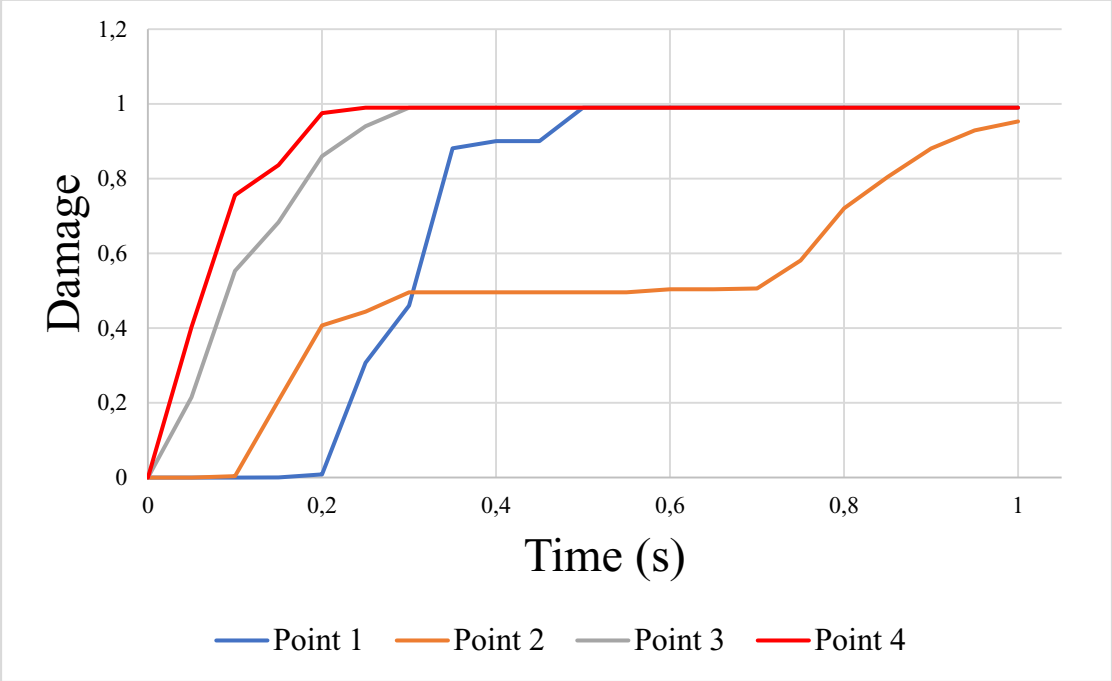

Figure 3.59. Tensile crack patterns in the beam at critical points

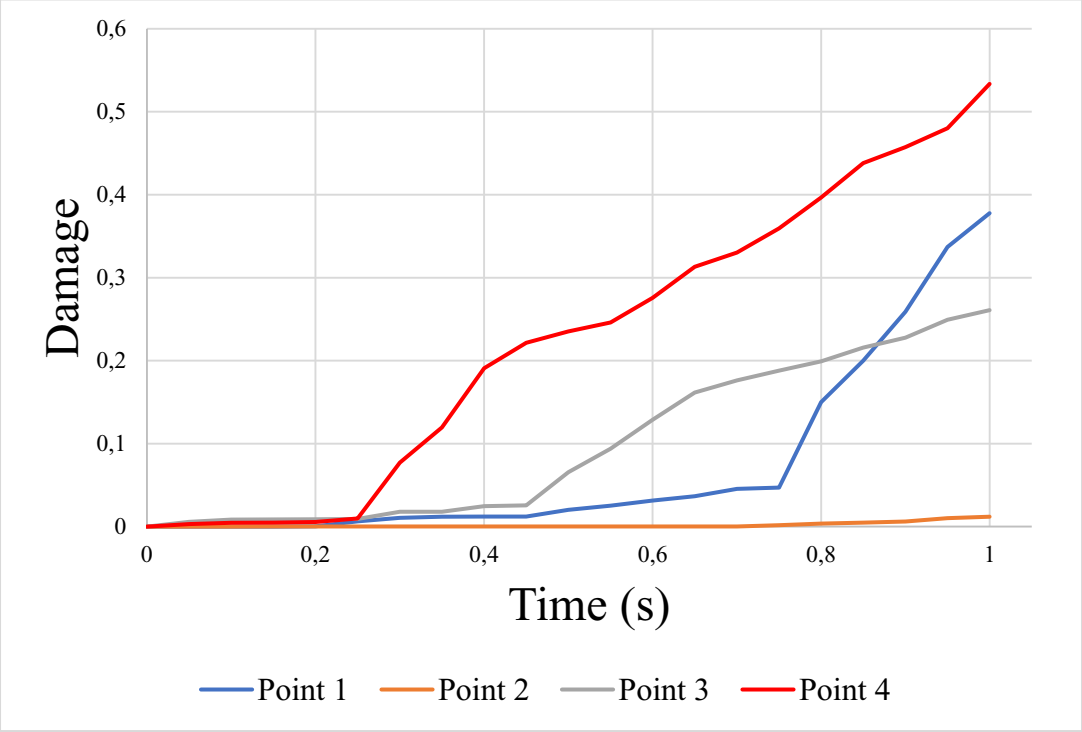

Figure 3.60. Compressive crack patterns in the beam at critical points

At the end of the test, we can conclude that flexural cracks first forms in the lower fibers of the mid spans of each span (points 3 and 4), extends upward and outward towards the supports with eventual crushing of the concrete in the mid spans of each span moving downward through the section of the beam in accordance with Buckhouse and also in accordance with Kachlakev. But the compressive damage magnitude is lower than that of tensile damage indicating that the failure is mostly caused by tension in the beam. This crack pattern also shows large similarities with those obtained by the studies of Leonhardt and Walter, and Darmansyah Tjitradi, Eliatun Eliatun and Syahril Taufik as stated earlier in the literature. So these results are validated with experimental results.

Load against mid span deflection curves for the outer and the middle spans are illustrated in figure 3.61 and this corresponds to ultimate loadings predictions for a reinforced concrete beam. From this graph we can see that the middle span (which is shorter), admits lower deflection of 7.734 mm before complete damage than the longer outer spans with a deflection of 10.866 mm before complete damage. Beyond these values of deflection, the deflection is no more proportional to the applied load. So the middle span is damaged before the outer spans.

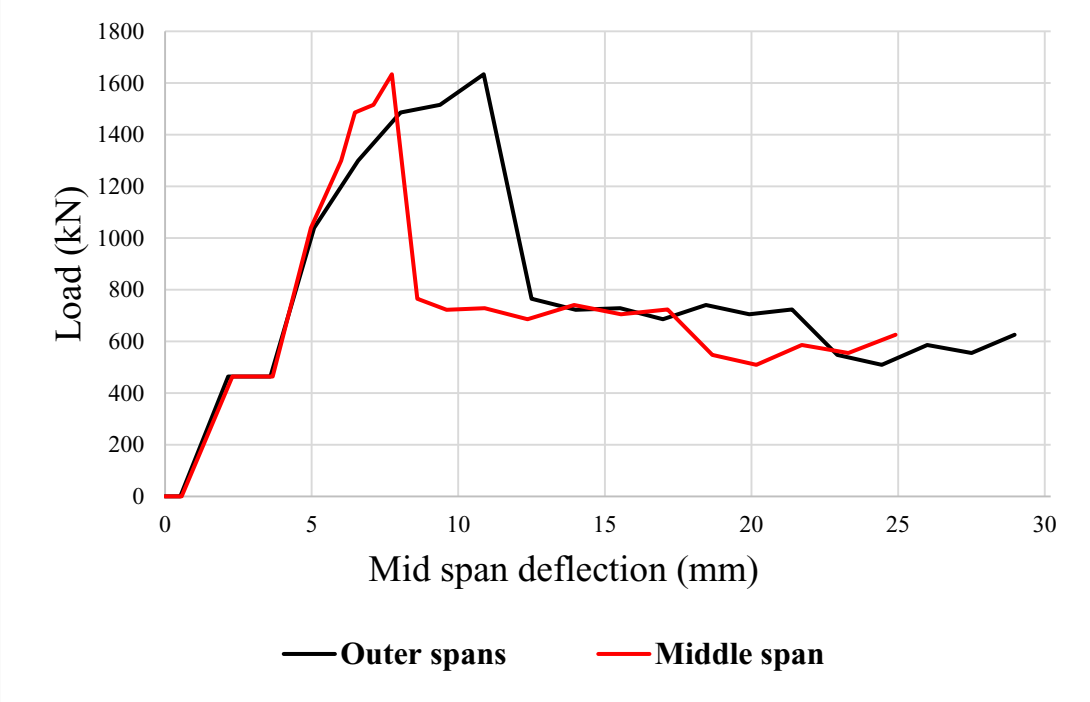

Figure 3.61. Load vs deflection plot

(b) Results on the steel reinforcements in the beam

Tensile stresses which could not be supported by the concrete has been transmitted to the steel reinforcements. Figures 3.62 to 3.64 shows the stresses in steel reinforcements of the beam at 3 different time steps.

(i) At time t= 0.1s

The tensile stresses recorded in the steel is over 350 MPa. It can be seen in figure 3.62 how the longitudinal steel starts being stressed at the lower part of the beam in areas where the concrete starts cracking.

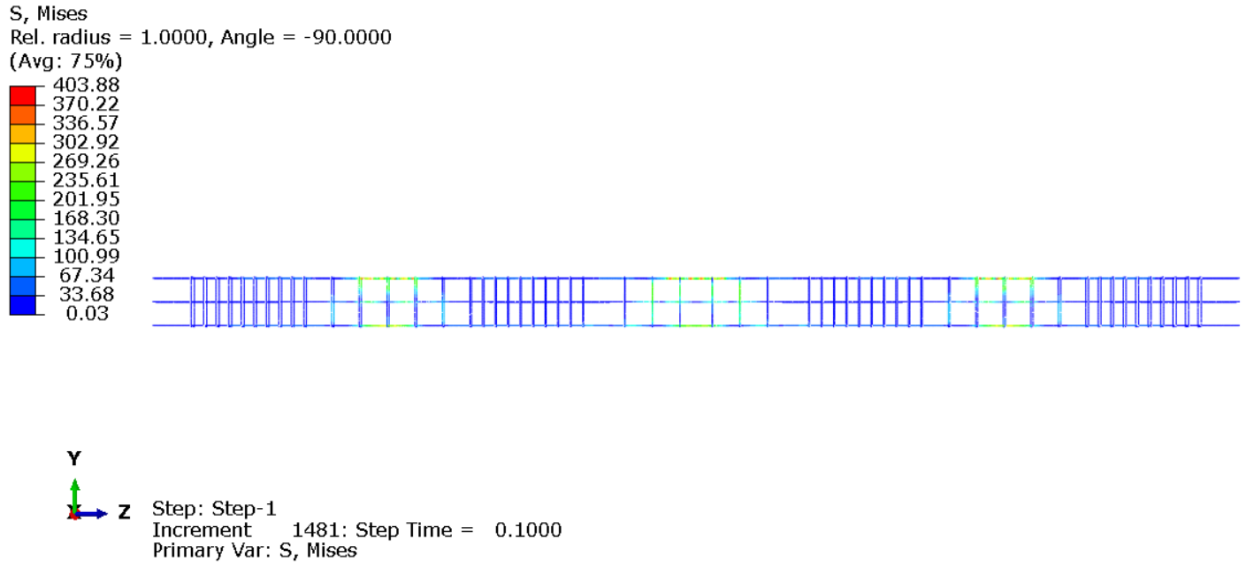

Figure 3.62. Tensile stresses in the steel reinforcements at time t=0.1s

(ii) At time t= 0.35s

The tensile stresses recorded in the steel has increased and is now over 400 MPa. It can be seen in figure 3.63 how the longitudinal steel has yielded at the lower part of the mid spans and upper part of the supports of the beam. Middle span steel reinforcements are all stressed indicating that concrete at this parts has already been damaged.

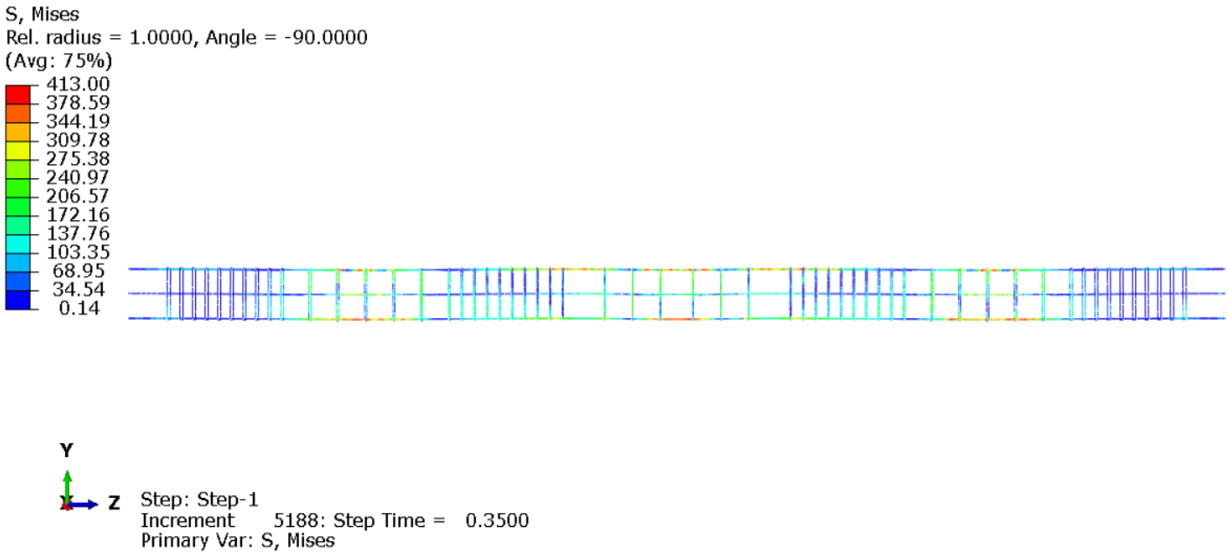

Figure 3.63. Tensile stresses in the steel reinforcements at time t=0.35s

(iii) At time t= 1s

Almost all the beam reinforcements exhibits tensile stress and can be seen in Figure 3.64.

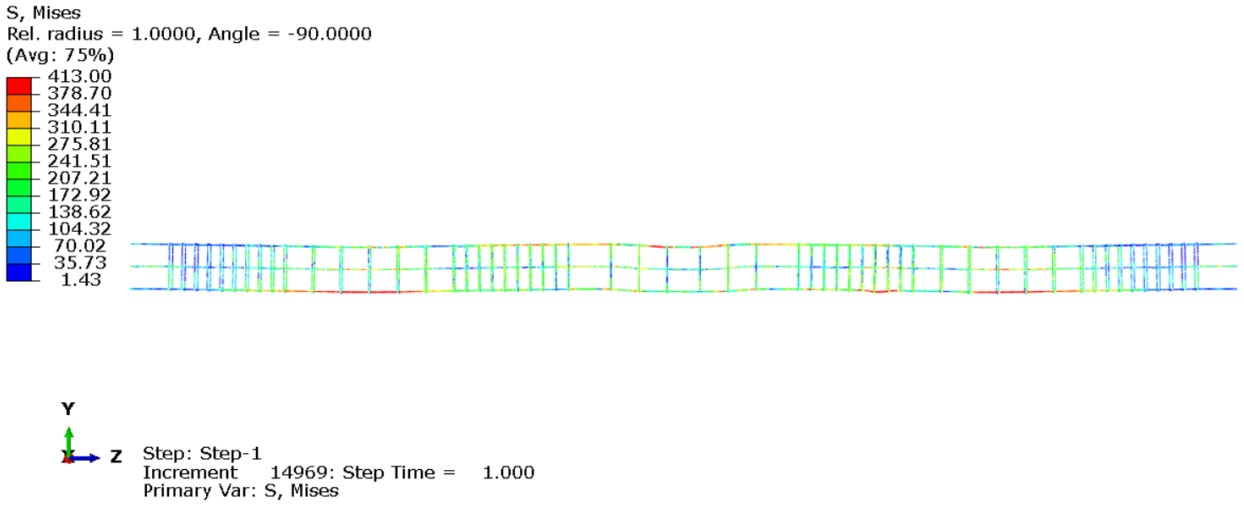

Figure 3.64. Tensile stresses in the steel reinforcements at time t=1s

It is clearly observed that in parts of the beam experiencing tensile stresses, the steel is under tension and it's responsible for the ductile behaviour of the beam. As predicted by Paulay and Priestly (1992), the steel reinforcements in tension zones is fully responsible for load transfer

3.5.3. Application of the results in the field of forensic engineering

Cracks, in themselves, are not "defects" but symptoms of distress within and around the fabric of the structure (Johnson 2002). As discussed in the literature, one of the most common

defect that causes cracking in reinforced concrete structures is the deflection of the beam. One of the biggest causes of why ceramic tiles or partition walls might crack is deflection in the sub floor as seen in figures 3.65 to3.68.

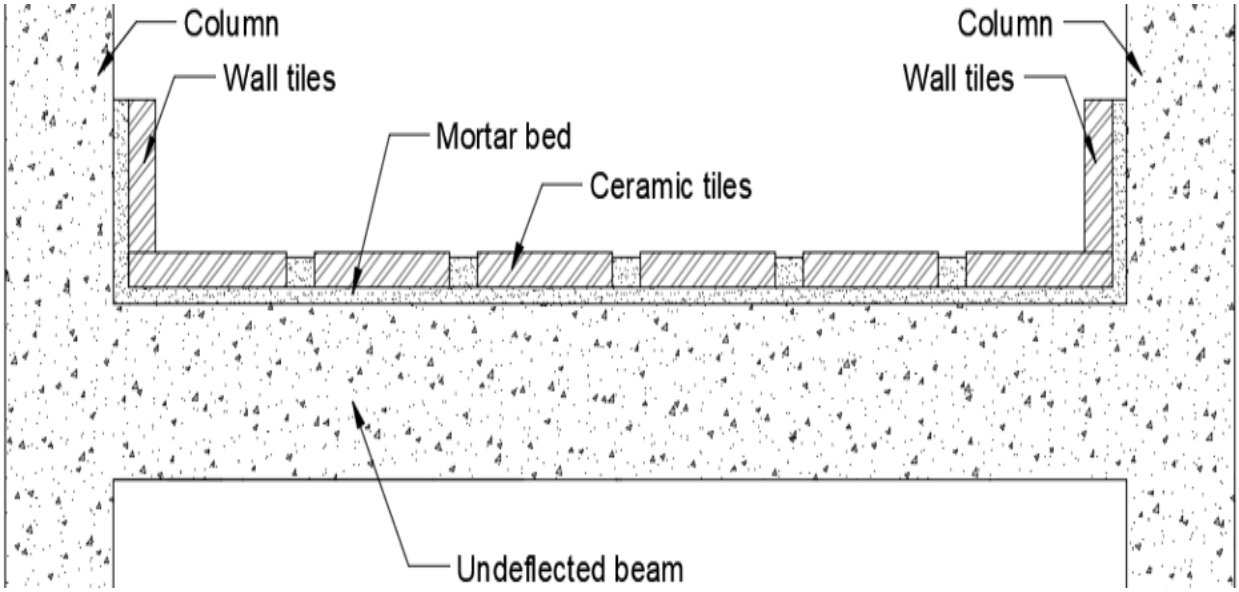

Figure 3.65. Ceramic tiles on undeflected beam

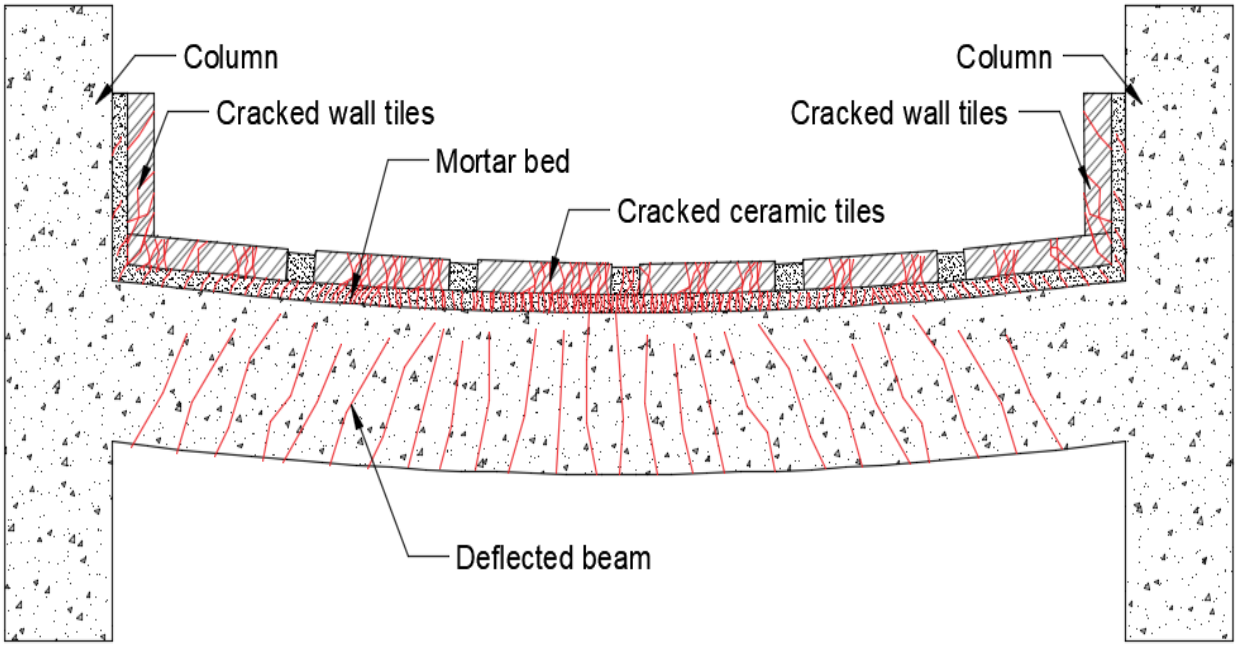

Figure 3.66. Ceramic tiles cracking due to deflected beam

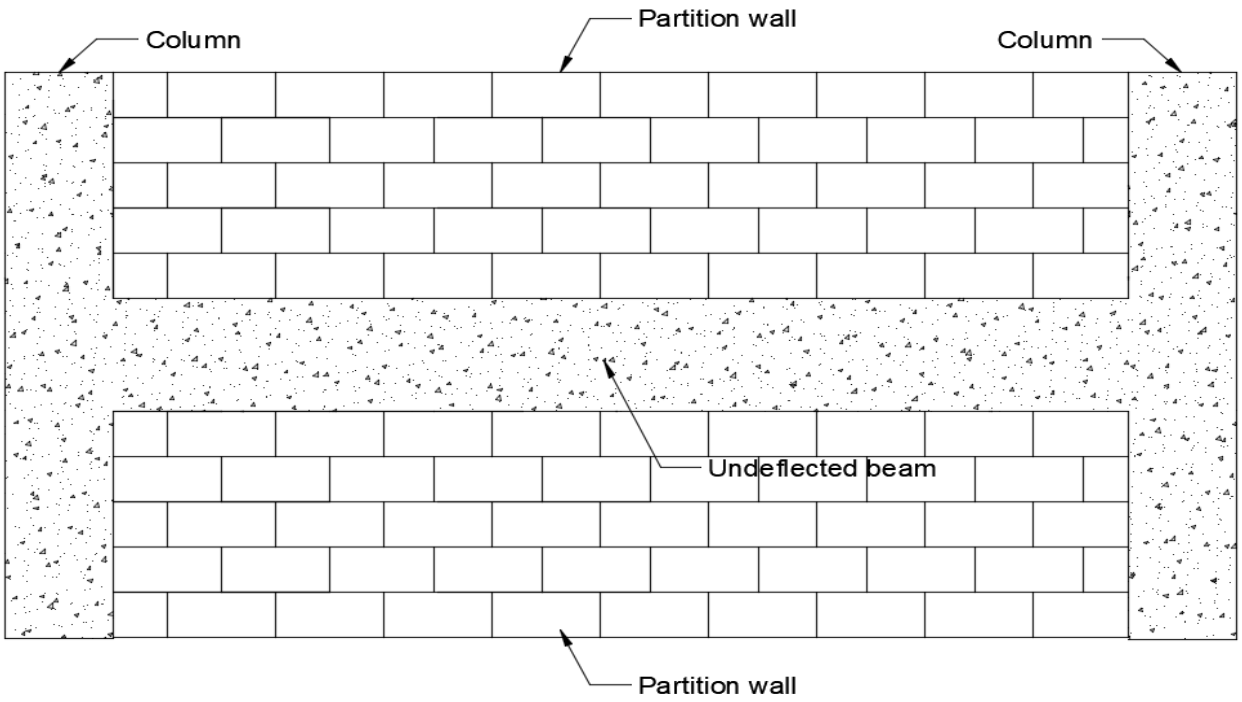

Figure 3.67. Partition wall on undeflected beam

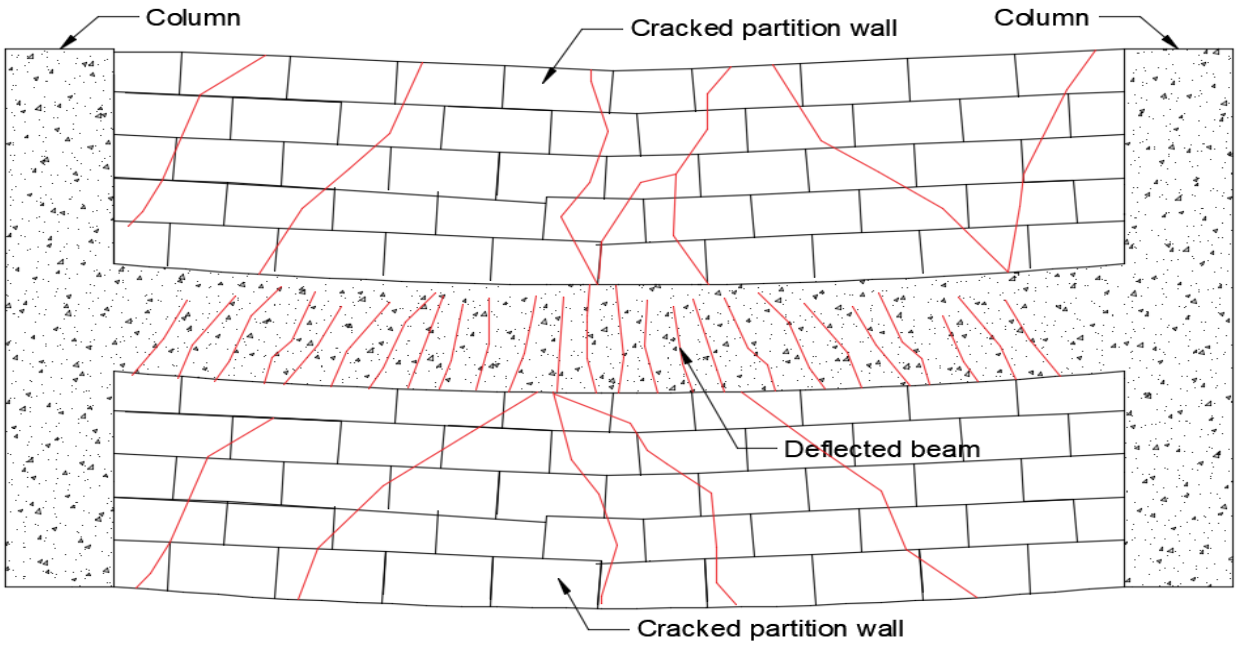

Figure 3.68. Partition wall cracking due to deflected beam

Notions on crack patterns and failure mechanism provided by this work can provide the lead information necessary for a structural forensic engineer to discover the actual source of the defects in the structure. Until the defect is properly identified, any remedial solution may not be effective;

the cracks may appear again, possibly in the same place, or close to it, with greater intensity, causing the structure to deteriorate at a faster rate (Grew 1996). An incorrect assessment of the causes of cracks can lead to expensive and unnecessary remedial works. It is important to note during preliminary inspection if the cracks are static or active. In the case of static cracks, a simple exercise of filling the cracks with appropriate binding materials and repainting may solve the problem. However, if the cracks are active, it requires further investigations to unearth the source; if left untreated, the underlying defects might affect the serviceability or the stability of the structure or its components as discussed in section 1.3.2.

Conclusion

The aim of this chapter was to present the case study, to perform the linear static analysis and the design of the beams, columns and footings considering the soil structure interaction and also to present the results of the crack pattern analysis of a numerical model that describes the nonlinear behaviour of reinforced concrete frame with the beams subjected to vertical displacements in order to capture the beams failure mechanism expressed by a continuous propagation of cracks throughout the beams section and spans. Concrete damage plasticity material model was applied to the numerical procedure as a distributed plasticity over the whole geometry of the specimens to appropriately simulate material nonlinearity. Also, results obtained in this work were compared to experimental results. The configuration of numerical model was implemented in finite element code ABAQUS. The finite element models were validated with experimental results. Finally, a discussion on how these results may be important in the field of forensic engineering was made.

GENERAL CONCLUSION

The main aim of this thesis was the study of a reinforced concrete beam, conducted using finite element analysis in order to understand the response of reinforced concrete beams due to transverse displacements, the way this response expresses itself in terms of cracks and why is such a knowledge important for a forensic engineer. To achieve this, basic practices in forensic engineering in concrete structures have been discussed in chapter 1 alongside a general knowledge on reinforced concrete building material making emphasis on its defects (particularly deflection). Also, notions on cracks and crack propagation were discussed. Chapter 2 presented the methodology to be used and the results presentation and interpretation was done in chapter 3. After the linear static analysis, the design of the beam, column and footings considering soil structure interaction were made. Next, the reinforced concrete beam with flexural and shear reinforcement was analyzed to failure and compared to experimental results. Efficient and accurate model for the simulation of the damage and failure of RC frame, which can be readily used in the analysis of multi-storey RC frame structures was presented, and employed in the analysis of a 6-storey RC frame structure. A displacement based control method was used, with an imposed displacement of 30mm to be applied incrementally in 1 second on the beam. At different time intervals, the level of cracks corresponding to a particular deflection of the beam were observed, to trace out the crack pattern from its initiation to complete beam failure. The analysed models were implemented in ABAQUS/CAE and special attention was given to flexural resisting mechanism. Corresponding crack pattern behaviour of the beam adequately modelled through the Concrete Damage Plasticity (CDP) material model applied to the numerical procedure as a distributed plasticity over the whole geometry of the specimens. The results were expressed in terms of damage in the concrete and tensile stresses in steel reinforcements recorded for different values of beam deflection. The validation of the model was shown by agreement between experimental and numerical results. In addition, this model can be calibrated to study crack patterns subjected to other types of loadings.

The results of the study performed demonstrated that under vertical displacements of a beam, flexural and diagonal tension cracks appears caused by tensile stresses and compressive cracks also appears caused by compressive stresses. Firstly, flexural cracks (at the lower fibres of the midspans) and compressive cracks (at the upper fibres of the midspans) appears. As midspans

displacements increases, flexural cracks extends upward towards the supports while compressive cracks moves downward through the beam section inclined at almost 45°, with the evolution of flexural cracks in terms of speed and magnitude faster than that of compressive cracks. Further displacements leads to the appearance of diagonal tensile cracks still almost inclined at 45°. Cracks due to tension later on appears at the supports and at the beam-column joints. The middle span is completely damaged at a deflection of 7.734 mm while the outer spans are completely damaged at a deflection of. 10.866 mm. The tensile stresses are resisted by the steel reinforcement bars as concrete is unable to resist tensile stresses. After the beam is completely damaged, the columns follow. Finally, the results obtained can provide the lead information necessary for a structural forensic engineer to discover the actual source of the defect (in this case deflection of the beam) during an investigation. Deflection in the beam causes wall and floor finishes to crack, so when cracks on these finishes are noticed, it should serve as a warning that it can be due to beam deflection avoiding any remedial solution which may not be effective.

The subject dealt with is very vast and it was necessary to limit the field of research for this work to beams experiencing gravity loads and flexural failure only. However, this model can be calibrated to study other types cracks such as shear cracks and torsional cracks and other types of loads acting on beams and columns. However, this work cannot be without imperfections due to the failure to carry out a self-experimental test to validate the results of the numerical model which was done with results already validated on different types of specimens.

BIBLIOGRAPHY

Robert T. Ratay (2000). *Forensic Structural Engineering Handbook.*

Marvin M. Specter (1987)**.** *Forensic Engineering Civil Engineering Edition Vol. I.*

Randall K. Noon (1992). *Introduction to Forensic Engineering.*

Randall K. Noon (2001). *Forensic Engineering Investigation.*

Kenneth L. Carper**.** *Forensic Engineering, Second Edition.*

E. T. Brown (2006). *Forensic engineering for underground construction.*

Jeffrey Garrett (2013). *Structural Forensic Engineering.*

Kardon J B (2012). *Guidelines for Forensic Engineering Practice Second Edition.*

Bill Mosley, John Bungey and Ray Hulse. *Reinforced concrete design to Eurocode 2.*

Georges Dreux, Jean Festa (1998). *''Nouveau guide du béton et de ses constituants.''*

Kosmatka, S.H., Kerkhoff, B. and Panarese, W.C. (2003). *Design and Control of Concrete Mixtures. 14th Edition.*

K.Ohno (2015). *Acoustic Emission and Related Non-Destructive Evaluation Techniques in the Fracture Mechanics of Concrete.*

Jean Lemaitre (1996).*A Course on Damage Mechanics Springer.*

Jean Lemaitre, Rodrigue Desmorat (2015). *Engineering damage mechanics, ductile, creep, fatigue and brittle failures Springer.*

Abaqus User Manual, 2008

Abhyuday, T. (2017). *Fundamentals of direct displacement based design procedure - A brief introduction. Disaster Advances*, 10(6), 40–43.

Filippou, F. C. (2015). *Mechanics and Materials Finite Element Analysis of Reinforced Concrete Structures.* July.

A. Borosnyói, G. L. Balázs*, Models for flexural cracking in concrete: the state of the art, Structural Concrete* 6(2) 2005 53-62

Chien-Kuo Chiu*, Kai-Ning Chi, and Bo-Ting Ho. (2018). *Experimental Investigation on Flexural Crack Control for High-Strength Reinforced-Concrete Beam Members*

Anthony J. Wolanski, B.S. (2004). *Flexural behaviour of reinforced and prestressed concrete beams using finite element analysis*

Darmansyah Tjitradi, Eliatun Eliatun, Syahril Taufik, *3D ANSYS Numerical Modeling of Reinforced Concrete Beam Behaviour under Different Collapsed Mechanisms, International Journal of Mechanics and Applications*, Vol.7 No.1, 2017, 14-23.

Saifullah I., Nasir-uz-zaman M., Uddin S.M.K., Hossain M.A., Rashid M.H. (2011). *Experimental and Analytical Investigation of Flexural Behaviour of Reinforced Concrete Beam,* International Journal of Engineering & Technology IJET -IJENS Vol: 11, No: 01, pp. 146-153, February

Tejaswi, S., and Eeshwar, R. J. (2015). *Flexural Behaviour of RCC Beams, Internasional Journal of Innovations in Engineering and Technology*, Vol. 5, February.

Faherty, K.F. (1972), *An Analysis of a Reinforced and a Prestressed Concrete Beam by Finite Element Method,* Doctorate's Thesis, University of Iowa, Iowa City.

Buckhouse, E.R. (1997), *External Flexural Reinforcement of Existing Reinforced Concrete Beams Using Bolted Steel Channels,* Master's Thesis, Marquette University, Milwaukee, Wisconsin

Grew, R. (1996). *The surveying of structural damage, Structural Survey*, 14(4) 4-9.

Hayes, F. X. (2006). *A proactive solution*, American School and University, 2006.

Johnson, R. W. (2002). *The significance of cracks in low-rise buildings, Structural Survey*, 155-161.

Kaklauskas, G., Bacinskas, D., and Simkus, R. (1999). *Deflection estimates of reinforced concrete beams by different methods,* V (4) 258-264.

Kennedy, M. (2008) *Ready to renovate*, American School and University. 14-18.

Pryke, J. F. S. (1983). *Understanding cracks in houses, Structural Survey*, 37-45.

Remoy, H., and Van der Voordt, T. (2014). *Adaptive reuse of office buildings into housing: opportunities and risks, Building Research and Information*, 1-10.

Suffian A. (2013). *Some common maintenance problems and building defects: Our experiences, Procedia Engineering* 54, 101-108.

E. Ogbeifun, J. H. Pretorius, and C. Mbohwa (2014). *Identifying the effects of excessive deflection in reinforced concrete beams.*

Maharajpur Gwalior (2014). *Cracks in Buildings (Causes and Prevention)*

Hippolito Sousa, Rui Sousa (2016). *Analysis of reinforcement techniques for partition walls subjected to vertical deformations of concrete slabs.*

A. R. Ingraffea and V. Saouma. *Numerical modeling of discrete crack propagation in reinforced and plain concrete*

J. Loss and E. Kennett. *Identification of Performance Failures in Large Scale Structures and Buildings*, College Park: University of Maryland. 1987.

ANNEX

Table A1. Values of Minimum cover, $C_{min,}$, requirements with regard to durability for reinforcement steel (EC2)

Environmental Requirement for $c_{min,dur}$ (mm)							
Structural Class	Exposure Class according to Table 4.1						
	X0	XC1	XC2 / XC3	XC4	XD1 / XS1	XD2 / XS2	XD3 / XS3
S1	10	10	10	15	20	25	30
S2	10	10	15	20	25	30	35
S3	10	10	20	25	30	35	40
S4	10	15	25	30	35	40	45
S5	15	20	30	35	40	45	50
S6	20	25	35	40	45	50	55

Table A2. Imposed loads on floors, balconies and stairs in buildings (EC 1 Part 1)

Categories of loaded areas	q_k [kN/m²]	Q_k [kN]
Category A		
- Floors	1,5 to 2,0	2,0 to 3,0
- Stairs	2,0 to 4,0	2,0 to 4,0
- Balconies	2,5 to 4,0	2,0 to 3,0
Category B	2,0 to 3,0	1,5 to 4,5
Category C		
- C1	2,0 to 3,0	3,0 to 4,0
- C2	3,0 to 4,0	2,5 to 7,0 (4,0)
- C3	3,0 to 5,0	4,0 to 7,0
- C4	4,5 to 5,0	3,5 to 7,0
- C5	5,0 to 7,5	3,5 to 4,5
category D		
- D1	4,0 to 5,0	3,5 to 7,0 (4,0)
- D2	4,0 to 5,0	3,5 to 7,0

Table A3. Categories of use of the building (EC 1 Part 1)

Category	Specific Use	Example
A	Areas for domestic and residential activities	Rooms in residential buildings and houses; bedrooms and wards in hospitals; bedrooms in hotels and hostels kitchens and toilets.
B	Office areas	
C	Areas where people may congregate (with the exception of areas defined under category A, B, and D[1)])	**C1**: Areas with tables, etc. e.g. areas in schools, cafés, restaurants, dining halls, reading rooms, receptions. **C2**: Areas with fixed seats, e.g. areas in churches, theatres or cinemas, conference rooms, lecture halls, assembly halls, waiting rooms, railway waiting rooms. **C3:** Areas without obstacles for moving people, e.g. areas in museums, exhibition rooms, etc. and access areas in public and administration buildings, hotels, hospitals, railway station forecourts. **C4**: Areas with possible physical activities, e.g. dance halls, gymnastic rooms, stages. **C5**: Areas susceptible to large crowds, e.g. in buildings for public events like concert halls, sports halls including stands, terraces and access areas and railway platforms.
D	Shopping areas	**D1:** Areas in general retail shops **D2**: Areas in department stores
[1)] Attention is drawn to 6.3.1.1(2), in particular for C4 and C5. See EN 1990 when dynamic effects need to be considered. For Category E, see Table 6.3		
NOTE 1 Depending on their anticipated uses, areas likely to be categorised as C2, C3, C4 may be categorised as C5 by decision of the client and/or National annex. NOTE 2 The National annex may provide sub categories to A, B, C1 to C5, D1 and D2 NOTE 3 See 6.3.2 for storage or industrial activity		

Table A4. Recommended values of Ψ factors for buildings (EC 8 Part 1)

Action	ψ_0	ψ_1	ψ_2
Imposed loads in buildings, category (see EN 1991-1-1)			
Category A : domestic, residential areas	0,7	0,5	0,3
Category B : office areas	0,7	0,5	0,3
Category C : congregation areas	0,7	0,7	0,6
Category D : shopping areas	0,7	0,7	0,6
Category E : storage areas	1,0	0,9	0,8
Category F : traffic area, vehicle weight ≤ 30kN	0,7	0,7	0,6
Category G : traffic area, 30kN < vehicle weight ≤ 160kN	0,7	0,5	0,3
Category H : roofs	0	0	0
Snow loads on buildings (see EN 1991-1-3)*			
Finland, Iceland, Norway, Sweden	0,70	0,50	0,20
Remainder of CEN Member States, for sites located at altitude H > 1000 m a.s.l.	0,70	0,50	0,20
Remainder of CEN Member States, for sites located at altitude H ≤ 1000 m a.s.l.	0,50	0,20	0
Wind loads on buildings (see EN 1991-1-4)	0,6	0,2	0
Temperature (non-fire) in buildings (see EN 1991-1-5)	0,6	0,5	0
NOTE The ψ values may be set by the National annex. * For countries not mentioned below, see relevant local conditions.			

Table A5. Indicative design working life (EC 0)

Design working life category	Indicative design working life (years)	Examples
1	10	Temporary structures (1)
2	10 to 25	Replaceable structural parts, e.g. gantry girders, bearings
3	15 to 30	Agricultural and similar structures
4	50	Building structures and other common structures
5	100	Monumental building structures, bridges, and other civil engineering structures
(1) Structures or parts of structures that can be dismantled with a view to being re-used should not be considered as temporary.		